

**Responses to lowered salinity in the Pacific spiny dogfish, *Squalus suckleyi*, a marginally euryhaline shark**

By

Dylan Montgomery Cole

A thesis submitted in partial fulfillment of the requirements for the degree of

Master of Science

In

Physiology, Cell and Developmental Biology

Department of Biological Sciences

University of Alberta

## Abstract

Euryhalinity is the ability to survive in multiple environmental salinities. Full euryhalinity is rare within the elasmobranchs (rays, skates, and sharks), however, marginal euryhalinity is comparatively more common. The physiology underlying these adaptations is relatively understudied in cartilaginous fishes compared to bony fishes. I investigated changes in both gill morphology and the kidney transcriptome in Pacific spiny dogfish (*Squalus suckleyi*), a marginally euryhaline shark, following an ecologically relevant 65% seawater exposure. Furthermore, I explored the evolutionary basis of salinity tolerance using the current literature on phylogenetic relationships in selachimorphs (sharks). Dogfish were exposed to 65% seawater for up to 48hrs and sampled throughout. After 24hrs, gills were excised for light microscopy, revealing a significant increase in the interlamellar cell mass and the appearance of both lamellar clubbing and epithelial lifting, suggesting reduced surface area and increased cellular damage, respectively. Total plasma osmolality was measured during the time course and exhibited a significant reduction. This was primarily attributed to the loss of plasma urea, as both  $\text{Na}^+$  and  $\text{Cl}^-$  showed minimal change. I employed RNA-seq to quantify changes in kidney mRNA expression after 0, 12, and 48hrs in 65% seawater. The role of the kidney in low salinity exposure has been previously studied using physiological methods, however, there is a substantial lack of molecular level studies. This technique revealed 1013 unique and differentially expressed transcripts, of which ~60% were functionally annotated. Generally, transcripts that were upregulated or downregulated after 12hrs remained so after 48hrs. Differentially expressed transcripts were involved in numerous cellular functions including protein chaperones, metabolic processes, cell signalling, and responses to stimuli and stress. Importantly, multiple heat shock protein transcripts were upregulated after 12hrs and numerous

transcripts encoding protein trafficking were downregulated. Overall, I showed that the transcriptomic response of the kidney to 65% seawater was highly integrative and relied on the regulation of a multitude of processes. Lastly, low salinity tolerance within elasmobranchs has arisen in multiple species and I postulate that the phylogenetic distance between these species has no bearing on the limits of salinity tolerance observed in the literature.

## **Preface**

The synthesis of cDNA libraries for sequencing were generated in collaboration with Dr. Andrew Whitehead and Jen Roach at UC Davis. Sequencing of these cDNA libraries and demultiplexing was performed by the UV Davis Genome Sequencing Centre.

## **Acknowledgements**

Firstly, thank you to Dr. Greg Goss. You have been an exceptional teacher and guide during my time at U of A. You allowed me to work independently knowing I always had a safety net if guidance was necessary. You allowed me to go places and perform research I might have otherwise only read about.

Thank you to my parents who have been incredibly supportive and helpful. The science conversations on the couch between gorging on chocolate chip cookies made this work much easier. Meghan Gal, thank you for being patient and encouraging while living in different cities, I am extremely grateful to you.

During my time at U of A I received funding from the Queen Elizabeth II Graduate Scholarship, the Dr. Richard (Dick) E Peter Memorial Graduate Scholarship, the Alberta Graduate Student Scholarship. I received travel funds from the Canadian Society of Zoologists, the U of A Graduate Student Association, the International Conference for the Biology of Fishes, and the Society for Experimental Biology. Funding for experiments was provided by NSERC Research Grant provided to Dr. Greg Goss. I am extremely appreciative of all these funding agencies.

Thank you to my committee member Dr. Warren Gallin, you have been extremely helpful in both the work presented in this thesis and in the technical expertise of oocyte injections outside of this thesis. Thank you to Dr. Andrew Whitehead and Jen Roach at UC Davis for providing the technical expertise while I visited your lab, it was an incredible experience. Thank you to the staff at Bamfield Marine Sciences Centre for providing the most beautiful place for blood sampling at 4 a.m. Thank you to the administration and building staff of the Biological Sciences department and the staff in MBSU.

Thank you to all the members of the Goss lab, past and present, that I was lucky enough to meet and learn from. You are all cherished friends and collaborators and have been a highlight of my time at the U of A.

## Table of Contents

<b>Introduction</b> .....	<b>1</b>
<i>Osmoregulatory strategies in fishes</i> .....	1
<i>Iono- and osmoregulatory organs in marine elasmobranchs</i> .....	3
<i>Iono- and osmoregulation in the kidney</i> .....	5
<i>Euryhalinity in elasmobranchs</i> .....	6
<i>Transcriptomics and physiology</i> .....	7
<i>Thesis goals</i> .....	9
<b>Materials and Methods</b> .....	<b>10</b>
<i>Dendrogram of marginally euryhaline elasmobranchs</i> .....	10
<i>Animal collection and exposure</i> .....	10
<i>Plasma measurements and tissue sampling</i> .....	11
<i>Gill morphology</i> .....	12
<i>RNA extraction, cDNA library preparation, and sequencing</i> .....	12
<i>Processing of reads and transcriptome assembly</i> .....	12
<i>Annotation, differential expression analysis, GO enrichment, and KEGG pathways</i> .....	13
<i>Statistical analysis</i> .....	14
<b>Results</b> .....	<b>14</b>
<i>Phylogeny of marginally euryhaline selachimorphs</i> .....	14
<i>Plasma osmolytes and total osmolality</i> .....	15
<i>Gill morphology</i> .....	16
<i>RNA-seq analysis</i> .....	16
<i>Assembly statistics and annotation</i> .....	16
<i>Differential expression and annotation</i> .....	17
<i>Gene level expression</i> .....	21
<i>GO enrichment and KEGG pathways</i> .....	21
<b>Discussion</b> .....	<b>63</b>
<i>Lack of relationship between phylogeny and extent of salinity tolerance</i> .....	63
<i>Osmolytes and gill morphology perturbations following salinity challenge</i> .....	64

<i>Responding to salinity exposure through changes in transcript expression</i> .....	65
<i>Limitations to the study</i> .....	71
<i>Future Directions</i> .....	72
<i>Conclusions</i> .....	75
<b>References</b> .....	<b>76</b>
<b>Appendix</b> .....	<b>86</b>

## List of Tables

<b>Table 1.</b> Descriptive statistics of the filtered <i>de novo</i> kidney transcriptome produced by the Trinity pipeline.....	23
<b>Table 2.</b> BUSCO scores of the <i>de novo</i> kidney transcriptome.....	24
<b>Table 3.</b> Differentially expressed transcripts with the greatest fold change from control to 12 hrs in 65% SW.....	25
<b>Table 4.</b> Differentially expressed transcripts with the greatest fold change from control to 48 hrs in 65% SW.....	26
<b>Table 5.</b> Differentially expressed transcripts with the greatest fold change from 12hrs to 48hrs in 65% SW.....	27
<b>Table 6.</b> Top 10 enriched GO terms in based on number of differentially expressed transcripts associated with each term.....	28
<b>Table 7.</b> Top 10 enriched GO terms associated with the differentially expressed transcripts based on lowest P-value of the term.....	29
<b>Table S1.</b> Complete list of the differentially expressed transcripts following 65% SW exposure.....	86
<b>Table S2.</b> Complete list of the differentially expressed genes following 65% SW exposure....	120
<b>Table S3.</b> RNA purity and integrity of extracted total RNA from kidney tissue.....	126
<b>Table S4.</b> Concordant and discordant alignment rates.....	127

## List of Figures

<b>Figure 1.</b> Dendrogram of salinity tolerant selachimorphs and the lowest salinities experienced in a natural and laboratory setting.....	30
<b>Figure 2.</b> Correlational analysis of pairwise phylogenetic distance and pairwise difference in salinity tolerance.....	32
<b>Figure 3.</b> Plasma osmolality and osmolytes over 48hrs in 65% SW.....	34
<b>Figure 4.</b> Alterations in gill morphology following 24hrs in 65% SW.....	36
<b>Figure 5.</b> Correlation and variance within whole kidney transcriptome.....	38
<b>Figure 6.</b> Differentially expressed transcripts from all biological replicates.....	40
<b>Figure 7.</b> Differentially expressed transcripts of averaged values across time points.....	42
<b>Figure 8.</b> Differentially expressed genes following exposure to 65% SW.....	44
<b>Figure 9.</b> Correlation and variance within the differentially expressed transcripts.....	46
<b>Figure 10.</b> REVIGO analysis and clustering of significantly enriched GO terms.....	48
<b>Figure 11.</b> Differentially expressed transcripts present in the endocytosis KEGG pathway.....	51
<b>Figure 12.</b> Differentially expressed transcripts present in the spliceosome KEGG pathway.....	54
<b>Figure 13.</b> Differentially expressed transcripts present in the RNA transport KEGG pathway..	56
<b>Figure 14.</b> Differentially expressed transcripts present in the general metabolism KEGG pathway.....	58
<b>Figure 15.</b> Differentially expressed transcripts present in the glycerophospholipid metabolism KEGG pathway.....	61
<b>Figure S1.</b> Sum of transcript expression in each replicate.....	128
<b>Figure S2.</b> Estimation of true number of different transcripts in the kidney transcriptome.....	130
<b>Figure S3.</b> Analysis of ExN50 values of the <i>de novo</i> assembled kidney transcriptome.....	132
<b>Figure S4.</b> MA and Volcano plots for each statistical comparison.....	134

## List of Abbreviations

AQP4	Aquaporin 4
ATP	Adenosine triphosphate
BAG4	Bcl2 associated athanogene 4
bp	Base pairs
BUSCO	Benchmarking universal single-copy orthologs
BW	Brackish water
CADH1	Cadherin 1
CASP6	Caspase 6
CCD22	Coiled-coil domain containing 22
CCL20	C-C motif chemokine ligand 20
cDNA	Complementary deoxyribonucleic acid
CFTR	Cystic fibrosis transmembrane conductance regulator
CGNL	Cingulin Like 1
CNP	C-type natriuretic peptide
Contigs	Contiguous sequences
CPM	Counts per million reads
CPSI	Carbamoyl-phosphate synthase I
CPSIII	Carbamoyl-phosphate synthase III
DIC	Dicarboxylate carrier (also SLC25A10)
DNase	Deoxyribonuclease
DSC3	Desmocollin 3
E2	Ubiquitin-conjugating enzymes
EKI1	Ethanolamine kinase 1
EPT1	Ethanolaminephosphotransferase 1
ERK1	Extracellular signal-regulated kinase 1 (also MAPK1)
ERK2	Extracellular signal-regulated kinase 2
FADD	Fas associated death domain
FC	Fold change
FTCD	Formimidoyltransferase cyclodeaminase
FW	Freshwater

g	x gravity
GFR	Glomerular filtration rate
GO	Gene ontology
GSase	Glutamine synthetase
HGD	Homogentisate 1,2-dioxygenase
HPETE	Arachidonic acid 5-hydroperoxide
hrs	hours
HSP	Heat shock protein
HSP30	Heat shock protein 30kDa
HSP71A	Heat shock protein 71 A
HSP71L	Heat shock protein 71 L
HSP80	Heat shock protein 80
I17RA	Interleukin 17 Receptor A
IL10	Interleukin 10
ILCM	Interlamellar cell mass
kDa	Kilodalton
KEGG	Kyoto encyclopedia of genes and genomes
kg	Kilograms
L	Litres
LOX5	Arachidonate 5-lipoxygenase
MAPK	Mitogen activated protein kinase
MAP2K5	Mitogen activated protein 2 kinase 5
MAP3K15	Mitogen activated protein 3 kinase 15
mins	Minutes
mL	Millilitres
mOsm	Milliosmoles
MRC	Mitochondria rich cells
mRNA	Messenger ribonucleic acid
NADH	Nicotinamide adenine dinucleotide
NF-kb	Nuclear factor kappa-light-chain-enhancer of activated B cells
NGS	Next generation sequencing

NHE	Sodium-hydrogen exchanger (also SLC9)
NHE2	Sodium-hydrogen exchanger 2
NHE3	Sodium-hydrogen exchanger 3
NKA	Sodium-potassium ATPase
NKCC	Sodium-potassium-2 chloride
NO	Nitric oxide
nt	Nucleotides
ORFS	Open reading frames
OSTF1	Osmotic stress transcription factor 1
OUC	Ornithine-urea cycle
P53	Tumor protein 53
PCA	Principal component analysis
PE	Phosphatidylethanolamine
PFA	Paraformaldehyde
PISD	Phosphatidylserine decarboxylase
ppt	Parts per thousand
PSA7	Proteasome subunit alpha 7
PTSS2	Phosphatidylserine synthase 2
RAB7	Ras associated protein 7
RBBP6	RB Binding protein 6 ubiquitin ligase
REVIGO	Reduce and visualize gene ontology
Rhag	Rh associated glycoprotein type A
Rhbg	Rh associated glycoprotein type B
Rhcg	Rh associated glycoprotein type C
RhoA	Ras homology family member A
Rhp2	Rh protein 2
RIN	RNA integrity number
RNA	Ribonucleic acid
RNA-seq	RNA-sequencing technology
RSEM	RNA-seq by expectation-maximization
SARDH	Sarcosine dehydrogenase

shUT	Shark urea transporter
SLC	Solute carrier family
SLC25A10	Solute carrier family 25 member 10 (also DIC)
SLC6A18	Solute carrier family 6 member 18
SLC6A5	Solute carrier family 6 member 5
SLC9A9	Solute carrier family 9 member 9
SNX14	Sorting nexin 14
SNX4	Sorting nexin 4
SW	Seawater
TJAP	Tight junction associated proteins
TMAO	Trimethylamine N-oxide
TNF6B	Tumor necrosis factor receptor superfamily member 6B
TPM	Transcripts per million reads
TRPV4	Transient receptor potential cation channel subfamily V member 4
TSC22D2	TSC22 Domain family member 2
UB2J1	Ubiquitin conjugating enzyme E2 J1
UBC12	Ubiquitin conjugating enzyme E2 M
UBE2C	Ubiquitin conjugating enzyme E2 C
UBE2T	Ubiquitin conjugating enzyme E2 T
UFR	Urine flow rate
UHRF1	Ubiquitin like with PHD and ring finer domains 1
UT-A1	Urea transporter 1
UT-A2	Urea transporter 2
VPS36	Vacuolar protein sorting 36 homolog
ZO1	Tight junction associated protein 1

## List of Definitions

**BUSCO score** - A measure of the completeness of a transcriptome. Vertebrates possess 2586 orthologs that should be present only once in the transcriptome, thus if all are present in a dataset it is likely more complete than one without all.

**Chondrichthyes** - All cartilaginous fishes, including elasmobranchs and holocephalans.

**Concordant alignment** - Successfully mapping both paired reads to a single location on the transcriptome.

**de Bruijn graphs** - A method of presenting the sequence variations in overlapping contigs.

**Disconcordant alignment** - Mapping of paired reads to separate locations, or, mapping of only a single contig of the pair.

**Elasmobranchs** - A subclass of Chondrichthyes consisting of sharks, rays, and skates.

**Euryhalinity** - The ability of an animal to survive in a wide range of environmental salinities.

**Ex90** - Represents the subset of transcripts that comprise 90% of the most highly expressed transcripts of the TMM normalized data.

**Ex90N50 value** - The N50 value calculated using only the Ex90 subset as the input, rather than the entire transcriptome.

**N50 value** - A weighted median statistic that represents a transcript length such that 50% of the assembly is equal to or greater than this value.

**Phred score** - The probability that a base is sequenced incorrectly, ranging from 0-40. A score of 40 has a 1 in 10000 chance of being identified incorrectly.

**Selachimorphs** - A superorder of elasmobranchs that contains only the true sharks.

**TPM** - Normalized expression values where raw counts are first divided by the length of genes in kilobases to get reads per kilobase (RPK), followed by dividing the sum of all RPK values by 1 million to get transcripts per million.

**TMM normalization** - Normalization method of TPM values which removes mRNA composition bias.

## Introduction

### *Osmoregulatory strategies in fishes*

Osmotic stress is an innate challenge for all aquatic organisms that is imposed simply due to physiochemical properties of the environment. Fishes are the most abundant vertebrate within the aquatic environment and have evolved multiple physiological strategies to overcome osmotic challenges (Kultz, 2015). Actinopterygians (ray finned, bony fishes) are the largest class of fishes and have evolved to simultaneously osmoregulate and ionoregulate, maintaining an internal plasma osmotic pressure of roughly 300-400 milliosmole (mOsm) (Kultz, 2015). The evolution of this strategy has supported widespread habitation in both marine and freshwater environments by many species. Actinopterygians living in a freshwater environment are hyperosmotic, resulting in simultaneous water influx and ion efflux. Inversely, Actinopterygians living in marine environments are hyposmotic and thus are constantly inundated with ion influx and dehydrating conditions. In both environments, the osmoregulatory systems are tailored precisely to maintain ion balance and total osmotic pressure. In contrast to the diverse Actinopterygians, the Myxini class (hagfish) employ a strategy in which they osmoconform and ionoconform causing the osmotic pressure within to match the surrounding water. These fishes are restricted to a marine environment and are unable to survive any freshwater exposure (Martini, 1998).

Another osmoregulatory strategy in the fishes is present in Chondrichthyes, or cartilaginous fishes, and in the rare, extant fossil clade Coelocanthiformes (Griffith, 1980). Marine elasmobranchs (sharks, rays, and skates) are naturally isosmotic (or slightly hyperosmotic) with the surrounding water, maintaining an extracellular osmolality of ~1000 mOsm (Wright and Wood, 2015). This has greatly reduced the need to imbibe water, contrary to their marine Actinopterygian counterparts. Together, plasma  $\text{Na}^+$  and  $\text{Cl}^-$  account for approximately 500-600 mOsm, producing an inward gradient for these electrolytes that must be excreted. The remaining 400-500 mOsm is primarily attributed to the unique addition of two nitrogenous compounds, urea and trimethylamine N-oxide (TMAO)(Yancey, 2015). Therefore, this is termed a ureosmotic strategy. Urea typically exerts an osmotic pressure of approximately 300-500 mOsm, while TMAO is substantially less at 50-100 mOsm (Yancey, 2015). Other

organic methylamines and amino acids such as betaine,  $\beta$ -alanine, sarcosine, and taurine also contribute to total osmotic pressure however in smaller quantities (totalling <50 mOsm). Early studies on elasmobranch physiology (reviewed in Smith, 1936) indicated urea was critical for proper cardiac function in a variety of species. *in vitro* experiments using four elasmobranch species (*Raja clavata*, *Raja blanda*, *Scyllium canicula*, and *Rhina squatina*) demonstrated the vital role of urea in cardiac contractions, while experiments on *Squalus suckleyi* cardiac tissue revealed an increase in irregular heart rate following replacement of urea with sucrose or thio-urea (Mines, 1912; Simpson and Ogden, 1932). It has since been concluded that almost all elasmobranchs require urea, with the exception being a small number of obligatory freshwater stingrays of the Myliobatiformes order (Ballantyne and Robinson, 2010). No teleosts species to date have shown to be ureosmotic, making the Chondrichthyes and Coelocanth unique. However, some such as Lake Magadi tilapia (*Alcolapia graham*) are known to be ureotelic, as opposed to the majority that are ammonotelic (Randall et al., 1989).

Retaining urea as a primary osmolyte comes with several major consequences. The first problem is that urea induces destabilizing effects on protein structure. This occurs through both hydrogen bonds forming with the protein amide group and a reduction in the hydrophobic effects that maintain proper protein structure (Zou et al., 1998). To rescue this negative effect, the previously mentioned methylamine compounds (particularly TMAO) act as chemical chaperones to enable proper protein folding and enzymatic function (Yancey and Somero, 1980). The ratio of urea to TMAO (and other organic chaperones) that optimizes protein stabilization is roughly 2:1, however, this is also impacted by depth in the water column, species, and tissue type (Forster and Goldstein, 1976; Laxson et al., 2011; Suyama and Tokuhiko, 1954; Yancey and Somero, 1979).

The second major consequence of the ureosmotic strategy is the metabolic price of urea synthesis. Urea is synthesized through the ornithine-urea cycle (OUC) and this predominantly occurs in the mitochondria (the purine degradation pathway is also present but does not contribute significantly) (Schooler et al., 1966). There are several important differences between the OUC in elasmobranchs and in similar ureotelic animals. First, elasmobranchs rely on glutamine as the initial nitrogenous substrate, rather than ammonia (Anderson and Casey, 1984). Secondly, the reliance on glutamine necessitates a different catalyzing enzyme for this reaction and therefore elasmobranchs employ carbamoyl-phosphate synthetase III (CPS III, substrate is

glutamine) rather than CPS I (substrate is ammonia). Third, both the initial reaction catalyzed by glutamine synthetase (GSase) and the final reaction catalyzed by arginase occur within the mitochondria, rather than in the cytosol (Casey and Anderson, 1982). The functional outcome of this last difference is likely an increase the shuttling of glutamine directly into the urea cycle rather other glutamine dependent processes and increased rate of return of ornithine back into the cycle (Anderson, 1991). The highest rates of urea biosynthesis in elasmobranchs are found in liver, nevertheless, extrahepatic sources are also involved. In particular, white muscle shows relatively low synthesis rates yet contributes significantly to total urea biosynthesis due to its large mass (Steele et al., 2005). Furthermore, GSase in these extra-hepatic tissues (except kidney) is located within the cytosol as opposed to the mitochondria, supporting the key role the liver plays in urea production (Anderson, 1991). The OUC is extremely expensive metabolically, requiring 5 mol of adenosine triphosphate (ATP) to produce a 1 mol of urea (Kirschner, 1993). Since retention of urea across the osmoregulatory organs is not perfect, continuous production of urea is necessary to maintain isosmotic status. A consequence of this constant urea production is that these animals are almost permanently in a nitrogen limited state. It is hypothesized that this high nitrogen demand contributes to the nearly ubiquitous role as carnivores (Ballantyne and Robinson, 2010; Wright and Wood, 2015).

#### *Iono- and osmoregulatory organs in marine elasmobranchs*

The elasmobranchs have evolved numerous sophisticated physiological mechanisms to deal with strong gradients directing salts inward and organic osmolytes outward, all while remaining isosmotic. The four main organs involved in regulating osmolytes are the intestine, rectal gland, gill, and kidney (Wright and Wood, 2015; Yancey, 2015). Briefly, the intestine does not typically play a large role as the drinking rate is almost zero due to their isosmotic status. However, during feeding, osmotic challenge, or alteration of the renin angiotensin via pharmacology, these animals may imbibe seawater and the intestine may become involved (Anderson et al., 2002; Anderson et al., 2007). The rectal gland is present in both elasmobranchs and coelacanth and shares similarities with salt glands found in birds and reptiles (Forey, 1980; Holmes and Phillips, 1985; Shoemaker and Nagy, 1977). It is critical in removing plasma  $\text{Na}^+$  and  $\text{Cl}^-$  and excreting a highly concentrated solution into the lower intestinal tract. It uses a

counter-current system and is populated with numerous mitochondrion-rich cells (MRCs), a hallmark of active ion transport (Wright and Wood, 2015).

The direct interface with the aquatic medium make the gills a principal location for salt influx and urea loss. The gross morphology differs only slightly from teleosts, however, the transport physiology is quite altered. Teleost gills are heavily involved in both acid-base homeostasis and ionoregulation while the elasmobranch gill plays a similar role in acid-base homeostasis, however its role in salt excretion may be secondary to rectal gland, but still functional (Evans et al., 2005; Wright and Wood, 2015). In both clades, salt secretion demands numerous MRCs with high abundance of the trademarks proteins  $\text{Na}^+/\text{K}^+$ -ATPase (NKA),  $\text{Na}^+/\text{K}^+/2 \text{Cl}^-$  co-transporter (NKCC), and cystic fibrosis transmembrane conductance regulator (CFTR)(Silva et al., 1977). Together, this system generates secondarily active NaCl excretion. Interestingly, in marine spiny dogfish, *Squalus acanthias*, surgical removal of rectal gland does not elicit an increase branchial NKA activity (to increase  $\text{Na}^+$  and  $\text{Cl}^-$  secretion) or alter salt homeostasis, suggesting that increased urinary output and the basal level of branchial secretion was sufficient to maintain homeostasis (Wilson et al., 2002). In contrast to this, marine houndsharks (*Triakis scyllium*) challenged with diluted seawater showed an increase in branchial NKA, in addition to NKCC (Takabe et al., 2016). The exact role of the elasmobranch gills in ionoregulation is contentious and remains to be discerned (Wright and Wood, 2015).

In contrast to this disputed ionoregulatory role, the gills undoubtedly contribute significantly to urea osmoregulation and are the primary route for the loss of nitrogenous compounds (Payan et al., 1973; Wood et al., 1995). Elasmobranch gills possess two mechanisms that limit urea loss against a steep chemical gradient. The first is an abnormal basolateral membrane composition in the epithelial cells. This membrane displays an extremely high ratio of cholesterol-to-phospholipids (3.68), promoting the tight packing of the phospholipids and ultimately decreasing the passive urea loss (Fines et al., 2001). The other mechanism of branchial urea regulation is the presence of urea transporters. The location (basolateral vs apical) and transport mechanism (facilitated, co-transporter, or exchanger) remains inconclusive, however, pharmacological inhibition studies using phloretin (NKA inhibitor) and isolated basolateral membrane suggest a  $\text{Na}^+$  dependent back transporter that maintains intracellular urea low (Fines et al., 2001). Alternatively, use of urea analogues thiourea and acetamide suggested an apical localization of a facilitative transporter (Wood et al., 2013). These are not mutually

exclusive and further work needs to be done to conclusively identify the proteins involved. Interestingly, the gills show an ability to acquire  $\text{NH}_3$  from the environment, providing another source of nitrogen (Wood and Giacomini, 2016).

#### *Iono- and osmoregulation in the kidney*

The elasmobranch kidney is a critical osmoregulatory organ primarily due to its role in urea homeostasis, wherein it achieves 70-99% reabsorption of the filtered urea (Kempton, 1953). This high rate of renal urea reabsorption is reflected in whole-animal urea excretion measurements where basal renal loss in *Raja erinacea*, a marine skate, only accounted for roughly 4% with branchial loss contributing the remaining 96% (Payan et al., 1973). Reabsorption is suggested to occur through active (primary and/or secondary) transport, or through a countercurrent manner of passive transport, or a combination (Hammerschlag, 2006; Schmidt-Nielsen et al., 1972). Morphologically, the nephron tubules are substantially more convoluted and longer than most other vertebrates, making them unique (Hazon et al., 2003). Tubules begin at the renal corpuscle and typically form a series of 4 hairpin loops that alternate between the bundle zone and sinus zone, before finally emptying into the collecting tubules (Lacy and Reale, 1985). Encasing each bundle tubule is a unique peritubular sheath which shares similarities in cellular arrangement to barrier structures in invertebrates and vertebrates, possibly suggesting a similar role (Lacy and Reale, 1986). The filtered, hyposmotic urine travels from collecting tubules into a duct and is then excreted from the animal through the cloaca. The countercurrent morphology arrangement of tubules in addition to the impermeable peritubular suggests the possibility of a passive renal transport system (Friedman and Hebert, 1990). The proportion of transport that can attributed to this passive movement has not been explored and warrants further analysis. An exception to this complex renal morphology is the Potamotrygonidae family of freshwater rays. These animals have lost the typical ureosmotic strategy present in marine elasmobranchs, and therefore may have no necessity for a complex, renal system to maintain urea and salt homeostasis (Hyodo et al., 2014).

Renal transport proteins are fundamental for the reabsorption of plasma osmolytes, irrespective of the overall transport mechanism (active, passive, or both). Like the rectal gland and gills, basolateral NKA in the renal tubules is a key generator of  $\text{Na}^+$  gradients that can be employed by numerous co-transporters. Renal reabsorption of urea is maintained at a ratio of

1.6:1 to  $\text{Na}^+$  regardless of environmental salinity, suggesting a strong link between the two osmolytes (Schmidt-Nielsen et al., 1972). Both a phloretin sensitive, facilitated urea transporter (shUT) and a phloretin sensitive,  $\text{Na}^+$  dependent transporter have been identified and are hypothesized to be the main participants in urea reabsorption (Morgan, 2003a). The shUT in Japanese-banded houndsharks showed localization restricted only to the collecting tubule and furthermore, this was predominantly in the apical side of the cells (Hyodo et al., 2004; Yamaguchi et al., 2009).

Other transport proteins that play important ionoregulatory roles have been identified in elasmobranch kidney tissues. Two members of the  $\text{Na}^+/\text{H}^+$  exchanger (NHE) family (NHE2 and NHE3) have been revealed, however these were suggested to have a much larger role in acid-base regulation than osmoregulation (Claiborne et al., 2008; Li et al., 2013). Four NKCC2 (a kidney-specific NKCC) variants have been identified (Gagnon et al., 2002). In addition to reabsorbing osmolytes, the kidneys also tightly regulates water balance. Aquaporin 4 (AQP4) has been identified in dogfish shark kidneys, however, that is the only member (Cutler et al., 2012). There is a lack of data about many of the other Solute Carrier (SLC) family transporters that are likely involved in retention of the organic methylamine osmolytes. Ammonia transporter Rhp2 is present in shark kidney and is localized only in the sinus zone (Nakada et al., 2010). In summation, several transporters have been identified, of which some have been localized to particular regions, however, the overall mechanism of osmolyte reabsorption and how each component fits together has not been resolved.

### *Euryhalinity in elasmobranchs*

Euryhalinity is the ability of an organism to live in a wide range environmental salinities. This trait exists as a gradient, ranging from true euryhalinity to marginal euryhalinity. FW habitation in the elasmobranch clade is relatively rare compared to the bony fishes. There are ~1,050 extant elasmobranchs and of this, 171 species are thought to enter BW or live in FW (Dulvy et al., 2014; Martin, 2005). Of these tolerant species, only ~8% are considered truly euryhaline and 21% are obligate FW species, compared to 41% in teleosts (Cohen, 1970; Martin, 2005). Therefore, approximately 120 elasmobranch species can be considered marginally euryhaline. Little is known about the extent of salinity tolerance in the vast majority of these marginally euryhaline species, yet some have been well studied (e.g. *Squalus suckleyi*, *Squalus*

*acanthias*, *Raja erinacea*, *Heterodontus portusjacksonii*, *Triakis scyllium*) The fully euryhaline species include a single shark family, Carcharhinidae (requiem sharks), and several ray and skate families including Pristidae (sawfish), Dasyatidae (whiptail rays), and Rajidae (skates)(Martin, 2005). From the known species, it is clear the rays and skates are considerably more successful at penetrating into freshwater and brackish environments than sharks (Martin, 2005). There may be several factors that limit the extent of FW invasions, however, it is hypothesized that urea physiology, rather than any morphological basis, is responsible due to the common occurrence of unspecialized ecomorphotypes in euryhaline and FW species (Martin, 2005).

Transition from a SW environment to a BW or FW environment induces many acute physiological changes. The most common and well documented change is a reduction of total plasma osmolality, primarily through the loss of plasma urea and TMAO and a similarly, a reduction in urea biosynthesis (Anderson et al., 2005a; Cooper and Morris, 1998; Deck et al., 2016; Guffey and Goss, 2014; MacLellan et al., 2015). This urea loss occurs predominantly through the kidney, as efflux from the gills stays relatively constant (Payan et al., 1973). A common response observed in the kidney is an increased urine flow rate (UFR) and glomerular filtration rates (GFR), both contributing to a decrease in urea reabsorption and an overall decrease in plasma urea (Cooper and Morris, 2004a; Goldstein and Forster, 1971; Payan et al., 1973). Increased GFR also likely contributes to water homeostasis as during this period there is increased water influx (Anderson et al., 2007; Guffey and Goss, 2014).

### *Transcriptomics and physiology*

Genetic sequencing technology and its applications have advanced significantly since its conception with Sanger sequencing, the first generation, low-throughput technique (Sanger and Coulson, 1975; Sanger et al., 1977). Sequencing by synthesis, or next-generation sequencing (NGS), was the next revolutionary technology that allowed high-throughput, parallel sequencing of entire DNA libraries, rather than single targets such as in Sanger sequencing (Heather and Chain, 2016). NGS employs fluorophore-conjugated nucleotides that can be laser stimulated to fluoresce following DNA polymerization, thus revealing the nucleotide identity (Shendure and Ji, 2008). This technology has also been applied to RNA (termed RNA-seq), although it requires reverse transcription to produce a cDNA library prior to sequencing. The development of RNA-seq has greatly benefited the field of transcriptomics (study of the mRNA profile), which

primarily aims to quantify transcript expression after treatment or between different tissue types, measure changes in gene splicing, and identify single nucleotide polymorphisms (Wang et al., 2009).

Prior to RNA-seq, quantification of mRNA expression levels in a high-throughput manner was largely accomplished by microarrays (tag-based methods were also possible however still relied on Sanger sequencing). Microarrays use a set of complementary nucleotide probes, either custom designed or general oligonucleotides, to bind to mRNA and fluoresce upon laser stimulation (Tarca et al., 2006). This hybridization-based method is relatively quick, easy, and inexpensive. However, probe design requires prior genetic knowledge, limiting its applications. Furthermore, some mRNA sequences may cross-hybridize with multiple probes, increasing background levels greatly (Okoniewski and Miller, 2006). Microarrays also possess a limited dynamic range of detection, decreasing the sensitivity (Wang et al., 2009). RNA-seq overcomes many of these issues, as well as providing other advantages. No prior genetic knowledge is necessary for RNA-seq, making it suitable for non-model species. RNA-seq has an extremely large dynamic range, allowing detection of transcripts with differences of >8000 fold, while microarrays are restricted to fold differences in the hundreds (Wang et al., 2009). In addition to its wide detection range, it has also been shown to be accurate in its quantification of transcripts (Mortazavi et al., 2008; Nagalakshmi et al., 2008). This technology is not without its own disadvantages and challenges. It requires extensive use of bioinformatics and computing resources for analysis due to the large amount of data generated. Furthermore, steps in cDNA library synthesis can introduce bias, however, most of these can be measured and corrected (Wang et al., 2009).

RNA-seq has become common in a physiological context to understand changes in organisms following treatment or experimental exposure. In teleost fishes RNA-seq has been used extensively to study several phenomena in multiple tissue types, e.g. thermal tolerance, salinity tolerance, hypoxia exposure, stress responses, immune response to infection and metal toxicity (Aballai et al., 2017; Beck et al., 2016; Gibbons et al., 2017; Metzger and Schulte, 2016; Naour et al., 2017; Nguyen et al., 2016; Song et al., 2017; Tomalty et al., 2015; Zhang et al., 2017a; Zhang et al., 2017b). Within elasmobranchs, RNA-seq has seen limited usage. The studies that have been performed have used it to catalogue the transcriptome, rather than performing any experimental treatment to quantify differential expression (Chana-Munoz et al.,

2017; King et al., 2011; Krishnaswamy Gopalan et al., 2014; Mulley et al., 2014; Richards et al., 2013). The potential of future investigation into elasmobranch genomes and transcriptomes using NGS is enormous.

### *Thesis goals*

Currently, there is a broad understanding of elasmobranch renal physiology following a salinity challenge (SW into BW or FW), however it is far from complete. Unsurprisingly, most studies that have examined changes at the molecular level have focused on critical transporters (such as urea transporters), excluding a plethora of other potential responses that may be occurring. Therefore, this thesis primarily sought to explore in greater detail the changes in expression of transcripts involved in ion transport, and ancillary transcripts that also likely contribute to successfully responding to osmotic challenges within the kidney. This was accomplished using RNA-seq technology and the Pacific spiny dogfish, *Squalus suckleyi*. As discussed previously, RNA-seq technology has been limited in its application in elasmobranch species, making the work in this thesis particularly novel. *S. suckleyi*, and its sister species *S. acanthias*, are marginally euryhaline elasmobranchs and have been extensively used in whole body, branchial, and rectal gland physiology studies, largely excluding the kidney (Claiborne et al., 2008; Deck et al., 2016; McMillan and Morse, 1999; Wilson et al., 2002; Wood et al., 1995; Wood et al., 2013). These animals have been previously caught in estuaries where salinity was measured at ~65% SW, and therefore this level was used for experiments. It is hypothesized that an acute salinity challenge will induce a reduction in the transcript expression of urea transporters as previously seen in *Triakis scyllium*, in addition to transcripts involved in organic osmolyte transport, ultimately to allow the conservation of isosmotic status (Yamaguchi et al., 2009). Consistent with this hypothesis, decreases in the expression of tight junction transcripts such as the claudin family is expected, allowing for increased paracellular loss of osmolytes. Furthermore, the abundance of aquaporins transcripts will likely increase to permit water loss and maintain water balance. Responding to any stimulus requires the activation of signal transduction pathways, and therefore transcripts involved in these pathways will likely be differentially expressed following an osmotic challenge, with increases and decreases in expression specific to each pathway (Fiol and Kültz, 2007). Consequently, there will likely be changes metabolic processes to accommodate the activation of these pathways and the extensive

responses these pathways activate or inhibit. The levels of protective osmolytes such as TMAO have an inverse relationship with the levels of heat shock proteins, and thus, as TMAO decreases there will likely be an increase in the expression of heat shock protein transcripts (MacLellan et al., 2015).

Additional to this primary goal, I aimed to characterize morphological changes seen in the dogfish gills following exposure to low salinity. This has not been documented in these sharks previous, however, teleosts have been shown to respond to changes in salinity through alterations to gill morphology (Blair et al., 2018). The last objective of this thesis was to explore the evolutionary history of the selachimorphs to elucidate whether the level of salinity tolerance was evolutionarily related to phylogenetic relationships.

## **Materials and Methods**

### *Dendrogram of marginally euryhaline elasmobranchs*

The literature was searched for publications containing information about the lowest salinity that selachimorphs are found at in a natural setting or tested within the laboratory. A representative dendrogram was generated to visualize the relationships between species based on (Ballantyne and Fraser, 2012) and Naylor et al. (2012). A semi-quantitative measure of the link between salinity tolerance and evolutionary history was performed by measuring the pairwise phylogenetic distance between each euryhaline species and correlating this to pairwise differences in the lowest published salinity. This was done under the hypothesis that species with a greater phylogenetic distance would likely display a greater difference in salinity tolerance. The phylogenetic distances between species were measured using ImageJ software and the phylogeny generated by Naylor et al. (2012) which used NADH2 sequences from 595 elasmobranch species.

### *Animal collection and exposure*

Pacific spiny dogfish (*Squalus suckleyi*) were collected from Barkley Sound (Vancouver Island, B.C., Canada) using hook and line and transported to Bamfield Marine Sciences Station where they were kept in a flow-through, circular housing tank (140,000 L). Dogfish were fed

commercial hake (*Merluccius productus*) to satiation every four days. Experimental animals were transferred to a smaller, flow-through, circular holding tank (1,500 L) to fast for five days. Following fasting experimental animals were transferred to individual, opaque, flow-through exposure tanks (135 L) and allowed to acclimate for at least eight hours. Upon completion of acclimation period, water was drained over 10 mins to ~65% tank volume and refilled with 100% FW to achieve the desired 65% SW (21ppt), an ecologically relevant exposure level (McMillan and Morse, 1999). Simultaneous inflows of 100% SW and 100% FW at different rates maintained the 65% SW exposure level throughout the length of the experiment. Five animals were kept at 65% SW for each time duration (0, 3, 6, 12, 24, and 48hrs) with continuous flow-through and an oxygen air-stone. Water salinity was measured using an electronic probe (YSI) and maintained via adjustments to the SW and FW inflow rates. Water temperature was maintained at environmental levels by the flow-through system. After completion of the full exposure duration, animals were euthanized using tricaine methanesulfonate ( $5 \text{ g L}^{-1}$ ) (Syndel Laboratories, Qualicum Beach, B.C., Canada) followed by severance of the spinal cord. All procedures using animals were approved by the University of Alberta and Bamfield Marine Sciences Centre animal use care committees (University of Alberta AUP#00001126).

#### *Plasma measurements and tissue sampling*

Whole blood (2mL) was sampled at each time point via caudal puncture using a 20 gauge needle rinsed beforehand with heparinized dogfish saline (in  $\text{mmol L}^{-1}$ : NaCl 280.0, KCl 6.0,  $\text{CaCl}_2$  5.0,  $\text{MgCl}_2$  3.0,  $\text{Na}_2\text{SO}_4$  0.5,  $\text{Na}_2\text{HPO}_4$  1.0,  $\text{NaHCO}_3$  4.0, Urea 350.0, TMAO 70.0, and glucose 5.0 at  $\text{pH} = 7.8$ ) (Guffey and Goss, 2014). Blood was immediately centrifuged at 12,000 xg for 2 min to obtain plasma. Plasma  $\text{Na}^+$ ,  $\text{Cl}^-$ , and urea were measured via, respectively, a Thermo Scientific model iCE 3300 Atomic Absorption Spectrometer, a Buchler digital chloridometer, and a colourimetric urea assay (urea diluted to 1:5000) (Rahmatullah and Boyde, 1980). Total plasma osmolality was measured using a Vapro vapour pressure osmometer. Tissue samples (gut, kidney, brain, heart, gills, white muscle, liver, and rectal gland) were excised at each time point immediately upon euthanasia and placed into appropriate solutions (e.g. RNAlater™ (Ambion) and then into liquid nitrogen or prepared for gill morphology).

### *Gill morphology*

Gills from three animals at both 0hrs and 24hrs were extracted and fixed in 4% PFA overnight at 4 °C and subsequently washed twice with ice-cold 70% ethanol. These were then dehydrated via a series of ethanol washes. Tissues were embedded in paraffin, sectioned at 5 µm and stained with hematoxylin and eosin before being imaged on Zeiss Scope A1 microscope combined with an optronic camera for imaging. Images were loaded in ImageJ and the line tool was used for measurements using a reference scale bar added during image capturing. Gill lamellar width measurements were performed by taking the average of ten random measurements along the length of a lamellae on five different lamellae. Five interlamellar cell mass (ILCM) measurements were made on each side of a gill by measuring from the outermost side of the ILCM to border.

### *RNA extraction, cDNA library preparation, and sequencing*

Total kidney RNA was extracted using TRIzol (Invitrogen) according to manufacturer's guidelines from sharks exposed to low salinity for 0hr, 12hr, and 48hr. RNA integrity and purity were analyzed on an Agilent 2100 Bioanalyzer and Nanodrop 1000, respectively, for quality control prior to cDNA library synthesis. All RNA integrity numbers (RINs) were above 8 (mean = 9.32). RNA concentration was measured using a Qubit fluorometer (Invitrogen). The cDNA libraries were produced using the NEBNext<sup>®</sup> Ultra Directional RNA Library Prep Kit for Illumina<sup>®</sup> and indexed using the NEBNext<sup>®</sup> Multiplex Oligos for Illumina<sup>®</sup>. The quality of the cDNA libraries was measured using an Agilent 2100 Bioanalyzer. Samples were pooled after indexing and sequenced on an Illumina HiSeq 4000 with 150bp, paired-end sequencing parameters at the UC Davis Genome Centre. Following sequencing, raw reads were demultiplexed by the UC Davis Genome Center.

### *Processing of reads and transcriptome assembly*

The quality of the raw reads was assessed using FastQC v0.11.5 and subsequently trimmed using Trimmomatic v0.36 software to remove both primer and adaptor sequences, low quality reads at the leading and trailing ends (Phred score <15), and reads that are <50 bp in length (Andrews, 2010; Bolger et al., 2014). Reads were also trimmed using the sliding window

function set at a window of 4 and a minimum Phred score of 10. Post-trimming quality was assessed again using FastQC to verify that all non-biological sequences were removed and remaining sequences were of high quality. These trimmed reads were *de novo* assembled using the Trinity v2.4.0 software (Grabherr et al., 2011). In short, Trinity is comprised of three modules that together generate a transcriptome. The Inchworm module assembles the trimmed reads into contiguous sequences (contigs) based on overlapping k-mers. The Chrysalis module then clusters similar contigs together and creates de Bruijn graphs for each cluster. Finally, the Butterfly module reconstructs transcript isoforms from each cluster de Bruijn graph. Reconstructed transcripts were filtered based on a minimum threshold of 1 transcript per million reads (TPM) in any sample. Following assembly and filtering of the transcriptome, numerous scripts within the Trinity package were run to analyze assembly statistics such as sample correlation, calculation of N50 and Ex90N50 value, and principal component analysis. BUSCO (Benchmarking Universal Single-Copy Orthologs) scores were calculated using online software gVolante v1.0.1 to estimate the completeness of the transcriptome (<https://gvolante.riken.jp/>; Nishimura et al., 2017). The Trinity script *align\_and\_estimate\_abundance.pl* wrapped Bowtie2 v2.3.2 for alignment of samples to the *de novo* transcriptome and RSEM v1.3.0 (RNA-seq by Expectation-Maximization) for alignment-based estimation of transcript abundances (Langmead and Salzberg, 2012; Li and Dewey, 2011). This script produced matrices of both transcript and gene counts, in addition to CPM normalized expression values, in each of the 15 samples. Gene level expression is the sum of all transcript isoform expression values.

#### *Annotation, differential expression analysis, GO enrichment, and KEGG pathways*

TransDecoder v5.0.0 was used to predict likely open reading frames (ORFs) in each transcript (Haas et al., 2013). Both nucleotide and predicted protein sequences were used with the Trinotate v3.0 pipeline (<http://trinotate.github.io/>). Briefly, this pipeline wraps multiple querying programs and databases together (including Blast+, SwissProt, HMMER/PFAM, and GO annotations) to extract homologous annotations from other species. Differential expression analysis was performed using the Trinity script *run\_DE\_analysis.pl* which wrapped edgeR, an analysis package within R (Robinson et al., 2009). Transcripts that showed significant differential expression (cutoff of  $P_{adj} < 0.05$  and  $\log_2FC > 1$ ) were extracted using the Trinity script *analyze\_diff\_expr.pl* (McCarthy et al., 2012). Similar analysis was also performed to find

changes in expression at the gene level. Heatmaps were produced in R Studio v1.0.143 using the “gplots” package. The Trinity script *run\_GOseq.pl* wrapped the R package GOseq to determine enriched GO terms (biological processes, molecular function, and cellular component) in the differentially expressed transcripts (Young et al., 2010). REVIGO online software was used to collapse semi-redundant biological process terms, cluster these terms and plot them (<http://revigo.irb.hr/>; Supek et al., 2011). Custom labels were added to these GO plots to summarize the general functional role of the major clusters. Functional annotations from differentially expressed transcripts were converted into *H. sapiens* homologs to identify and visualize enriched KEGG pathways using online software DAVID v6.8 (<https://david.ncifcrf.gov/>; (Huang et al., 2009a; Huang et al., 2009b).

### *Statistical analysis*

Significant differences in plasma osmolality and osmolyte concentrations were tested using a one-way ANOVA followed by a Tukey’s post hoc test which compared the data from each group to every other group. This was done with a p-value threshold of 0.05. Analysis of the gill morphology was performed using an unpaired T-test, with a similar P-value threshold of 0.05. Differential expression within RNA-seq was performed by the edgeR program and corrected for using the Benjamini-Hochberg correction.

## **Results**

### *Phylogeny of marginally euryhaline selachimorphs*

The literature of selachimorphs was reviewed to investigate both the prevalence and limits of salinity tolerance in elasmobranchs. The occurrence of marginal euryhalinity is much more common than what has previously been suggested by Ballantyne and Fraser (2012). The bullshark, *Carcharhinus leucas*, remains the only completely euryhaline selachimorph. There are six orders of marginally euryhaline selachimorphs, including Sphyrnidae, Triakidae, Heterodontidae, Squalidae, and Hemiscyllidae, and Scylorhinidae. The Triakidae order contains the greatest number of marginally euryhaline animals, possessing four species that can tolerate salinity from 10 ppt up to 26 ppt. Of this group, *Triakis scyllium* exhibits the greatest salinity tolerance, capable of surviving as low as 10 ppt water (Yamaguchi et al., 2009).

This dendrogram (Fig. 1) highlights the diverse clades that exhibit marginal salinity tolerance, however, it doesn't distinguish whether there is a relationship between the phylogeny of these species and differences in salinity tolerance. This is essential for understanding whether salinity tolerance is an ancestral trait shared by all members within an order or whether it has evolved multiple times both within orders and between orders. Therefore, using the phylogeny created by Naylor et al. (2015) the pairwise phylogenetic distance between each known euryhaline (marginal and full) species was measured and plotted against the pairwise difference in lowest salinity experienced in either a lab or natural setting (Fig 2). There was no observable correlation between these two parameters, suggesting salinity tolerance is not dependent on phylogenetic relationships and has likely evolved multiple times independently.

#### *Plasma osmolytes and total osmolality*

Dogfish transferred from 100% SW to 65% SW exhibited a time-dependent, significant decrease in total plasma osmolality from  $843.8 \pm 1.6$  mOsm/kg to  $662.2 \pm 15.3$  mOsm/kg over 48hrs ( $P < 0.05$ ,  $n=5$ ) (Fig. 3a). This decrease was non-linear and approached an asymptote at 650 mOsm/kg, roughly equivalent with the environment. No significant alterations were seen in plasma  $\text{Na}^+$  as concentrations in control animals was  $325.7 \pm 8.8$  mmol  $\text{L}^{-1}$  and decreased minimally to  $308.1 \pm 12.7$  mmol  $\text{L}^{-1}$  following 48hrs of exposure (Fig. 3b). However, plasma  $\text{Na}^+$  reached the lowest levels at  $298.3 \pm 6.5$  mmol  $\text{L}^{-1}$  after 24hrs (Fig. 3b). Similarly, resting plasma  $\text{Cl}^-$  was  $248.6 \pm 5.9$  mmol  $\text{L}^{-1}$  and decreased to  $221.4 \pm 6.0$  mmol  $\text{L}^{-1}$ , with a significant decrease after 24hrs (Fig. 3b). Urea levels demonstrated larger changes than both  $\text{Na}^+$  and  $\text{Cl}^-$  however no significant changes were detected (Fig. 3b). Control plasma concentration was  $358.0 \pm 73.6$  mmol  $\text{L}^{-1}$ , which decreased after 6hrs to  $184.3 \pm 73$  mmol  $\text{L}^{-1}$ . Interestingly after 24hrs, urea had risen to  $254.6 \pm 31.3$  mmol  $\text{L}^{-1}$  before levels decreased again to the lowest concentration measured of  $118.1 \pm 42$  mmol  $\text{L}^{-1}$ . The osmolyte concentration data was reformatted to provide a measure of the change from control which highlighted the large change in urea and the tight link between  $\text{Na}^+$  and  $\text{Cl}^-$  (Fig. 3c).

### *Gill morphology*

Changes in gross gill morphology were quantified in control animals and animals after 24hrs in 65% SW. Lamellar widths of control and experimental animals was measured, however no significant differences were detected (Fig. 4c). Conversely, there was a ~2-fold significant increase in ILCM of exposed fish (Fig. 4d). There were notable changes to the lamellar structures after 24hrs in 65% SW, including both epithelia lifting and lamellar clubbing (Fig. 4a & b). Furthermore, there appears to be the development of pyknosis (nucleus and chromatin collapse), a process associated with apoptosis and necrosis.

### *RNA-seq analysis*

#### *Assembly statistics and annotation*

The total number of fragments for each sample ranged between ~2 million up to 18 million (Supp. Fig. 1). These were used in the *de novo* assembly, which after filtering of low expression transcripts, 479,976 transcripts were retained, contained within 361,284 genes (Table 1). This number of transcripts and genes assembled is likely an overestimation of the true numbers, possibly caused by the process of *de novo* assembly. Most of the transcripts and genes identified were expressed at very low levels and if these low-expression contigs (<10 TPM) are excluded from calculations, then 15,082 transcripts were assembled (Supp. Fig. 2). The quality of the assembled transcriptome was assessed in a variety of ways. The assembly had a N50 value of 361bp and a Ex90N50 value of 1855. The average contig length was 407 bp, however there were 79 transcripts that were longer than 10,000 bp and 30,843 transcripts longer than 1,000 bp. BUSCO score analysis showed that of the 2,586 BUSCO groups searched, 1,935 (74.8%) were found as complete sequences within the transcriptome (Table 2). Of these 1,935 groups, 1,202 (46.5%) were found as complete and single-copy while 733 (28.3%) were found as complete and duplicated. The total mapping coverage of aligned reads to the *de novo* transcriptome also served as an indication of assembly quality (a higher alignment suggests a better assembly). Approximately 27% of paired reads did not align concordantly (of which 18% aligned discordantly, and the remaining 9% never aligned), 16% aligned concordantly once, while 56% aligned more than once, with an overall alignment rate of 92.75% (Supp. Table 4).

Correlation between sample expression profiles using were also computed and suggested minimal correlation (Fig 5a). Furthermore, PCA showed that global expression patterns did not separate into distinct clusters based on sampling times (Fig. 5b).

### *Differential expression and annotation*

Analysis using edgeR revealed 1013 transcripts that underwent significant differential expression ( $P_{\text{adj}} < 0.05$  and  $\log_2\text{FC} > 1$ ). Only 179 genes were differentially expressed under matching parameters. A heatmap including each biological replicate shows within treatment variation is quite high (Fig 6). Therefore, the expression of biological replicates was averaged and centered on control values (Fig 7). This produced more distinct clusters of upregulated and downregulated transcripts. The heatmap highlights a general trend over time; most transcripts that were upregulated in the short term, stayed upregulated to later time points, and similarly, those downregulated in the early response remain downregulated. Of the 1013 transcripts, there were 240 that showed a reversal in the direction of change; undergoing upregulation at 12 hrs to downregulation at 48hrs, or *vice-versa*. Furthermore, 63 transcripts show expression values equal to control levels at 12hrs or 48hrs. At the gene level, similar trends exist in the expression pattern over time (Fig 6). Pearson correlation analysis and principal component analysis on the differentially expressed transcripts show similar patterns of expression and low variance within treatments (Fig 7). Only ~15% of all transcripts were annotated using Trinotate, however, ~60% of the differentially expressed transcripts were annotated. At the gene level, 45 out of 179 differentially expressed genes were annotated. A full listing of differentially expressed transcripts and genes can be found in Supplementary Material, but below I will review results with respect to specific physiological functions.

### *Transcripts involved in trans- and paracellular transport*

The significant role of the kidneys in osmoregulation suggests an osmotic stress would induce changes in the expression of a variety of transporters and tight junctions (NKA, urea transporter, members of the SLC family, aquaporins, claudins, etc) to regulate transcellular and paracellular ion/molecular flux. Transcripts and genes encoding proteins in the NKA complex showed no significant changes in expression over the exposure. Only a single NHE, SLC9A9, was upregulated after 12hrs, but returned to control levels after 48hrs. Other members of the

SLC family such as SLC6A18 (neutral amino acid transporter) SLC6A5 (glycine transporter), SLC22A2 (polyspecific organic cation transporter) were all upregulated after 12 hrs. Multiple transcripts encoding SLC25A10 (mitochondrial dicarboxylate carrier, DIC) was significantly upregulated and exhibited one of the high fold changes in the annotated transcripts. Interestingly only a single contig was annotated as CFTR, and showed no change in expression levels. NKCC transcripts were identified however expression remained constant throughout the exposure. Calcium ATPase Type 2C was also downregulated after 48hrs. Numerous aquaporins were detected in the transcriptome however none showed significant changes in expression. The urea transporter, UT-A1, was not detected, however, UT-A2 (mammalian UT-A2 is 66% amino acid homologous to shUT) was detected at low levels and showed no change in expression levels. No changes were present in transcript expression of the ammonia transporters Rhag, Rhbg, or Rhcg, although they were detected. A number of transporter transcripts were among the most highly altered following 65% SW exposure such as mitochondrial dicarboxylate transporter, thiamine transporter 2, cationic amino acid transporter 3, and mitochondrial calcium uptake 1 (Table 3, Table 4, Table 5).

Paracellular leakage is another route of possible osmolyte loss. Two transcript isoforms of claudin 10 were differentially expressed. Both showed a significant reduction, however one was reduced at 12hrs and one at 48hrs compared to control. No changes were seen in the expression of occludin transcripts. Tight junction protein 1 (ZO1) was significantly upregulated from 12hrs to 48hrs. No changes were seen in any transcripts encoding tight junction associated proteins (e.g. TJAPs, and CGNLs). Transcripts of the cell adhesion protein cadherin 1 (CADH1) and the desmosome adhesion protein desmocollin 3 (DSC3) were both downregulated after 48hrs. In conclusion, most transcripts related to tight junctions and paracellular leakage were either downregulated or unchanged.

#### *Protein chaperones, degradation and transport*

The highly conserved family of heat shock proteins (HSPs) act as molecular chaperones in a similar method to the chemical chaperones (i.e. TMAO) to reduce stress associated protein misfolding and promote correct protein maturation (Georgopoulos and Welch, 1993). This family has been implicated in the response of elasmobranchs to osmotic challenges (MacLellan et al., 2015; Morash et al., 2016). Transcripts within this family that were differentially

expressed were all upregulated following the salinity challenge, including HSP70, HSP71A, HSP71L, and HSP30.

Damaged proteins that cannot be rescued through the action of chaperones or proteins that are no longer needed must be degraded. This can occur through the ubiquitin-proteasome pathway or transport into lysosomes for hydrolysis. Transcripts within the ubiquitination-proteasome pathway were detected, however, only transcripts encoding E2 enzymes (UB2J1, UBE2T, UBE2C, UBC12) and E3 enzymes (UHRF1, RBBP6) were differentially expressed (both up and downregulated). A single subunit of the 20S proteasome (PSA7) was significantly downregulated, however, this may be of little consequence as there are a total of 28 subunits within this complex (Tanaka, 2009). Numerous lysosomal peptidases (including cathepsins, carboxypeptidases, dipeptidyl peptidase) were detected however none were differentially expressed following exposure.

An essential function within cells is the distribution of newly synthesized proteins in addition to the removal and recycling of mature proteins from the plasma membrane or organelles. An abundance of transcripts (e.g. RAB7, SNX4, SNX14, SNX6, VPS36) involved in protein transport were differentially expressed following exposure to 65% SW. The majority of these were downregulated, particularly those related to early-to-late endosome transport and endosome to lysosome.

#### *Metabolism and signal transduction*

Several transcripts of interest involved in metabolic processes were differentially expressed. Interestingly, sarcosine dehydrogenase (SARDH) was downregulated after both 12 and 48hrs, suggesting an accumulation of sarcosine. Transcripts for formimidoyltransferase-cyclodeaminase (FTCD), an enzyme involved in amino acid degradation, were also downregulated after both 12 and 48hrs. Inversely, another amino acid catabolizing enzyme, homogentistate 1,2-dioxygenase (HGD), was upregulated after both 12 and 48hrs. Multiple transcripts involved in oxidative phosphorylation (NADH dehydrogenase, cytochrome C oxidase, V-type ATPase, ubiquinol-cytochrome C reductase complex) were differentially expressed but showed no distinct pattern of co-expression.

Signal transduction is an essential component in eliciting a response to a stimulus, including salinity stress (Fiol and Kültz, 2007). Within the dogfish kidney, numerous MAP

kinases were identified, however only MAP2K5 and MAP3K15 were differentially expressed; the former was consistently upregulated and the latter was consistently downregulated. Nitric oxide synthase 2 (NOS2) produces NO, a potent signalling molecule, was upregulated after 12hrs. Transcripts encoding various targets in fish signalling cascades (including 14-3-3 proteins, c-Jun N-terminal kinases, osmotic response elements, TSC22D2, and TRPV4) were detected yet none showed significant changes in expression (Fiol et al., 2007; Kültz et al., 2001; Liedtke et al., 2000; Lopez-Bojorquez et al., 2007; Marshall, 2005; Wang and Kültz, 2017). Osmotic stress transcription factor 1 however was not detected.

### *Immune related function*

Salinity induced stress response is common in fish and many of the proteins involved in this response have immunological functions (Cuesta et al., 2005; Gu et al., 2018). Cytokines play an important role in propagating immune response. Multiple transcripts encoding the cytokine C-C motif chemokine ligand 20 (CCL20) were upregulated after 12 hrs. Importantly, interleukin 10 (IL10), an inhibitor of cytokine production, was downregulated after both 12 and 48hrs (de Waal Malefyt et al., 1991). Another major mediator in regulating cytokine production and stress responses is NF- $\kappa$ b complex. The coiled-coil domain containing protein 22 (CCD22) is an activator of the NF- $\kappa$ b complex and was downregulated after both 12hrs and 48hrs (Starokadomskyy et al., 2013). NF- $\kappa$ b was detected however no significant changes occurred. Expression of select cytokine receptors were also changed. Tumor necrosis factor receptor member 6b (TNF6B) was upregulated while inversely interleukin 17 receptor A (IL17RA) was significantly downregulated. A regulator in the signal transduction from the death receptors on the cell surface, Fas associated death domain (FADD), was down regulated after 48hrs (Kim, 2002). Transcripts for Bcl2 associated athanogene 4 (BAG4), a protein involved in suppressing activity of death receptors via interactions with HSPs, were upregulated after both 12hrs and 48hrs (Briknarová et al., 2002). In contrast to the general pattern of downregulation in cytokines and receptor transcripts, caspase 6 (CASP6), a promotor of apoptosis, was upregulated after both 12 and 48hrs (Riedl and Shi, 2004). Another pro-apoptotic protein, tumour protein P53 (P53) was upregulated after 12hrs and downregulated after 48hrs (Fridman and Lowe, 2003).

Importantly, prostaglandin-endoperoxide synthase 2 was upregulated after both 12 and 48hrs, which would correspond to an increase in prostaglandin H<sub>2</sub> from arachidonic acid. Prostaglandin H<sub>2</sub> is a precursor for a suite of hormonally active compounds, some of which have immunological functions (Ricciotti and FitzGerald, 2011). Arachidonic acids can also be converted into immunologically active leukotrienes via 5-lipoxygenase (LOX5), which catalyzes both the conversion of arachidonic acid into hydroperoxyeicosatetraenoic acid (HPETE) and HPETE into leukotriene A<sub>4</sub>, a pro-inflammatory mediator (Samuelsson, 1983). Transcripts for LOX5 were downregulated after 12hrs and upregulated after 48hrs.

### *Gene level expression*

The sum of transcript expression values within the Trinity gene was also used to quantify changes in expression (Supp. Table 2). The Trinotate annotation pipeline does not provide annotations at the gene level and therefore annotations for this level were based on the consensus of transcript level annotations. The changes that were observed at the gene level show similarity to the transcript level. Of note, HSP71A and HSP30C were both consistently upregulated at the gene level. Multiple immunological genes were also altered included interferon induced protein 44-like (IF44L), immune-response gene 1 (IRG1), NLR family pyrin domain containing 3 (NALP3), and C-C motif chemokine ligand 20 (CCL20).

### *GO enrichment and KEGG pathways*

The Goseq package was used to quantify the enrichment of GO terms (biological processes, molecular functions, and cellular components) in the differentially expressed transcripts in each time point comparison, while REVIGO software was used reduce redundancy, cluster, and visualize these GO terms. One possible way to examine and interpret the Goseq results is to rank the enriched GO terms based on terms that contain the most differentially expressed transcripts (Table 6). The top terms enriched in 0hrs vs 12hrs were “extracellular region part”, “regulation of biological quality”, and “cellular response to stimulus”. The three most common terms in 0hrs vs 48hrs were “positive regulation of biological process”, “integral component of the membrane”, and “intrinsic component of the membrane”. Interestingly, the most common enriched terms from 12hrs to 48hrs were “localization”, “establishment of localization”, and “transport”. Most of these terms are extremely broad and therefore by default

will likely be more common. Additionally, in some cases they may be too broad to provide useful conclusions. Therefore, ranking the enriched terms based on P-value is another possible method to draw conclusions (Table 7). Compared to control, 12hrs in low salinity cause chaperone related GO terms to be most enriched based on P-value. Again, compared to control, 48hrs elicited “ribosome assembly” and “hormone activity”. Interestingly, from 12hr to 48hrs GO terms related to bacterial infections such as “cellular response to molecule of bacterial origin” and “cellular response to lipopolysaccharide” were strongly enriched.

REVIGO software was used to reduce redundancy and visualize clustered GO terms based on similarity of terms. A multitude of generalized functional groups were identified and of these, a select few were consistently enriched in each comparison (Fig. 10a, b, c). These consistent functional groups were “regulatory processes”, “signalling pathways”, and “response to stimulus or stress”. The cluster “cell differentiation and maturation” was only present comparing 0hrs with 48hrs. Other semi common clusters were “ion, molecular, and protein transport”, “protein and molecular complexes”, and “metabolic processes”.

There were no significantly enriched KEGG pathways, however, multiple pathways contained numerous transcripts that were differentially expressed. These include RNA transport, endocytosis, spliceosome, glycerophospholipid metabolism, general metabolism (Fig. 11-15). Of note, numerous transcripts within the endocytosis pathway functioning in the early-to-late endosome phase were differentially expressed (Fig. 11). Transcripts within the general metabolic pathways were sporadic and not limited to a single metabolic process (Fig. 14). Within the glycerophospholipid metabolism KEGG pathway, transcripts related to production of phosphatidylethanolamine and phosphoethanolamine (e.g. PISD, EPT1, PTSS2, EKI1) were variable in response, however, expression patterns indicate a reduction in phosphatidylethanolamines.

**Table 1.** Descriptive statistics of the filtered de novo kidney transcriptome produced by the Trinity pipeline

Statistics were calculated using online software gVolante online software and Trinity scripts (TrinityStats.pl and contig\_ExN50\_statistic.pl). Filtering of transcripts was performed using Trinity script filter\_low\_expr\_transcripts.pl with a minimum expression level of 1 TPM.

<b>Descriptive statistic</b>	<b>Value</b>
Total transcripts	479,976
Total genes	361,284
Total nucleotide	195,303,735
Longest sequence (nt)	26092
Shortest sequence (nt)	201
Average contig length	407
Median length	238
# of transcripts > 1k	30,843
# of transcripts > 10k	79
N50 value (nt)	361
Ex90N50 value (nt)	1,855
GC content (%)	45.39

**Table 2.** BUSCO scores of the *de novo* kidney transcriptome.

BUSCO scores were calculated using online software gVolante with the Vertebrata reference gene set. A higher percent of complete BUSCO's suggests a more complete transcriptome.

<b>Category</b>	<b>Percent</b>
Complete BUSCOs	74.8%
Complete and single copy	46.5%
Complete and duplicated copy	28.3%
Partial BUSCOs	8.2%
Missing BUSCO	17.0%

**Table 3.** Differentially expressed transcripts with the greatest fold change from control to 12 hrs in 65% SW.

Trinotate software was used to annotate the *de novo* assembly of the kidney transcriptome and edgeR was used to calculate differentially expressed transcripts. Fold change expression values are compared to control samples. P-values were adjusted for multiple comparisons using Benajmini-Hochberg correction.

<b>Trinity ID</b>	<b>Protein annotation</b>	<b>log<sub>2</sub>FC</b>	<b>P<sub>adj</sub> value</b>
TRINITY_DN180862_c3_g1_i21	Chaperon containing TCP1 subunit 2	12.35	2.73E-15
TRINITY_DN210149_c0_g2_i20	Dicarboxylate transporter	11.90	1.01E-10
TRINITY_DN196335_c1_g1_i12	Mitochondrial calcium uptake 1	11.62	2.01E-11
TRINITY_DN210149_c0_g2_i4	Dicarboxylate transporter	11.48	2.48E-21
TRINITY_DN208164_c8_g1_i16	Eukaryotic translation initiation factor 6	11.33	2.19E-07
TRINITY_DN200423_c2_g1_i9	Triosephosphate isomerase	11.27	3.05E-06
TRINITY_DN185152_c7_g1_i5	Plasmolipin	11.06	2.38E-05
TRINITY_DN194352_c0_g1_i3	Nucleoside disphosphate kinase C	10.95	6.31E-10
TRINITY_DN198669_c2_g1_i14	Pyrimidine nucleotide carrier	10.73	5.07E-05
TRINITY_DN177301_c1_g2_i7	Hexamethylene bisacetamide inducible 1	10.73	9.89E-14
TRINITY_DN200898_c1_g1_i4	SEC14 like lipid binding protein 1	-10.72	1.73E-02
TRINITY_DN180862_c3_g1_i19	Chaperon containing TCP1 subunit 2	-11.06	1.30E-02
TRINITY_DN193809_c1_g2_i10	Ubiquinol cytochrome C reductase complex assembly factor 3	-11.09	1.37E-02
TRINITY_DN190775_c2_g3_i6	Citrate synthase	-11.12	9.31E-04
TRINITY_DN212659_c3_g3_i2	Proteasome subunit alpha 7	-11.38	1.45E-04
TRINITY_DN208373_c1_g4_i7	Arginine methyltransferase 5	-11.44	7.85E-07
TRINITY_DN191009_c0_g8_i5	Mitochondrial ribosomal protein L9	-12.00	1.48E-07
TRINITY_DN203597_c4_g2_i1	Calcium binding protein	-12.51	3.20E-04
TRINITY_DN209298_c7_g1_i9	D-glutamate cyclase	-12.82	1.09E-02
TRINITY_DN211819_c6_g2_i5	Eukaryotic translation initiation factor 5A	-13.40	9.55E-03

**Table 4.** Differentially expressed transcripts with the greatest fold change from control to 48 hrs in 65% SW.

Trinotate software was used to annotate the *de novo* assembly of the kidney transcriptome and edgeR was used to calculate differentially expressed transcripts. Fold change expression values are compared to control samples. P-values were adjusted for multiple comparisons using Benajmin-Hochberg correction.

<b>Trinity ID</b>	<b>Protein Annotation</b>	<b>log<sub>2</sub>FC</b>	<b>P<sub>adj</sub> value</b>
TRINITY_DN185653_c1_g1_i15	Coatomer protein complex delta subunit	11.67	2.34E-04
TRINITY_DN210149_c0_g2_i20	Dicarboxylate transporter	11.56	3.62E-04
TRINITY_DN180862_c3_g1_i21	Chaperon containing TCP1 subunit 2	11.52	3.83E-03
TRINITY_DN209642_c7_g1_i8	Cytochrome C oxidase subunit 5a	11.48	8.94E-03
TRINITY_DN211526_c9_g1_i13	Homogentisate 1,2-Dioxygenase	11.43	4.23E-03
TRINITY_DN204320_c4_g1_i7	Osteoclast-stimulating factor 1	11.36	7.83E-04
TRINITY_DN191624_c11_g1_i1	Secretogranin B	11.33	3.38E-03
TRINITY_DN210258_c5_g3_i3	Forkhead Box K1	10.82	1.91E-02
TRINITY_DN186925_c3_g1_i11	BRCA2 and CDKN1A interacting protein	10.68	1.63E-02
TRINITY_DN196335_c1_g1_i12	Mitochondrial calcium uptake 1	10.61	8.24E-03
TRINITY_DN208735_c2_g1_i1	ATPase secretory pathway Ca <sup>2+</sup> Transporting 1	-10.71	7.24E-05
TRINITY_DN207838_c1_g2_i1	Family with sequence similarity 210 member B	-10.78	2.39E-02
TRINITY_DN204054_c2_g1_i11	Thiamine transporter 2	-10.80	6.06E-05
TRINITY_DN207619_c2_g1_i4	Eukaryotic translation initiation factor 2	-10.83	1.57E-03
TRINITY_DN193809_c1_g2_i10	Ubiquinol cytochrome C reductase complex assembly factor 3	-10.84	1.92E-02
TRINITY_DN208809_c1_g1_i9	DEAD-box helicase 18	-10.96	1.33E-03
TRINITY_DN206991_c0_g1_i9	Ring finger protein 10	-11.10	8.51E-03
TRINITY_DN175437_c8_g3_i10	Kruppel like factor 13	-11.50	5.44E-05
TRINITY_DN204676_c3_g2_i2	MAL proteolipid protein 2	-11.53	6.46E-04
TRINITY_DN209298_c7_g1_i9	D-glutamate cyclase	-12.57	1.60E-02

**Table 5.** Differentially expressed transcripts with the greatest fold change from 12hrs to 48hrs in 65% SW.

Trinotate software was used to annotate the *de novo* assembly of the kidney transcriptome and edgeR was used to calculate differentially expressed transcripts. Fold change expression values are compared to 12hr samples. P-values were adjusted for multiple comparisons using Benajmin-Hochberg correction.

<b>Trinity ID</b>	<b>Protein Annotation</b>	<b>Log<sub>2</sub>FC</b>	<b>P<sub>adj</sub> value</b>
TRINITY_DN191624_c11_g1_i2	Secretogranin B	13.08	1.07E-03
TRINITY_DN211927_c2_g1_i9	Integrin subunit beta 2	12.54	9.72E-20
TRINITY_DN198092_c12_g1_i1	Transmembrane P24 trafficking protein 2	12.07	3.71E-04
TRINITY_DN212085_c0_g1_i7	Calcium and integrin binding 1	11.58	3.98E-04
TRINITY_DN180862_c3_g1_i19	Chaperon containing TCP1 subunit 2	11.54	1.08E-02
TRINITY_DN209642_c7_g1_i8	Cytochrome C oxidase subunit 5A	11.40	9.30E-03
TRINITY_DN200898_c1_g1_i4	SEC14 like lipid binding protein 1	11.39	9.90E-03
TRINITY_DN212233_c1_g1_i3	Potassium channel tetramerization domain containing 10	11.03	6.90E-03
TRINITY_DN205377_c3_g2_i19	GTP binding protein 2	10.86	3.19E-15
TRINITY_DN212659_c3_g3_i2	Proteasome subunit alpha 7	10.79	1.00E-02
TRINITY_DN204054_c2_g1_i11	Thiamine transporter 2	-10.19	3.21E-03
TRINITY_DN211557_c0_g1_i32	Aldehyde oxidase 1	-10.22	9.36E-05
TRINITY_DN205218_c1_g2_i6	MYB binding protein 1A	-10.24	1.48E-02
TRINITY_DN194776_c2_g2_i4	Sjogren syndrome antigen B	-10.24	8.28E-05
TRINITY_DN198669_c2_g1_i14	Pyrimidine nucleotide carrier	-10.39	2.17E-02
TRINITY_DN212850_c8_g1_i1	Complement C6	-10.52	2.11E-02
TRINITY_DN207619_c2_g1_i4	Eukaryotic translation initiation factor subunit alpha	-10.54	2.62E-03
TRINITY_DN176676_c3_g1_i11	TBC1 domain family member 10A	-10.56	1.98E-02
TRINITY_DN204108_c2_g3_i10	Cationic amino acid transporter 3	-10.67	3.47E-04
TRINITY_DN211062_c4_g1_i8	Cadherin 3	-11.48	2.87E-05

**Table 6.** Top 10 enriched GO terms in based on number of differentially expressed transcripts associated with each term.

Trinotate was used to extract GO terms for each transcript and Goseq was used to perform functional enrichment tests for each transcript. CC represents cellular component and BP represents biological process.

<b>Comparison</b>	<b>GO Term</b>	<b>Ontology</b>	<b>No. of transcripts</b>	<b>P-Value</b>
0hrs vs 48hrs	positive regulation of biological process	BP	77	1.99E-03
0hrs vs 48hrs	integral component of membrane	CC	68	3.63E-02
0hrs vs 48hrs	intrinsic component of membrane	CC	68	4.79E-02
0hrs vs 48hrs	positive regulation of cellular process	BP	67	3.53E-03
0hrs vs 48hrs	response to stimulus	BP	61	1.86E-02
0hrs vs 48hrs	negative regulation of biological process	BP	60	4.12E-02
12hrs vs 48hrs	localization	BP	58	3.34E-02
0hrs vs 48hrs	negative regulation of cellular process	BP	57	3.30E-02
0hrs vs 12hrs	extracellular region part	CC	56	3.25E-02
0hrs vs 48hrs	establishment of localization	BP	55	2.30E-02

**Table 7.** Top 10 enriched GO terms associated with the differentially expressed transcripts based on lowest P-value of the term.

Trinotate was used to extract GO terms for each transcript and Goseq was used to perform functional enrichment tests for each transcript. CC represents cellular component, MF represents molecular function, and BP represents biological process.

<b>Comparison</b>	<b>GO Term</b>	<b>Ontology</b>	<b>No. of transcripts</b>	<b>P-Value</b>
0hrs vs 12hrs	zona pellucida receptor complex	CC	5	1.35E-06
0hrs vs 48hrs	ribosome assembly	BP	5	1.11E-05
0hrs vs 12hrs	chaperone-mediated protein complex assembly	BP	4	1.28E-05
12hrs vs 48hrs	cellular response to biotic stimulus	BP	8	2.03E-05
12hrs vs 48hrs	cellular response to lipopolysaccharide	BP	7	2.07E-05
0hrs vs 12hrs	chaperonin-containing T-complex	CC	4	2.13E-05
12hrs vs 48hrs	cellular response to molecule of bacterial origin	BP	7	2.24E-05
12hrs vs 48hrs	hormone activity	MF	4	2.56E-05
0hrs vs 12hrs	binding of sperm to zona pellucida	BP	5	4.06E-05
0hrs vs 48hrs	hormone activity	MF	4	4.22E-05

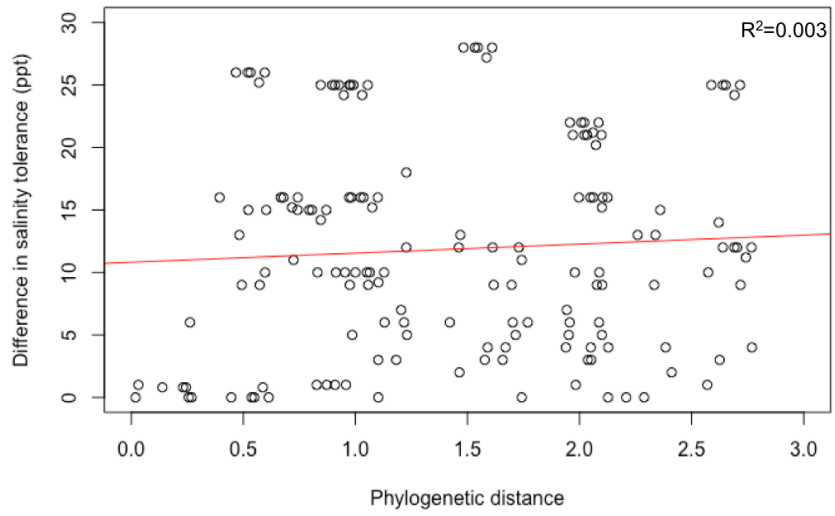
**Figure 1.** Dendrogram of salinity tolerant selachimorphs and the lowest salinities experienced in a natural and laboratory setting.

The literature was searched for selachimorphs that were caught in BW or FW and a dendrogram was adapted from Ballantyne and Fraser (2012) and Naylor et al. (2012) to visualize the evolutionary relationships between these animals. Colours at the dendrogram terminals separate species by order. N.d. indicates no data.

Species name	Environment exposure (ppt)	Laboratory exposure (ppt)	Reference
Negaprion brevirostris	26	n.d	Morrissey and Gruber (1993)
Glyphis fowlerae	n.d	n.d	Martin (2005)
Glyphis gangeticus	nd	n.d	Martin (2005)
Glyphis glyphis	0	n.d	Lyon et al. (2017)
Glyphis garricki	n.d	n.d	Martin (2005)
Carcharhinus leucas	0	0	Pillans and Franklin (2004)
Carcharhinus limbatus	16	n.d	Froeschke, Stunz, and Wildhaber (2010)
Sphyrna tiburo	15	25	Mandrup-Poulsen (1981), Ubeda and Simpfendorfer (2008)
Triakis scyllium	n.d	10	Yamaguchi et al. (2009)
Triakis semifasciata	n.d	16	Dowd et al. (2010)
Mustelus antarcticus	n.d	25	Morash et al. (2016)
Galeorhinus galeus	n.d	25	Morash et al. (2016)
Scyliorhinus canicula	n.d	28	Anderson, Takei, and Hazon (2002)
Chiloscyllium punctatum	25	25	Cramp, Hansen, and Franklin (2015)
Chiloscyllium plagiosum	n.d	12	Wong and Chan (1977)
Heterodontus portusjacksoni	n.d	16	Cooper and Morris (1998)
Squalus suckleyi	21	21	MacMillan (1999), Guffey and Goss (2014)
Squalus acanthias	21	22	MacMillan (1999), MacLellan et al. (2015)

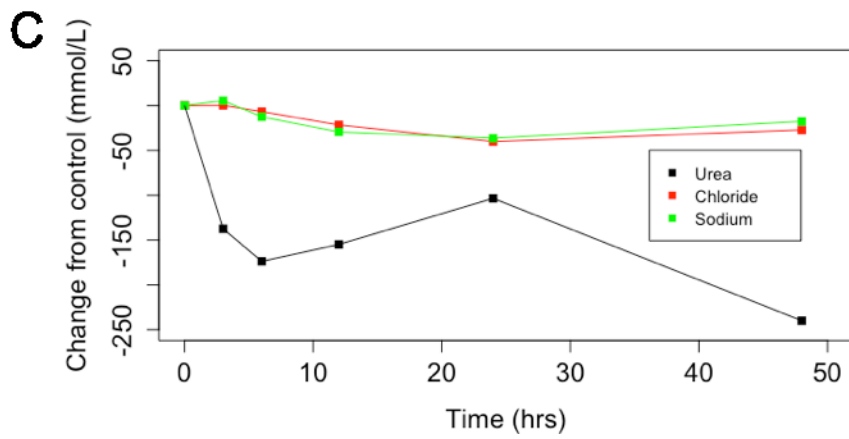
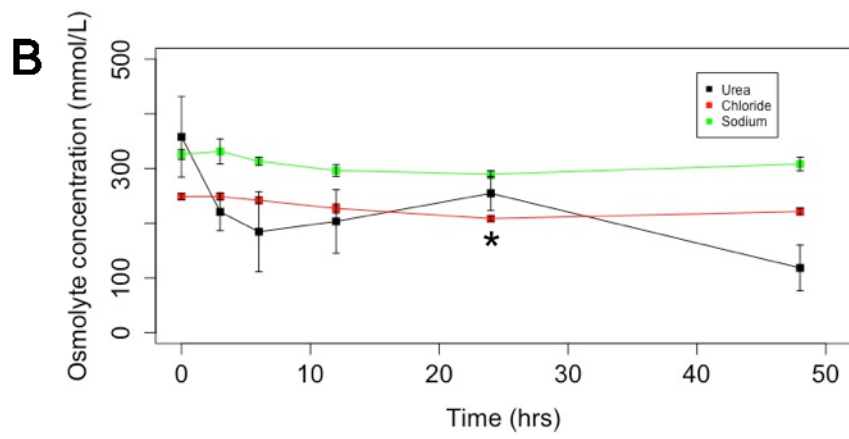
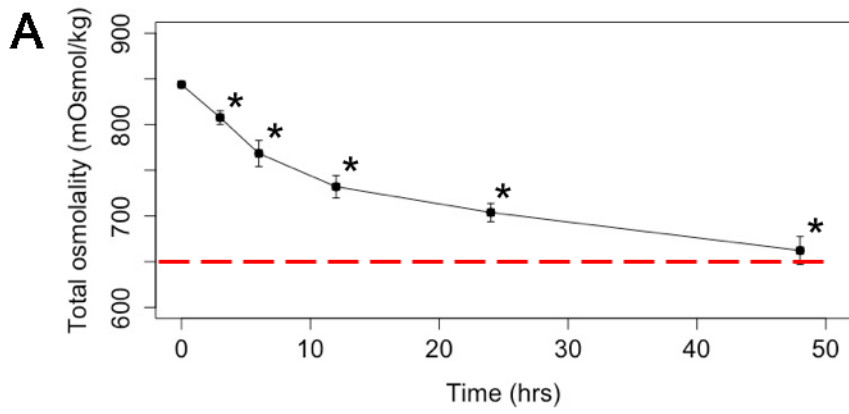
**Figure 2.** Correlational analysis of pairwise phylogenetic distance and pairwise difference in salinity tolerance.

The pairwise phylogenetic distance between each species in Figure 1 was quantified using the phylogeny in Naylor et al. (2012) plotted against to the pairwise difference in the lowest salinity (environmental or salinity) from Figure 1. Each dot represents a different species comparison. The red line indicates the linear regression.  $R^2 = 0.003$ .



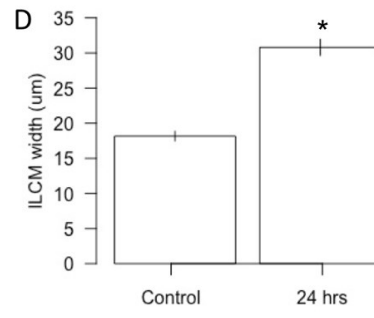
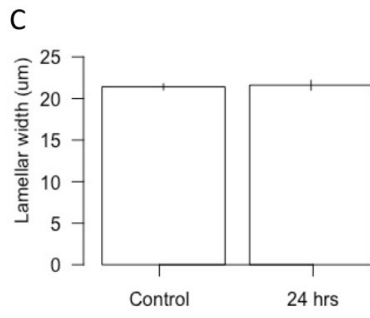
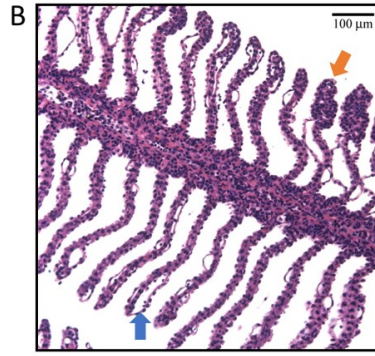
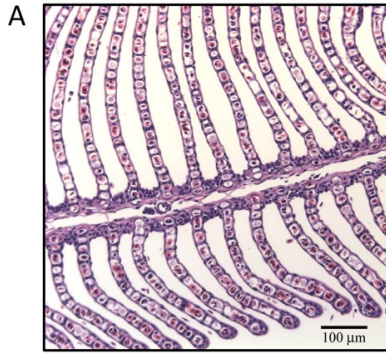
**Figure 3.** Plasma osmolality and osmolytes over 48hrs in 65% SW.

Time course (hrs) of the total osmolality ( $\text{mOsm kg}^{-1}$ )(A), osmolyte concentration ( $\text{mmol L}^{-1}$ )(B), and osmolyte change from control ( $\text{mmol L}^{-1}$ )(C) of the plasma in Pacific spiny dogfish following exposure to 65% SW ( $n \geq 3$ ). Values are presented as means  $\pm$  SEM. Significant differences from control (0hrs) are represented by \* ( $P < 0.05$ ) based on a ANOVA and Tukey's post-hoc test. The red dashed line (A) indicates the environmental salinity.



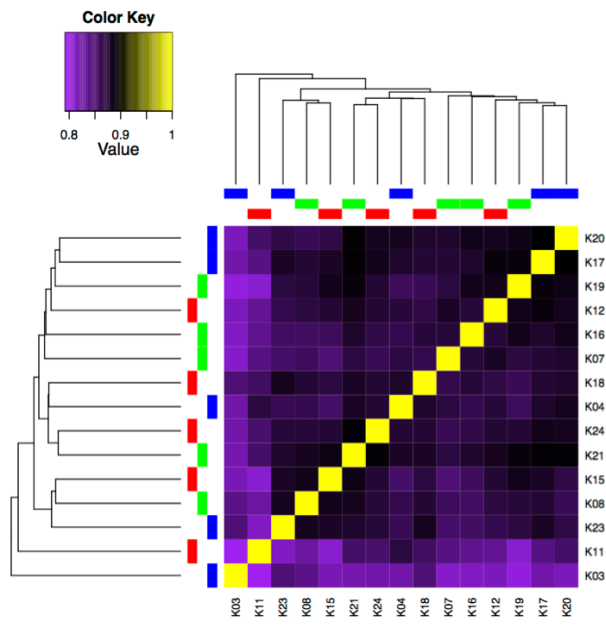
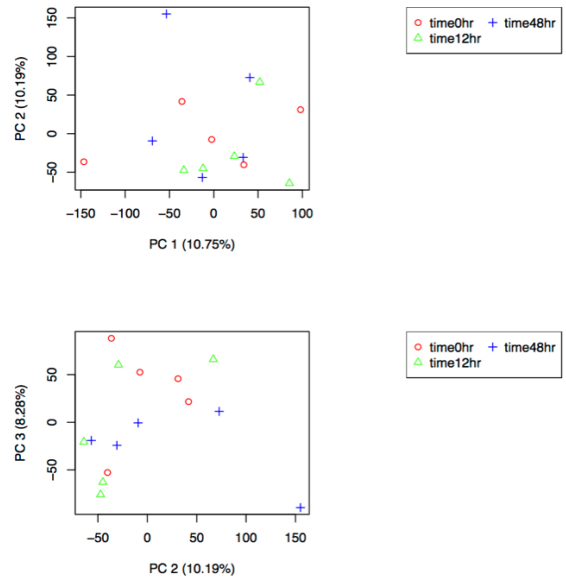
**Figure 4.** Alterations in gill morphology following 24hrs in 65% SW.

Representative light microscopy images with H&E staining of gills from Pacific spiny dogfish in control (A) and 24hrs in 65% SW (B). Morphological measurements of the gills were taken to quantify lamellar width (C) and interlamellar cell mass (D) (n=3). Values are presented as means±SEM. The orange arrow indicates an example of lamellar clubbing, while the blue arrow indicates epithelial lifting. Significant differences from control (0 hr) are represented by \* (P<0.05) and were calculated by unpaired Students t-test.



**Figure 5.** Correlation and variance within whole kidney transcriptome

A Pearson correlation analysis (A) was performed comparing the transcript expression ( $\log_2$  CPM) across all samples where purple indicates lower levels of correlation and yellow indicates high levels. The dendrogram in the margin depicts clustering based on similarity in expression. Time points are indicated by the colours in the margin; control (0hrs) = red, 12hrs = green, and 48hrs = blue. Rows and columns are both biological replicates. A principal component analysis (B) was computed from the  $\log_2$  CPM expression values of transcripts. Shown are PC1 vs PC2 (upper) and PC2 vs PC3 (lower).

**A****B**

**Figure 6.** Differentially expressed transcripts from all biological replicates.

Heatmap of 1013 differentially expressed transcripts (cutoff  $P_{adj} < 0.05$  and  $\text{Log}_2\text{FC} > 1$ ) from kidney tissue in control (0hrs), 12hrs in 65% SW, and 48hrs in 65% SW. Each row indicates a differentially expressed transcripts and each column is an individual animal. Legend indicates the  $\log_2$ , median-centered expression (TMM-normalized TPM) values where yellow indicates upregulation and blue indicates downregulation. Columns under the red bar indicate control (0hrs) samples, while columns under the green bar and blue bar are after 12hrs and 48hrs in 65% SW, respectively.

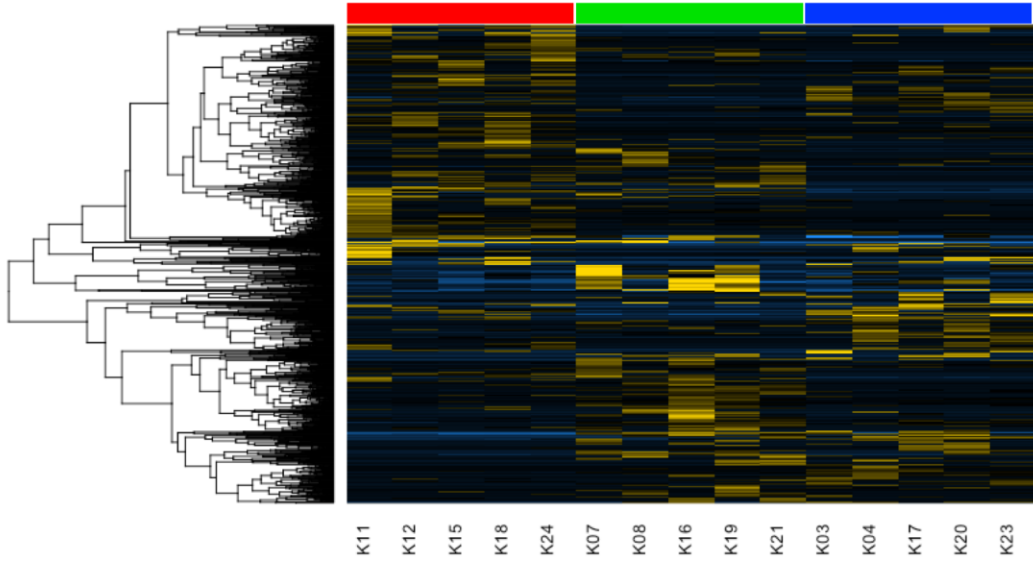
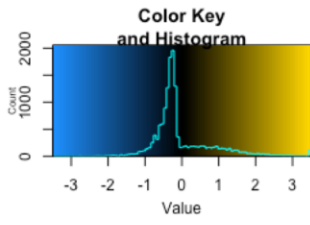


**Figure 7.** Differentially expressed transcripts of averaged values across time points. Heatmap of 1013 differentially expressed transcripts (cutoff  $P_{adj} < 0.05$  and  $\text{Log}_2\text{FC} > 1$ ) in control, 12hrs, and 48hrs in 65% SW. Each rows indicates a differentially expressed transcript and each columns is a different time point. The legend indicates the average  $\log_2$  expression (TMM-normalized TPM) centered on control expression levels (n=5). Colour corresponds to expression levels; blue indicates lower than control while yellow indicates higher than control. The dendrogram in the margin represents the clustering of different transcripts based on similarity in expression patterns.

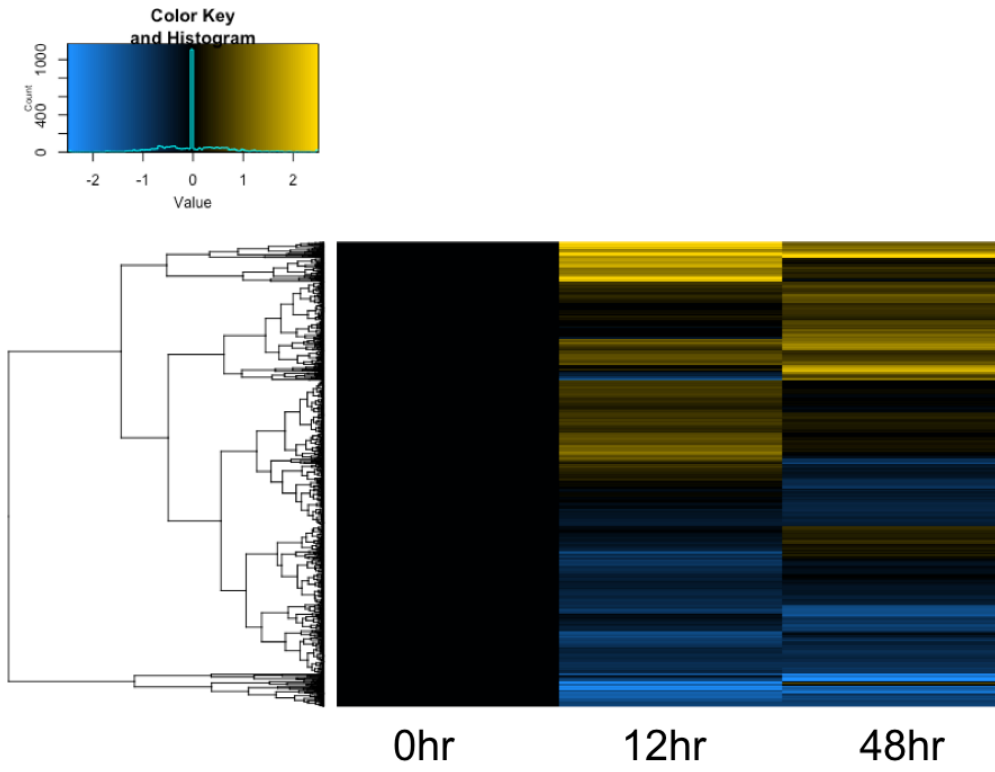


**Figure 8.** Differentially expressed genes following exposure to 65% SW

Heatmap of 179 differentially expressed genes in kidney tissue from animals exposed to 65%SW for 0hr (control), 12hrs, and 48hrs. Each rows indicates a differentially expressed gene and each columns is a different time point. The legend indicates the average  $\log_2$  expression value (TMM-normalized TPM) centered on control expression levels (n=5). Colour corresponds to expression levels; blue indicates lower than control while yellow indicates higher than control. The dendrogram in the margin represents the clustering of different transcripts based on similarity in expression patterns.

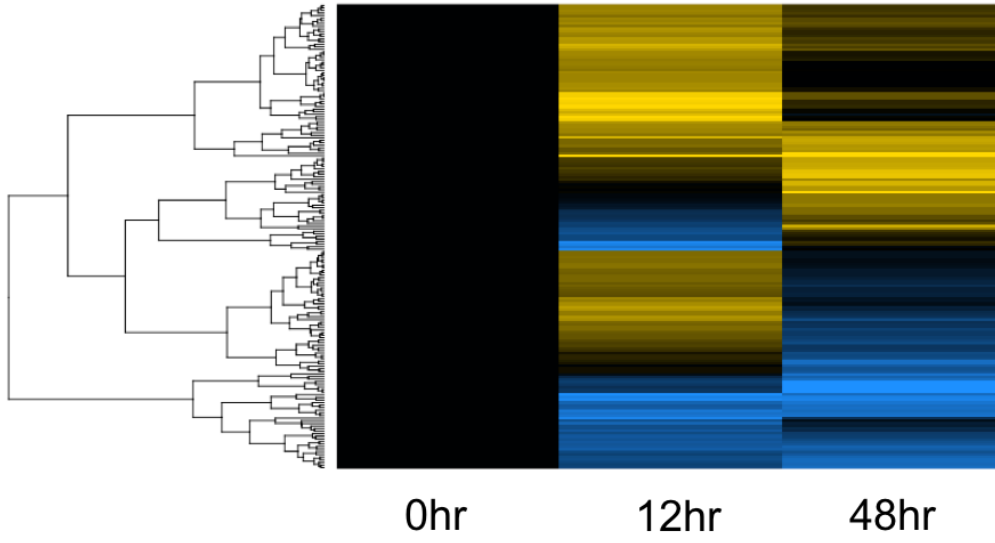
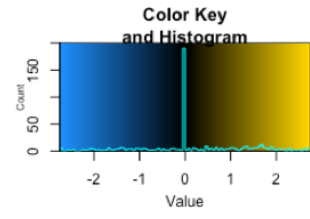


**Figure 9.** Correlation and variance within the differentially expressed transcripts

A Pearson correlation analysis (A) was performed comparing the expression of the salinity responsive transcripts ( $\log_2$  CPM) across samples where green indicates lower levels of correlation and red indicates high levels. The dendrogram in the margin depicts clustering based on similarity in expression. Time points are indicated by the colours in the margin; control (0hrs) = red, 12hrs = green, and 48hrs = blue. Rows and columns are both biological replicates. A principal component analysis (B) was computed from the  $\log_2$  CPM expression values of differentially expressed transcripts. Shown are PC1 vs PC2 (upper) and PC2 vs PC3 (lower).

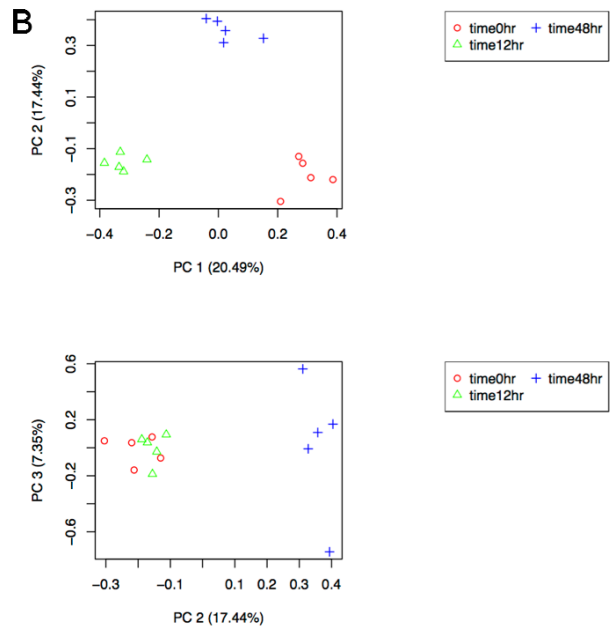
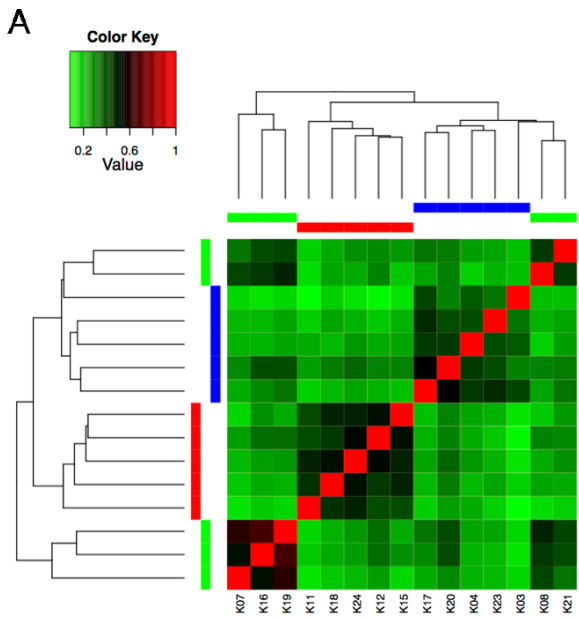
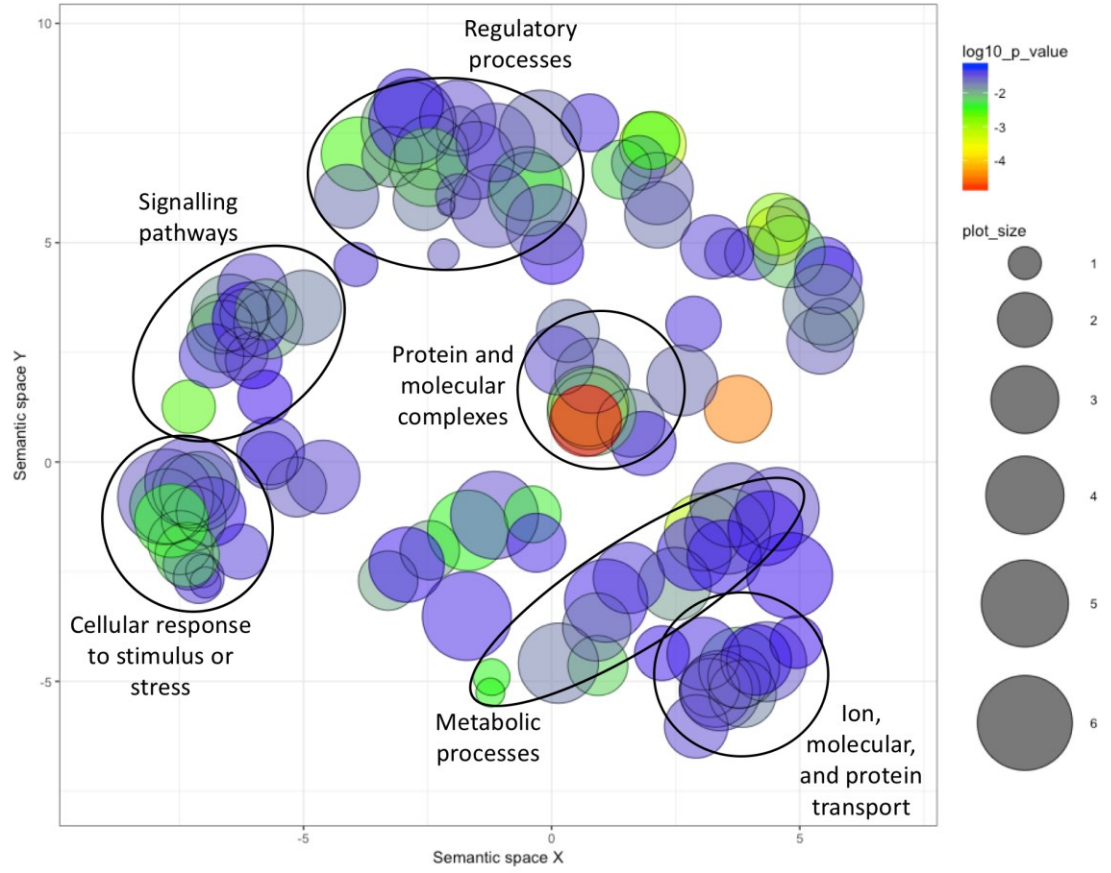


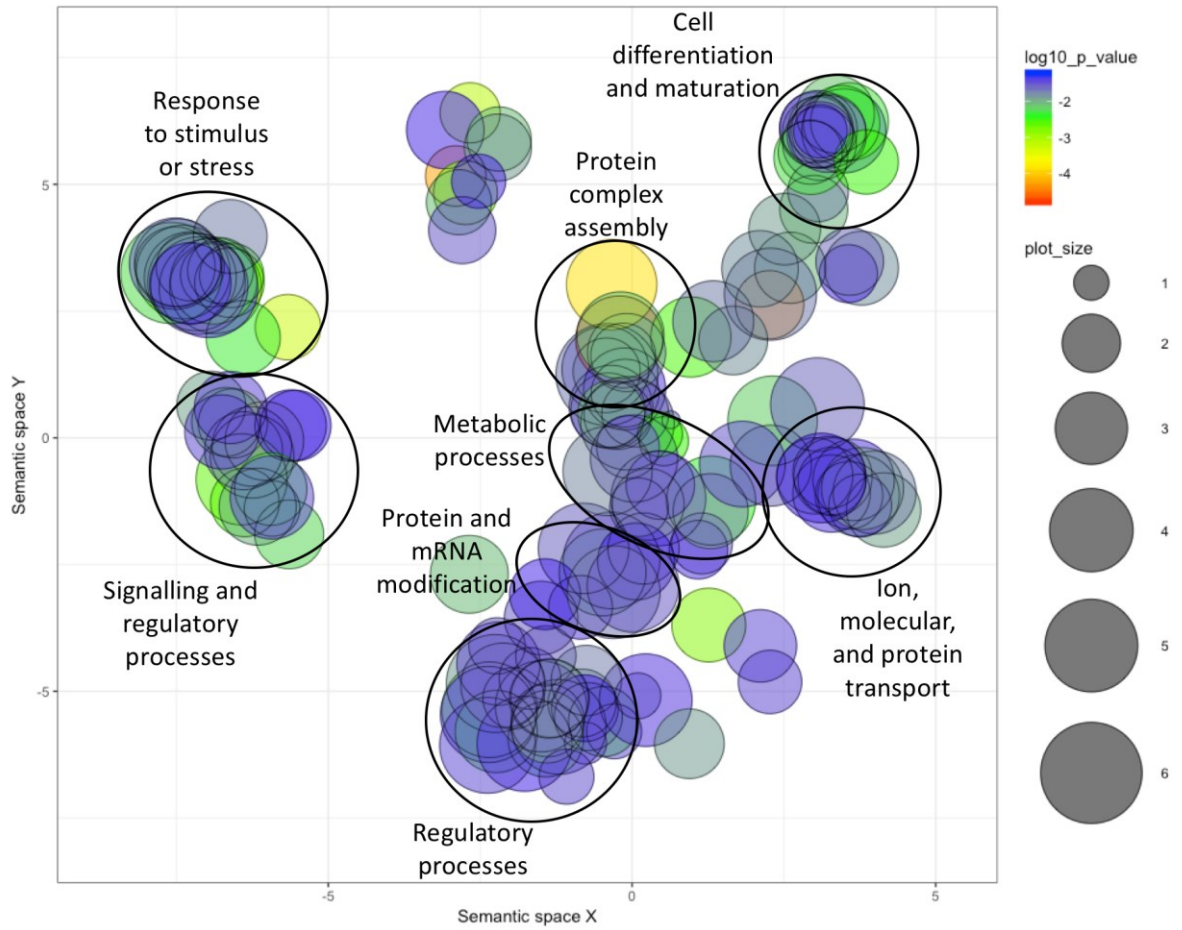
**Figure 10.** REVIGO analysis and clustering of significantly enriched GO terms

REVIGO software reduced redundancy in GO terms by collapsing similar terms, in addition to clustering and visualizing these collapsed terms in each statistical comparison, (A) 0hrs vs 12hrs, (B) 0hrs vs 48hrs, and (C) 12hrs vs 48hrs. Customized labels were added post REVIGO analysis. Individual bubbles indicate collapsed GO terms associated with the differentially expressed transcripts. Bubble colour indicates the P-value of enrichment. Bubble size indicates the frequency of the GO term in the reference data base (broader terms are larger). Each rows indicates a differentially expressed transcript and each columns is a different time point. The legend indicates the average  $\log_2$  expression (TMM-normalized TPM) centered on control expression levels (n=5). Colour corresponds to expression levels; blue indicates lower than control while yellow indicates higher than control. The dendrogram in the margin represents the clustering of different transcripts based on similarity in expression patterns.

A



B



C

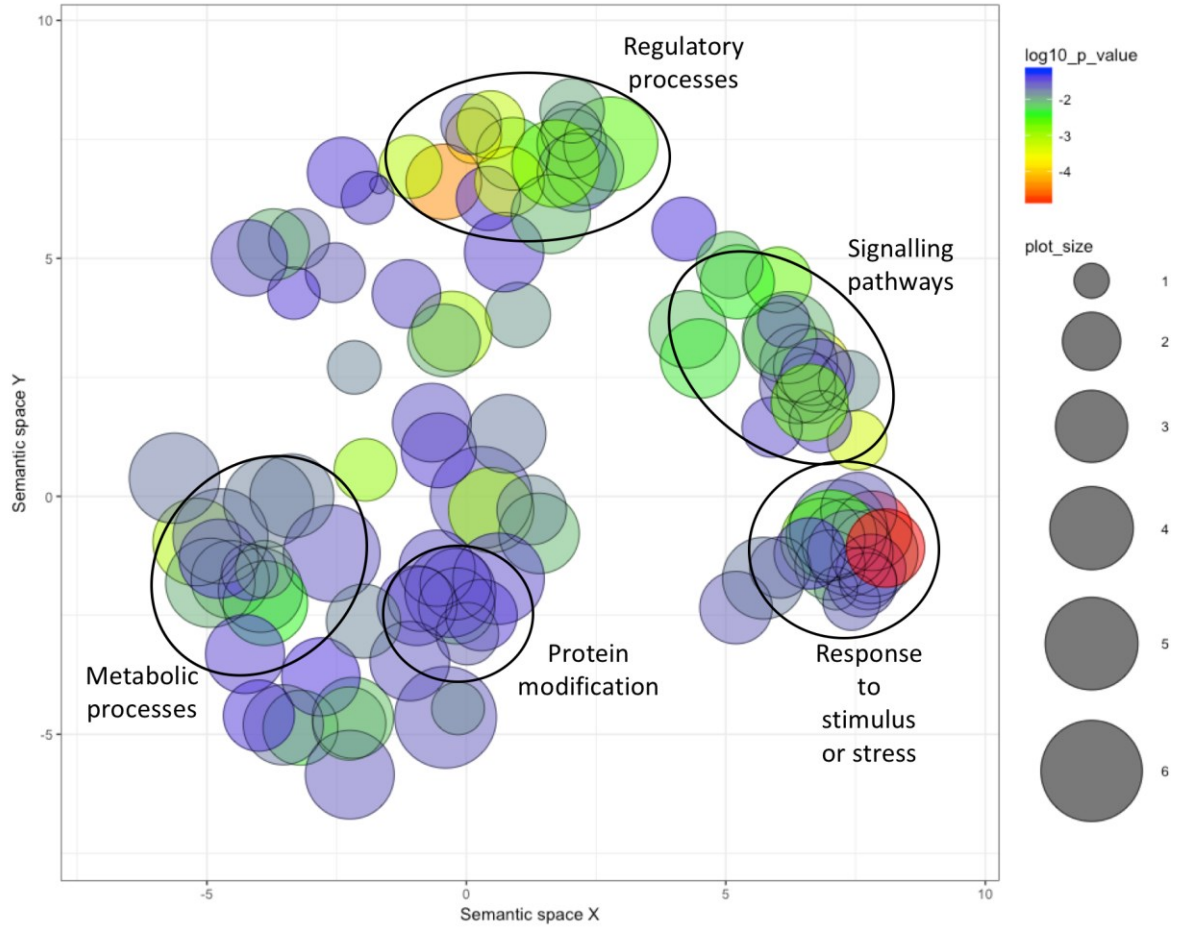


**Figure 11.** Differentially expressed transcripts present in the endocytosis KEGG pathway.

Protein annotations were submitted to DAVID online software to examine the enrichment in KEGG pathways. A heatmap generated using the gplot package in R was used to demonstrate the expression profile of the transcripts involved in the endocytosis pathway. Differentially expressed transcripts are indicated by red boxes on the KEGG pathway.



**Figure 12.** Differentially expressed transcripts present in the spliceosome KEGG pathway. Protein annotations were submitted to DAVID online software to examine the enrichment in KEGG pathways. A heatmap generated using the gplot package in R was used to demonstrate the expression profile of the transcripts involved in the endocytosis pathway. Differentially expressed transcripts are indicated by red boxes on the KEGG pathway.

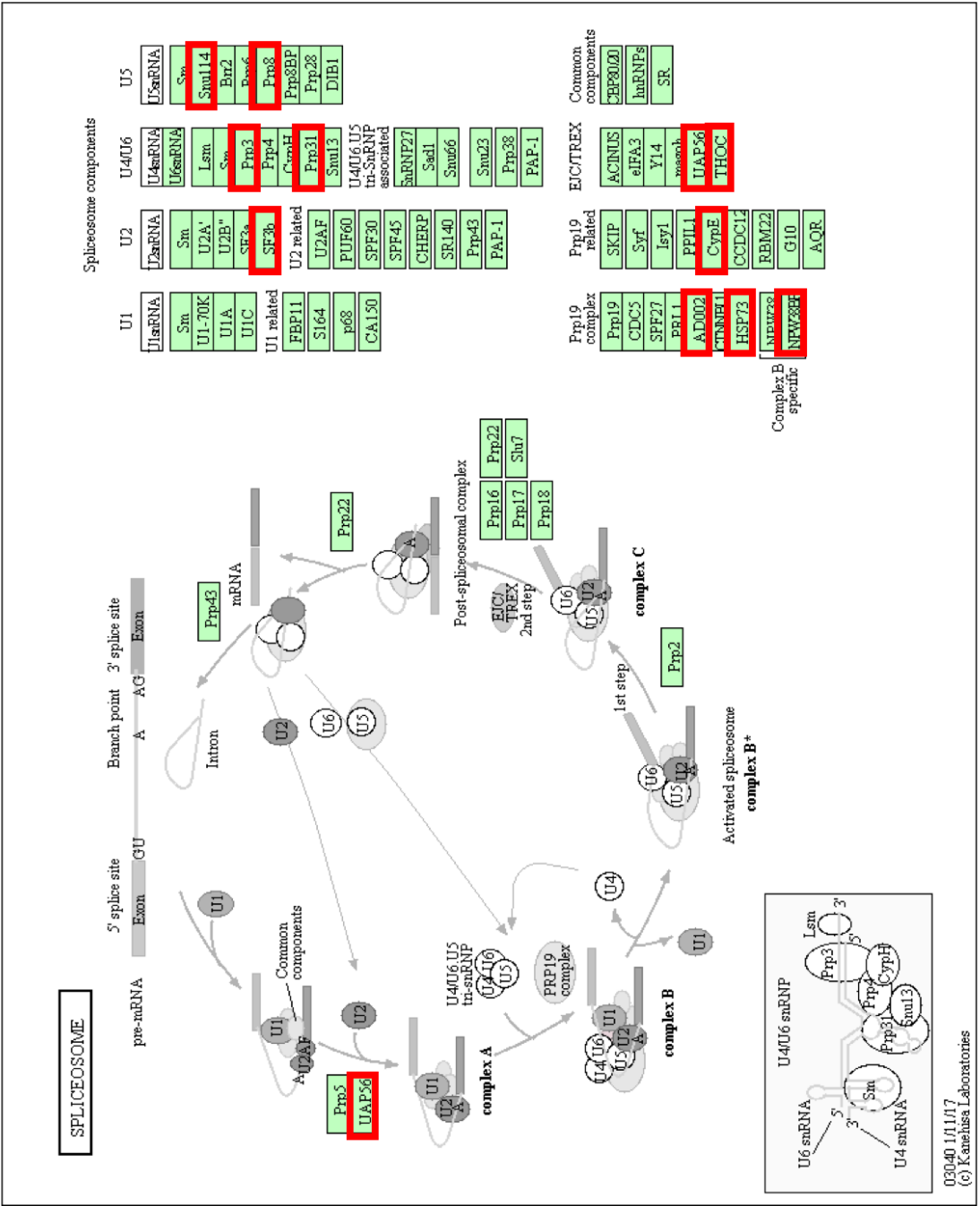


**Figure 13.** Differentially expressed transcripts present in the RNA transport KEGG pathway. Protein annotations were submitted to DAVID online software to examine the enrichment in KEGG pathways. A heatmap generated using the gplot package in R was used to demonstrate the expression profile of the transcripts involved in the endocytosis pathway. Differentially expressed transcripts are indicated by red boxes on the KEGG pathway.



**Figure 14.** Differentially expressed transcripts present in the general metabolism KEGG pathway.

Protein annotations were submitted to DAVID online software to examine the enrichment in KEGG pathways (A). A heatmap (B) generated using the gplot package in R was used to demonstrate the expression profile of the transcripts involved in the endocytosis pathway. Differentially expressed transcripts are indicated by red boxes on the KEGG pathway.



B.

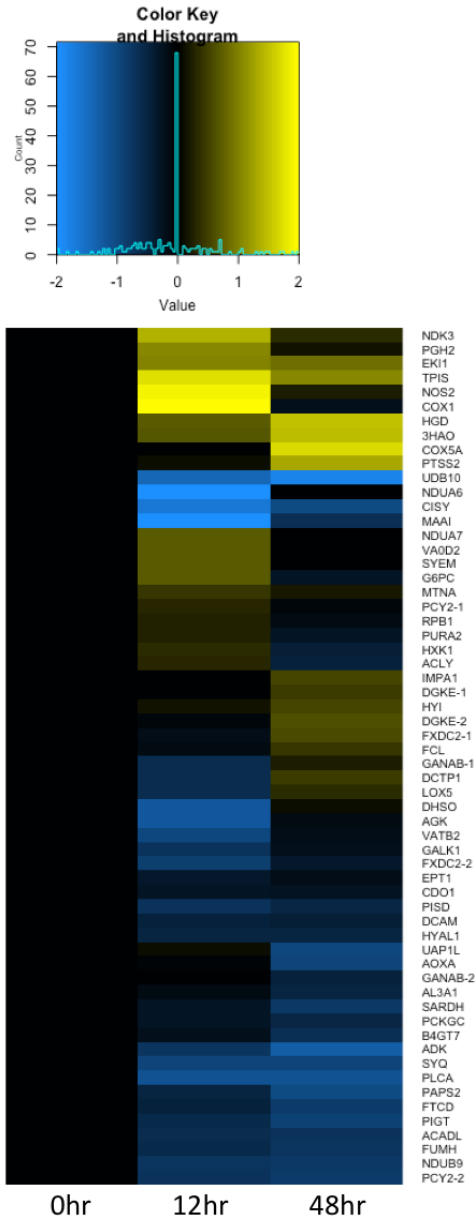
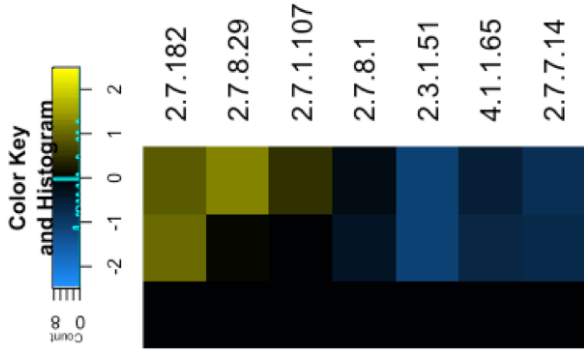
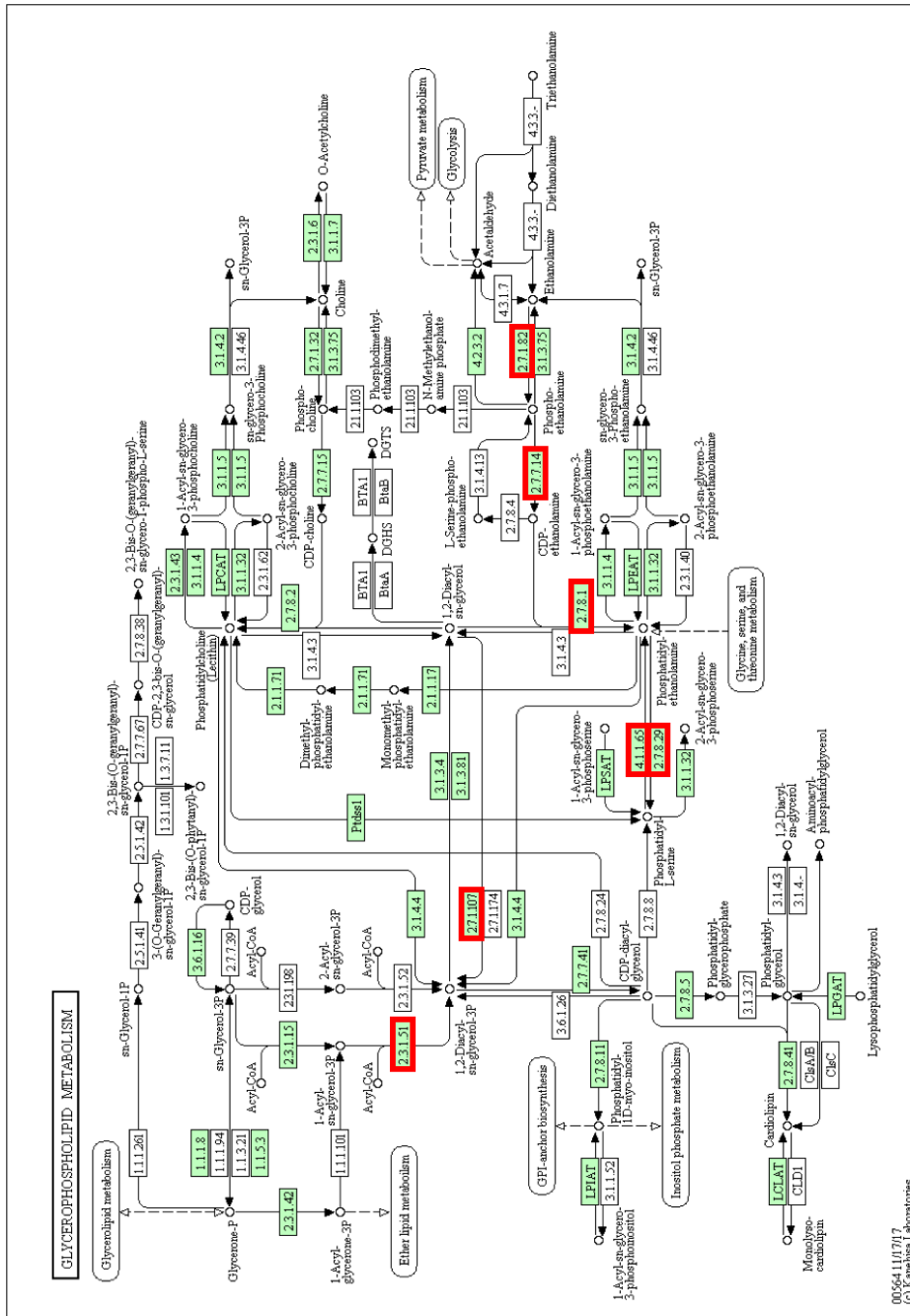


**Figure 15.** Differentially expressed transcripts present in the glycerophospholipid metabolism KEGG pathway.

Protein annotations were submitted to DAVID online software to examine the enrichment in KEGG pathways. A heatmap was generated using the gplot package in R was used to demonstrate the expression profile of the transcripts involved in the endocytosis pathway. Differentially expressed transcripts are indicated by red boxes on the KEGG pathway.



## Discussion

The work presented within this thesis is the first example of using RNA-seq technology to quantify the differential expression of transcripts following an experimental exposure in elasmobranchs. The use of differential expression analysis, as opposed to catalogue-based studies (which have been previously performed), significantly improves the conclusions that can be drawn regarding responses to salinity stress. Furthermore, data presented here offers numerous possible directions for future studies to use biochemical and physiological techniques to test the results shown and expand further. The gill morphology presented in this thesis is similarly novel. Prior work has characterized alterations to protein localization via immunofluorescence and mRNA abundance in the gills following salinity challenge, however, this is the first study to characterize alterations to gross morphology of the gill lamellae (Reilly et al., 2011; Takabe et al., 2016). The gill morphology work in this thesis is in no way fully comprehensive, however, serves as an indication that further work should be devoted to this area.

### *Lack of relationship between phylogeny and extent of salinity tolerance*

Low salinity tolerance in teleosts has evolved independently multiple times (Schultz and McCormick, 2013). It is likely that a similar process has unfolded in the elasmobranchs, although with fewer apparent invasions into BW/FW based on current knowledge. The variety of apparent osmotic strategies used by elasmobranchs during BW/FW invasions can be inferred by the range in plasma urea following salinity challenges (Ballantyne and Robinson, 2010). Only the stenohaline FW potamotrygonid rays from the Amazon basin that have been inhabiting a complete FW environment for millions of years are no longer ureosmotic, while many of the other euryhaline elasmobranchs have a range of urea levels suggesting multiple strategies are likely being used for invasions (Lovejoy et al., 1998). The data presented within this thesis suggests the degree of BW/FW tolerance in the selachimorphs appears to have no relation to the phylogeny; supporting the hypothesis that it has arisen multiple times and that the genetic machinery used for invasions is a phylogenetically ancient trait. However, as research into this relatively understudied group of fishes progresses, the list of marginally euryhaline elasmobranchs continues to grow and thus this subject of a phylogenetic basis for BW/FW invasion should be regularly revisited.

### *Osmolytes and gill morphology perturbations following salinity challenge*

Consistent with other studies using dogfish, animals in the current study experienced a reduction in total osmolality which was primarily through the loss of urea (Deck et al., 2016; Guffey and Goss, 2014). This is part of the larger trend in the marginally euryhaline elasmobranchs which all experience a similar occurrence during hyposmotic exposure. However, a more substantial NaCl loss appears more prevalent in other species experiencing BW stresses (Cooper and Morris, 1998; Cramp et al., 2015; Dowd et al., 2010). Most selachimorphs are considered osmoconformers and therefore as environmental osmolality drops, plasma osmolality follows accordingly. This would function to maintain appropriate osmolyte gradients, minimizing homeostatic disturbances in water balance. However, the changes in plasma osmolytes and total osmolality are clearly not instantaneous and therefore animals were hyperosmotic for the length of exposure causing an inward gradient for water, as reflected by an increase in body weight detailed in Guffey and Goss (2014). The preservation of water balance in the face of this inward flux is suggested to occur via through increased kidney function, specifically via an increase UFR and GFR (Cooper and Morris, 1998; Schmidt-Nielsen et al., 1972). While these changes are insufficient to completely combat the water-loading, the involvement of the kidney in early stage (<48hrs) responses to lowered salinity is apparent.

Alterations to gross gill morphology have been noted previously in teleosts and are commonly associated with the osmo-respiratory compromise (Nilsson, 2007). This compromise is typically seen as hypoxia-induced remodelling of gill morphology to increase surface area for oxygen uptake, while simultaneously conceding ion balance due to increased surface area (Nilsson et al., 2012). This phenomenon has been demonstrated in elasmobranchs using dogfish wherein acute severe hypoxia elicited increased branchial urea and ammonia efflux (Zimmer and Wood, 2014). Changes to environmental salinity have also been shown to induce morphological changes in the gills of teleosts (Blair et al., 2018). In the current study, an increase in ILCM was observed following 24hrs in 65% SW. This likely corresponds to a decrease in total surface area of the gills and thus a smaller area for ion and osmolyte loss, possibly mitigating the effects of the increased gradients during hyposmotic challenge. Constant branchial urea loss, despite increased osmotic gradients, was seen in the euryhaline skate, *Raja erinacea*, remained stable following transfer from 100% SW to 75% SW (Payan et al., 1973). The influence of these changes on O<sub>2</sub> uptake has not been fully elucidated, however, total O<sub>2</sub> consumption was

unchanged in the dogfish (Guffey and Goss, 2014) and the Port Jackson shark (Cooper and Morris, 2004b). Alteration to morphology of the gills is likely only one of the numerous responses available to elasmobranchs. Other possible mechanisms that would work to maintain a constant branchial efflux rate of urea include increasing the cholesterol content of the gill epithelium or increasing the back transport rate of urea. The effects of low salinity exposure on the gross gill morphology of elasmobranchs should be further investigated with a more detailed microscopy study.

#### *Responding to salinity exposure through changes in transcript expression*

Given the key role of the kidney in responding to salinity stress, the main objective of my thesis focused on the transcriptome level responses of this tissue during the first 48hrs of BW exposure. This work revealed extensive modifications in multiple cellular processes. Below I will discuss some of these changes and how they might contribute to low salinity tolerance observed in the dogfish.

#### *Amino acid and regulation*

Following 65% SW exposure, there was upregulation of the neutral amino acid transporter SLC6A18. This protein functions in a sodium-chloride dependent manner and is the main amino acid transporter in the kidney (Singer et al., 2009). Increased reabsorption of amino acids via SLC6A18 may be required to accommodate increased protein synthesis needed for induction of new cellular functions. In opposition of this, multiple translation initiation factors were downregulated during hyposmotic exposure suggesting there were at least some decreases in function of specific protein synthesis pathways. Furthermore, multiple transcripts within the endocytosis KEGG pathway, particularly in the early to late endosome phase, were also downregulated. Correspondingly, numerous GO terms related to protein localization and secretion were enriched in the differentially expressed transcripts. This may be indicative of decreased protein turnover and protein trafficking, and as a result, a possible reduction in protein synthesis. Taken together, the data suggests protein synthesis was not the driving force for increased amino acid retention. An alternative cause for increased amino acid retention is an increased rate of amino acid catabolism (possibly as a nitrogen source) or conversion. However, there were minimal changes in amino acid degradation pathways and therefore this justification

is unlikely. The increased expression of SLC6A18 may also be due to the increased GFR and UFR that is associated with low salinity exposure (Cooper and Morris, 2004a; Schmidt-Nielsen et al., 1972). These higher filtration and flow rates increase the total filtrate passing through the nephron tubule, and thus increasing the rate of amino acid loss. Therefore, to maintain post-exposure amino acid levels similar to that of pre-exposure levels, there would need to be increased expression of transporters to offset the increased rates of loss by passive filtration. Intracellular amino acids contribute to a small, but notable portion of the total osmotic pressure within tissues (Yancey, 2015). Therefore, as urea is being offloaded amino acids may contribute more significantly to the total cellular osmolality. Clearly, further work is needed to characterize the role of amino acids and amino acid transporters in elasmobranch following low salinity exposure.

#### *Urea transporter expression*

Interestingly, no change was seen in the expression of UT-A2 transcripts. The reduction in plasma urea during hyposmotic exposure would suggest a decreased level of renal urea transporters. Following exposure to 50% SW the little skate (*Raja erinacea*) demonstrated a reduction in the skate urea transporter mRNA (Morgan, 2003b), while the Atlantic stingray (*Dasyatis sabina*) did not exhibit substantial changes (Janech et al., 2003). The mRNA levels of urea transporters in the collecting tubules of the banded houndshark (*Triakis scyllium*) showed a non-significant reduction following 30% SW exposure, however, protein levels were significantly diminished (Yamaguchi et al., 2009). Furthermore, this reduction in protein abundance occurred primarily in the apical membrane. This not only suggests that the response is species-specific (supporting the independent evolution of these adaptations), but also highlights the possible discontinuous relationship between mRNA expression and protein abundance (discussed below). The stable expression of UT-A2 observed in this thesis implies that the increased GFR and UFR rates may be sufficient in eliminating urea to remain isosmotic, however, further work at the protein level would be needed to confirm this.

#### *Regulating paracellular loss*

The differential expression of transcripts involved in paracellular transport of osmolyte was expected following hyposmotic exposure. The osmoconforming strategy of elasmobranchs

necessitates that osmolytes are lost to the environment and one possible route is via paracellular loss. Claudins are a major component of tight junctions and contribute greatly in regulating this loss (Krause et al., 2008). Within teleosts there are ~63 different claudin genes which produce functional proteins that act as either pore forming (anion or cation selective) or barrier forming (Kolosov et al., 2013). Unfortunately, no work has been done to examine the molecular identities of claudins in elasmobranchs. The claudin 10 gene displays multiple splice variants that encode for either cation and anion pores (Krause et al., 2008). The current study noted that two claudin 10 transcripts were differentially expressed and displayed opposite transcriptome profiles. One of the transcripts was upregulated following 12hrs and substantially downregulated after 48hrs, while the second was the inverse of this. The trend observed may be the result of splice variants with functional differences, though the identity as either an anion or cation selective pore is unknown for these two transcripts. However, all claudin 10 isoforms are pores and therefore a reduction in these would limit the loss of osmolytes. Previous work has demonstrated teleost claudins are altered by environmental salinity to maintain homeostasis (Bui and Kelly, 2014; Marshall et al., 2018). In the euryhaline Japanese medaka (*Oryzias latipes*), long term FW acclimation was associated with decreased mRNA expression of certain renal claudins compared to SW acclimated fish (Bossus et al., 2015). Importantly, this response was isoform specific; claudin 10b1 (anion pore) and 10b2 (cation pore) were both downregulated in FW, however 10c, 10d, and 10f showed no change. Thus, the variation in claudin 10 isoforms seen in Pacific spiny dogfish is reasonable. Furthermore, tight junction protein 1 (ZO-1) was downregulated slightly following 12hrs and upregulated to a much greater degree after 48hrs. This protein functions as a scaffold, tethering the transcellular tight junction proteins (such as claudins and occludins) to the intracellular actin cytoskeleton (Chasiotis et al., 2012). The significant upregulation of ZO-1 after 48hrs allows for increased localization of tight junction proteins (either pore or barrier), further contributing to regulation paracellular loss. Cadherin 1 and desmocollin 3 are both involved in cell-cell adhesion and were downregulated during low salinity exposure. The alteration to cell adhesion, in conjunction with changes in transcripts directly involved in tight junctions, strongly suggests paracellular loss is tightly regulated and important element of marginal euryhalinity in the Pacific spiny dogfish.

### *Regulation of tight junctions*

The MAPK signalling pathway has been shown to alter the expression of both barrier and pore forming claudins and the expression of ZO-1 (González-Mariscal et al., 2008). The primary effector of these actions is MAPK/ERK1. Therefore, alteration to the expression of MAP3K15 and MAP2K5 (upstream of MAPK), supported by enrichment of GO term “positive regulation of ERK1 and ERK2 cascade”, may function to enhance MAPK activity and consequently, alter tight junction leakiness. RhoA was upregulated after 48hrs in 65% SW and functions through different actions from MAPK to achieve the similar results (González-Mariscal et al., 2008). RhoA is an activator of the actin remodelling, and thus can regulate actin-myosin mediated contraction of the cell to break tight junctions between adjacent cells (Capaldo and Nusrat, 2009; Hall, 1998). Cytokines also have established effects on paracellular leakage including interleukins (Capaldo and Nusrat, 2009). Knockout of IL-10 from mice resulted in reduced localization of ZO-1 to the tight junctions (Mazzon et al., 2002). A similar occurrence may have occurred in dogfish kidney as a result decreased IL-10 expression. In conclusion, a multitude of factors may be working in unison to regulate paracellular loss through the presence of tight junction proteins, the localization of intracellular elements, and use splice variants.

### *Osmosensing transcription factors and proteins*

The lack of extensive modifications to key transcription factors previously implicated in salinity acclimation was surprising, though justifiable. An important regulator of cell signalling following an osmotic challenge is the osmotic stress transcript factor 1 (OSTF1). This transcription factor was first identified in Mozambique tilapia (*Oreochromis mossambicus*) as an early response gene that increased 6-fold after a 2hr transfer from FW to SW (Fiol and Kültz, 2005). It has since been identified in a variety of teleosts, although never in an elasmobranch (Tse, 2014). The early onset of this transcription factor, in addition to its primary localization in the gills, suggests that if it were detected, it may not have been differentially expressed. A mammalian homolog of OSTF1, TSC22D2, was detected however no change was observed, suggesting these early response transcription factors are present in the dogfish but may not contribute to acclimation in the kidney. The annotation as TSC22D2 rather than OSTF1 is likely due to the lack of OSTF1 in the databases used by Trinotate, highlighting the difficulties of using

non-model species. Lastly, the 14-3-3 gene has been implicated as a major regulator for branchial osmosensory signalling in the euryhaline teleost *Fundulus heteroclitis* (Kültz et al., 2001). 14-3-3 transcripts in this study showed no significant changes in the dogfish over the course of 48hrs. Similarly, no change in 14-3-3 mRNA levels were detected *F. heteroclitus* intestine, suggesting a strong tissue dependence (Scott et al., 2006). The presence of numerous osmosensing transcription factors suggests that elasmobranchs have the genetic machinery in place to elicit a response, however, the lack of differential expression suggests that the kidney is not involved in osmosensing. Therefore, this finding warrants further exploration using gill tissues and earlier time points during salinity challenges.

### *Protein damage and chaperones*

Heat shock proteins (HSPs) are a large family of protein chaperones that reduce unwanted conformational changes and prevent protein aggregation (Georgopoulos and Welch, 1993). The uniform upregulation of multiple HSP at both the transcript and gene level, and enrichment of GO terms “chaperone-mediated protein complex assembly”, “protein stabilization”, and “regulation of protein stabilization” following 12hrs in 65% SW suggests a dramatic increase in protein stress. Ubiquitin protein levels can function as an indirect measure of protein damage and in the absence of direct protein quantification, expression levels of ubiquitination transcripts was used (MacLellan et al., 2015). Surprisingly, differentially expressed ubiquitin were inconsistent in their expression patterns making it difficult to evaluate the degree of protein damage. However, the observation that HSPs operate predominantly in a time dependent manner (much greater FC after 12hrs than 48hrs compared to control) suggests that protein damage or stress had ceased, or reduced dramatically, after 48hrs. The dogfish appeared to be approaching the isosmotic line after 48hrs, and congruently, HSPs had almost returned to control levels at that point. Conversely, other studies have demonstrated that HSP levels in dogfish gills remained elevated after 48hrs in 70% SW and HSP abundance in school shark and gummy shark gills after 48hrs in 75% SW were decreased and unchanged, respectively (MacLellan et al., 2015; Morash et al., 2016). Likewise, teleost HSP expression levels are altered by salinity. A chronic salinity stress (8 months) challenge by Deane et al. (2002) using Black Sea Bream demonstrated that HSPs were more abundant in both hyperosmotic and hyposmotic

conditions and less in fish maintained in isosmotic water (12 ppt). In summary, the role of HSPs in salinity stress appears to be substantial yet vary with tissue and species.

#### *Immune functions*

Alterations to apoptotic factors and pathways have been previously identified in fishes following a salinity challenge, however, this response is typically studied in the gills (Blair et al., 2018; Ching et al., 2013; Kammerer and Kültz, 2009). Mozambique tilapia (*Oreochromis mossambicus*) undergo an extensive apoptotic process that is localized to the branchial MRCs following transfer from FW to SW (Kammerer and Kültz, 2009). This is suggested to increase the reorganization of branchial cell populations to replace FW MRCs with SW MRCs. This unique cell type has not been identified in the elasmobranch kidney, however, the increased expression of pro-apoptotic factors P53 and caspase 6 may still result in alterations to the makeup of renal cell populations. Multiple GO terms associated with the cell cycle and cell differentiation were enriched, particularly after 48hrs, suggesting this is temporally dependent response (e.g. “mitotic cell cycle”, “regulation of cell cycle process”, and “positive regulation of cell cycle arrest”). Thus, modifications to the cell populations may be occurring, however it is impossible to determine the exact changes in cell composition without using specific markers of cell types.

#### *Metabolic processes*

While I did detect alterations to certain transcripts with metabolic functions, the changes were spread across multiple pathways. Numerous transcripts involved in the glycerophospholipid pathway were differentially expressed and exhibited expression patterns that would contribute to reduced production of phosphatidylethanolamine (PE). This phospholipid is highly enriched in the inner membrane of the lipid bilayer and functions in membrane fusion (Chernomordik and Kozlov, 2008). Endocytosis and vesicle fusion was repressed transcriptionally and decreased levels of PE may act in concert to further reduce these processes. The functional outcome of this may lead to decreased transport of proteins inwards, reducing the protein turnover rates. PE also plays a role in cytokinesis during mitosis, enabling the separation of cells (Emoto et al., 1996). Therefore, decreased PE would also suggest a reduction in cell cycle rates, further supporting the conclusion that low salinity challenges require alterations to composition of renal cell populations. The phospholipid composition within teleost gills is altered in response to

environmental salinity, however, a similar occurrence has not been demonstrated in elasmobranchs (Shivkamat and Roy, 2005). No progress has been made to quantify changes in elasmobranch gill membranes in response to changes in salinity, however, composition of elasmobranch gills has been investigated (Fines et al., 2001). However, it is apparent that the specific membrane composition in the kidneys must be altered to accommodate the osmotic stress.

The downregulation of sarcosine dehydrogenase (SARDH), responsible for enzymatic conversion of sarcosine to glycine, suggests an accumulation of this organic osmolyte. This was unexpected due to the osmoconforming strategy of the dogfish and thus the need for offloading of osmolytes. A similar enzyme, sarcosine oxidase, isolated from *Raja erinacea* (a euryhaline skate) hepatocytes showed osmolarity-dependent activity wherein lower osmolarity induced activity (Ballantyne et al., 1986). It may be possible these divergent results can be attributed to different rates of sarcosine catabolism in these two tissues, and thus the functional outcome of downregulation in the dogfish may not contribute significantly to total sarcosine levels. Sarcosine can act to stabilize proteins and therefore increased retention of this compound, in conjunction with HSPs, may help to ensure functional proteins (Street et al., 2006). To my knowledge no studies have detailed the regulation sarcosine during salinity challenges.

#### *Limitations to the study*

There are several potential limitations to this thesis. The first is reliance on homologous annotation and the relatively low annotation rate. The use of non-model species in comparative physiology is particularly valuable in understanding how certain adaptations function, however, accompanying this value is the lack of genomic data and extensive gene annotation. While RNA-seq is able to overcome this problem via *de novo* assembly and large scale homologous annotation pipelines, it is not a perfect method and incomplete transcripts are often assembled that can be annotated incorrectly. Furthermore, homologous annotations are not always obtained unless a compromise in strictness of the annotation program is made, reducing the confidence in the results. Using the data generated to conduct further homology searches using multiple sequence alignments may be possible, however, time consuming. In this study, there were approximately 400 contigs that showed significant differential expressed during the exposure, yet no annotation was found. Identification of these 400 contigs could reveal a multitude of important transcripts and pathways involved in salinity tolerance. Second, the correlation

between transcript expression levels and abundance of protein is not always correct (Maier et al., 2009). However, it has been demonstrated that differentially expressed transcripts are more likely to match their protein counterpart levels, compared to transcripts that are unresponsive to an experimental treatment (Koussounadis et al., 2015). While it may not be a completely accurate representation of the true intracellular environment, RNA-seq still provides valuable clues that can be pursued using other specialized techniques, such as protein level assays. Without RNA-seq, these clues may be missed. Third, RNA-seq in this study was performed on whole tissue. This can be important for tissues such as the kidney where adjacent sections are functionally different and therefore any localized changes would likely be lost. It would be possible to overcome this limitation through detailed dissection of sinus zones and bundle zones, however, the complicated kidney morphology would likely make this difficult. A detailed understanding of changes in mRNA along the length of the kidney would be a substantial improvement to this study.

One particular caveat for the present study is that the health of many of the sharks held at Bamfield Marine Sciences Centre was compromised as ~2 weeks prior to experimentations with a likely bacterial infection. Many experienced lesions in the snout and had obvious eye infections. While animals used in this study were from this group as a whole, care was taken to select fish with minimal overt clinical signs (e.g. negligible nose wounds) for experiments described in this thesis. Upon sacrifice, a limited number of sharks that appeared healthy externally exhibited significant changes in the texture and consistency of the liver, and in addition, some displayed a substantial reduction in the size of a lobe. However, the presence of non-presenting effects of either infection or recent recovery may have some influence on the results of this study and care should be taken when interpreting the results. Regardless, all results are compared to control animals from the same population and I am therefore confident in the validity of the changes in gene expression resulting from salinity stress.

### *Future Directions*

The work described in this thesis is primarily concerned with changes in gene expression in the kidney. However, the kidney is not the only organ involved heavily in ion and water balance. During sacrifice, I also took tissue samples from the gills, rectal gland, intestine, and liver from all the same animals. Therefore, an immediate goal would be the sequencing of the

transcriptome from each of these important osmoregulatory tissues and to compare findings with the current study. These other tissues may display more prominent alterations to select cellular functions, such as metabolic changes in the liver or osmosensing and signalling in the gills.

An alternative, equally important approach to understanding salinity tolerance might be to use a similar RNA-seq approach, but instead expose dogfish to multiple salinities for a single duration, rather than multiple durations at a single salinity. This study design would identify whether the osmosensory system within these animals can operate in a graduated manner depending on environmental salinity to fine tune downstream response. Furthermore, the use of multiple salinities may reveal that the changes in expression are consistent across multiple, or conversely, the level of osmotic stress induces different responses. Using the Pacific spiny dogfish, a graduated range of salinities that could be test include 32ppt, 28ppt, 24ppt, and 21ppt. An additional treatment could be included to examine the recovery of animals in 32ppt after exposure to 21 ppt.

Diverging from physiological studies may be necessary to understand the ecological reasons of entering BW or FW environments. For instance, female bull sharks can give birth in FW and as the pups mature, they migrate down rivers as they become larger before finally entering the marine environment (Simpfendorfer et al., 2005). This is hypothesized to give the pups protection from larger predators found in marine environments (Ballantyne and Fraser, 2012). However, very little is known about the purpose of BW invasions for other marine elasmobranchs such as the dogfish. Furthermore, very little is known about the duration of incursions. There are multiple likely motives that these animals might move into BW. Similar to bull sharks pups, dogfish are prey for a number of other larger animals. BW environments may provide added protection as opposed to pelagic and benthic environments further from the coast. Additionally, BW environments have very high primary production can therefore support a high population of fishes (Correll, 1978; Houde and Rutherford, 1993). This may be an additional food source that the dogfish take advantage of during invasions into low salinity environments in estuaries. Therefore, ecological studies need to be performed where animals near estuaries are tagged with sensors for environmental parameters (salinity, water temperature, and depth) to record details of possible incursions. Ideally, recapture of these animals following BW or FW incursions would be performed to allow for inspection of the intestinal contents. This would give indications about food sources within the estuary and if they differ from marine environments.

A key element missing from the majority of this study is the role of hormonal influence on renal function. Transcripts involved in enzymatic synthesis of prostaglandins were altered in this study however the role of this compound in osmoregulation has never been investigated. There are at least four components that contribute to endocrine based ion and water homeostasis in elasmobranch including the hypothalamic-pituitary-interrenal axis, c-type natriuretic peptide (CNP), vasoactive intestinal polypeptide, and the renin-angiotensin system (Gelsleichter and Evans, 2004). Importantly, CNP in *Scyliorhinus canicula* increased renal clearances of osmolytes (Wells et al., 2006). This peptide is synthesized in response to water loading and therefore is likely contributing significantly during low salinity invasions (Anderson et al., 2005b). The receptors for CNP were detected in the dogfish kidney transcriptome, however no changes were observed. Further work needs to be done to explore the role of this peptide in these animals during BW/FW incursion. This could be accomplished via transfusion of blood from hyposmotically challenged dogfish into naïve sharks. If a response was elicited this would demonstrate that circulating hormones are the primary drivers signalling for alterations to renal function. This could be measured via osmolyte clearance rates and changes in protein abundance and mRNA expression of targets downstream of the receptor.

The central aim, of which the work in this thesis is just one component, is to understand the physiological mechanisms that permit BW and FW invasions in elasmobranchs, and contextualize this within the evolution of these traits. Therefore, comparative physiology is essential. Using the data generated from this thesis as a starting point, a similar study could be performed using a variety of marginally euryhaline elasmobranchs with varied salinity tolerances. Salinity challenge could either be in the form of each species lowest limit, or to a consistent level that can be tolerated by most species (e.g. 70% SW). Multiple tissues could be collected for each species and using either RNA-seq experiment or proteomic methods. This would elucidate interspecific differences in the same tissue, as well as the intraspecific differences in across tissues. There is the possibility that all elasmobranchs use generally the same trends just regulated to different levels, or conversely, different species use distinctive adaptations to overcome the same challenge. Both are exciting possibilities and may provide a new outlook on the evolution of BW and FW invasions.

## *Conclusions*

This thesis presented multiple novel aspects, the most prominent of which was the application of RNA-seq for differential expression analysis in an elasmobranch. My work revealed that the response of the kidney in the marginally euryhaline elasmobranch *Squalus suckleyi* was extremely multifactorial and complicated following low salinity exposure. Some of the important changes in mRNA expression were discussed and future studies that directly use the data presented within this thesis were reviewed. As the fields of transcriptomic and genomics progress in the future, the ease at which elasmobranch transcriptome data can be accurately mapped and annotated will only increase. My work is the first step in this direction.

## References

- Aballai, V., Aedo, J. E., Maldonado, J., Bastias-Molina, M., Silva, H., Meneses, C., Boltaña, S., Reyes, A., Molina, A. and Valdés, J. A.** (2017). RNA-seq analysis of the head-kidney transcriptome response to handling-stress in the red cusk-eel (*Genypterus chilensis*). *Comp. Biochem. Physiol. - Part D Genomics Proteomics* **24**, 111–117.
- Anderson, P. M.** (1991). Glutamine-dependent urea synthesis in elasmobranch fishes. *J. Biochem. Cell Biol.* **69**, 317–319.
- Anderson, P. M. and Casey, C. A.** (1984). Glutamine-dependent synthesis of citrulline by isolated hepatic mitochondria from *Squalus acanthias*. *J. Biol. Chem.* **259**, 456–462.
- Anderson, W. G., Takei, Y. and Hazon, N.** (2002). Osmotic and volaemic effects on drinking rate in elasmobranch fish. *J. Exp. Biol.* **205**, 1115–22.
- Anderson, W. G., Good, J. P., Pillans, R. D., Hazon, N. and Franklin, C. E.** (2005a). Hepatic urea biosynthesis in the euryhaline elasmobranch *Carcharhinus leucas*. *J. Exp. Zool. Part A Comp. Exp. Biol.* **303**, 917–921.
- Anderson, W. G., Hyodo, S., Tsukada, T., Meischke, L., Pillans, R. D., Good, J. P., Takei, Y., Cramb, G., Franklin, C. E. and Hazon, N.** (2005b). Sequence, circulating levels, and expression of C-type natriuretic peptide in a euryhaline elasmobranch, *Carcharhinus leucas*. *Gen. Comp. Endocrinol.* **144**, 90–98.
- Anderson, W. G., Taylor, J. R., Good, J. P., Hazon, N. and Grosell, M.** (2007). Body fluid volume regulation in elasmobranch fish. *Comp. Biochem. Physiol. A. Mol. Integr. Physiol.* **148**, 3–13.
- Ballantyne, J. S. and Fraser, D. I.** (2012). *Euryhaline Elasmobranchs*. Elsevier Inc.
- Ballantyne, J. S. and Robinson, J. W.** (2010). Freshwater elasmobranchs: A review of their physiology and biochemistry. *J. Comp. Physiol. B Biochem. Syst. Environ. Physiol.* **180**, 475–493.
- Ballantyne, J. S., Moyes, C. and Moon, T. W.** (1986). Osmolarity affects oxidation of sarcosine by isolated hepatocytes and mitochondria from a euryhaline elasmobranch. *J. Exp. Zool.* **238**, 267–271.
- Beck, B. H., Fuller, S. A., Li, C., Green, B. W., Zhao, H., Rawles, S. D., Webster, C. D. and Peatman, E.** (2016). Hepatic transcriptomic and metabolic responses of hybrid striped bass (*Morone saxatilis* × *Morone chrysops*) to acute and chronic hypoxic insult. *Comp. Biochem. Physiol. - Part D Genomics Proteomics* **18**, 1–9.
- Blair, S. D., Matheson, D. and Goss, G. G.** (2018). Physiological and morphological investigation of Arctic grayling (*Thymallus arcticus*) gill filaments with high salinity exposure and recovery. **5**, 1–12.
- Bolger, A. M., Lohse, M. and Usadel, B.** (2014). Trimmomatic: A flexible trimmer for Illumina sequence data. *Bioinformatics* **30**, 2114–2120.
- Bossus, M. C., Madsen, S. S. and Tipsmark, C. K.** (2015). Functional dynamics of claudin expression in Japanese medaka (*Oryzias latipes*): Response to environmental salinity. *Comp. Biochem. Physiol. -Part A Mol. Integr. Physiol.* **187**, 74–85.
- Briknarová, K., Takayama, S., Homma, S., Baker, K., Cabezas, E., Hoyt, D. W., Li, Z., Satterthwait, A. C. and Ely, K. R.** (2002). BAG4/SODD protein contains a short BAG domain. *J. Biol. Chem.* **277**, 31172–31178.
- Bui, P. and Kelly, S. P.** (2014). Claudin-6, -10d and -10e contribute to seawater acclimation in the euryhaline puffer fish *Tetraodon nigroviridis*. *J. Exp. Biol.* **217**, 1758–1767.

- Capaldo, C. T. and Nusrat, A.** (2009). Cytokine regulation of tight junctions. *Biochim. Biophys. Acta - Biomembr.* **1788**, 864–871.
- Casey, C. A. and Anderson, P. M.** (1982). Subcellular location of glutamine synthetase and urea cycle enzymes in liver of spiny dogfish (*Squalus acanthias*). *J. Biol. Chem.* **257**, 8449–53.
- Chana-Munoz, A., Jendroszek, A., Sønnichsen, M., Kristiansen, R., Jensen, J. K., Andreasen, P. A., Bendixen, C. and Panitz, F.** (2017). Multi-tissue RNA-seq and transcriptome characterisation of the spiny dogfish shark (*Squalus acanthias*) provides a molecular tool for biological research and reveals new genes involved in osmoregulation. *PLoS One* **12**, 1–23.
- Chasiotis, H., Kolosov, D., Bui, P. and Kelly, S. P.** (2012). Tight junctions, tight junction proteins and paracellular permeability across the gill epithelium of fishes: A review. *Respir. Physiol. Neurobiol.* **184**, 269–281.
- Chernomordik, L. V. and Kozlov, M. M.** (2008). Mechanics of membrane fusion. *Nat. Struct. Mol. Biol.* **15**, 675–683.
- Ching, B., Chen, X. L., Yong, J. H. A., Wilson, J. M., Hiong, K. C., Sim, E. W. L., Wong, W. P., Lam, S. H., Chew, S. F. and Ip, Y. K.** (2013). Increases in apoptosis, caspase activity and expression of p53 and bax, and the transition between two types of mitochondrion-rich cells, in the gills of the climbing perch, *Anabas testudineus*, during a progressive acclimation from freshwater to seawater. *Front. Physiol.* **4**, 1–21.
- Claiborne, J. B., Choe, K. P., Morrison-Shetlar, A. I., Weakley, J. C., Havird, J., Freiji, A., Evans, D. H. and Edwards, S. L.** (2008). Molecular detection and immunological localization of gill Na<sup>+</sup>/H<sup>+</sup> exchanger in the dogfish (*Squalus acanthias*). *AJP Regul. Integr. Comp. Physiol.* **294**, R1092–R1102.
- Cohen, D. M.** (1970). How many recent fishes are there? *Proc. Calif. Acad. Sci. 4th Ser.* **37**, 341–346.
- Cooper, A. R. and Morris, S.** (1998). Osmotic, ionic and haematological response of the Port Jackson shark *Heterodontus portusjacksoni* and the common stingaree *Trygonoptera testacea* upon exposure to diluted seawater. *Mar. Biol.* **132**, 29–42.
- Cooper, A. R. and Morris, S.** (2004a). Osmotic, sodium, carbon dioxide and acid-base state of the Port Jackson shark, *Heterodontus portusjacksoni*, in response to lowered salinity. *J. Comp. Physiol. B Biochem. Syst. Environ. Physiol.* **174**, 223–236.
- Cooper, A. R. and Morris, S.** (2004b). Haemoglobin function and respiratory status of the Port Jackson shark, *Heterodontus portusjacksoni*, in response to lowered salinity. *J. Comp. Physiol. B Biochem. Syst. Environ. Physiol.* **174**, 223–236.
- Correll, D.** (1978). Estuarine productivity. *Bioscience* **28**, 646–650.
- Cramp, R. L., Hansen, M. J. and Franklin, C. E.** (2015). Osmoregulation by juvenile brown-banded bamboo sharks, *Chiloscyllium punctatum*, in hypo- and hyper-saline waters. *Comp. Biochem. Physiol. Part A Mol. Integr. Physiol.* **185**, 107–114.
- Cuesta, A., Laiz-Carrión, R., Martín Del Río, M. P., Meseguer, J., Miguel Mancera, J. and Ángeles Esteban, M.** (2005). Salinity influences the humoral immune parameters of gilthead seabream (*Sparus aurata* L.). *Fish Shellfish Immunol.* **18**, 255–261.
- Cutler, C. P., MacIver, B., Cramb, G. and Zeidel, M.** (2012). Aquaporin 4 is a ubiquitously expressed isoform in the dogfish (*Squalus acanthias*) shark. *Front. Physiol.* **2**, 1–9.
- Deane, E. E., Kelly, S. P., Luk, J. C. Y. and Woo, N. Y. S.** (2002). Chronic salinity adaptation modulates hepatic heat shock protein and insulin-like growth factor I expression in black

- sea bream. *Mar. Biotechnol. (NY)*. **4**, 193–205.
- de Waal Malefyt, R., Abrams, J., Bennett, B., Figdor, C. G. and de Vries, J. E.** (1991). Interleukin 10(IL-10) inhibits cytokine synthesis by human monocytes: An autoregulatory role of IL-10 produced by monocytes. *J. Exp. Med.* **174**, 1209–1220.
- Deck, C. A., Bockus, A. B., Seibel, B. A. and Walsh, P. J.** (2016). Effects of short-term hyper- and hypo-osmotic exposure on the osmoregulatory strategy of unfed North Pacific spiny dogfish (*Squalus suckleyi*). *Comp. Biochem. Physiol. Part A Mol. Integr. Physiol.* **193**, 29–35.
- Dowd, W. W., Harris, B. N., Cech, J. J. and Kültz, D.** (2010). Proteomic and physiological responses of leopard sharks (*Triakis semifasciata*) to salinity change. *J. Exp. Biol.* **213**, 210–224.
- Dulvy, N. K., Fowler, S. L., Musick, J. A., Cavanagh, R. D., Kyne, P. M., Harrison, L. R., Carlson, J. K., Davidson, L. N. K., Fordham, S. V., Francis, M. P., et al.** (2014). Extinction risk and conservation of the world's sharks and rays. *Elife* **3**, 1–34.
- Emoto, K., Kobayashi, T., Yamaji, a, Aizawa, H., Yahara, I., Inoue, K. and Umeda, M.** (1996). Redistribution of phosphatidylethanolamine at the cleavage furrow of dividing cells during cytokinesis. *Proc. Natl. Acad. Sci. U. S. A.* **93**, 12867–12872.
- Evans, D. H., Piermarini, P. M. and Choe, K. P.** (2005). The Multifunctional Fish Gill : Dominant Site of Gas Exchange , Osmoregulation , Acid-Base Regulation , and Excretion of Nitrogenous Waste. *Physiol. Rev.* **85**, 97–177.
- Fines, G. A., Ballantyne, J. S. and Wright, P. A.** (2001). Active urea transport and an unusual basolateral membrane composition in the gills of a marine elasmobranch. *Am. J. Physiol. Regul. Integr. Comp. Physiol.* **280**, R16–24.
- Fiol, D. F. and Kültz, D.** (2005). Rapid hyperosmotic coinduction of two tilapia (*Oreochromis mossambicus*) transcription factors in gill cells. *Proc. Natl. Acad. Sci.* **102**, 927–932.
- Fiol, D. F. and Kültz, D.** (2007). Osmotic stress sensing and signaling in fishes. *FEBS J.* **274**, 5790–5798.
- Fiol, D. F., Mak, S. K. and Kültz, D.** (2007). Specific TSC22 domain transcripts are hypertonically induced and alternatively spliced to protect mouse kidney cells during osmotic stress. *FEBS J.* **274**, 109–124.
- Forey, P. L.** (1980). Latimeria : a paradoxical fish. *Proc. R. Soc. B Biol. Sci.* **208**, 369–384.
- Forster, R. P. and Goldstein, L.** (1976). Intracellular osmoregulatory role of amino acids and urea in marine elasmobranchs. *Am. J. Physiol.* **230**, 925–31.
- Fridman, J. S. and Lowe, S. W.** (2003). Control of apoptosis by p53. *Oncogene* **22**, 9030–9040.
- Friedman, P. A. and Hebert, S. C.** (1990). Diluting segment in kidney of dogfish shark. I. Localization and characterization of chloride absorption. *Am. J. Physiol.* **258**, R398–408.
- Gagnon, É., Forbush, B., Flemmer, A. W., Giménez, I., Caron, L. and Isenring, P.** (2002). Functional and molecular characterization of the shark renal Na-K-Cl cotransporter: novel aspects. *Am. J. Physiol. - Ren. Physiol.* **283**, F1046–F1055.
- Gelsleichter, J. and Evans, A. N.** (2004). Hormonal Regulation of Elasmobranch Physiology. In *Biology of Sharks and their relatives*, pp. 313–348.
- Georgopoulos, C. and Welch, W. J.** (1993). Role of the major heat shock proteins as molecular chaperones. *Annu. Rev. Cell Biol.* **9**, 601–634.
- Gibbons, T. C., Metzger, D. C. H., Healy, T. M. and Schulte, P. M.** (2017). Gene expression plasticity in response to salinity acclimation in threespine stickleback ecotypes from different salinity habitats. *Mol. Ecol.* 2711–2725.

- Goldstein, L. and Forster, R. P.** (1971). Urea biosynthesis and excretion in freshwater and marine elasmobranchs. *Comp. Biochem. Physiol.* **39**, 415–421.
- González-Mariscal, L., Tapia, R. and Chamorro, D.** (2008). Crosstalk of tight junction components with signaling pathways. *Biochim. Biophys. Acta - Biomembr.* **1778**, 729–756.
- Grabherr, M. G., Haas, B. J., Yassour, M., Levin, J. Z., Thompson, D. A., Amit, I., Adiconis, X., Fan, L., Raychowdhury, R., Zeng, Q., et al.** (2011). Full-length transcriptome assembly from RNA-Seq data without a reference genome. *Nat. Biotechnol.* **29**, 644–652.
- Griffith, R. W.** (1980). Chemistry of the body fluids of the coelacanth, *Latimeria chalumnae*. *Proc. R. Soc. B Biol. Sci.* **208**, 329–347.
- Gu, J., Dai, S., Liu, H., Cao, Q., Yin, S., Lai, K. P., Tse, W. K. F., Wong, C. K. C. and Shi, H.** (2018). Identification of immune-related genes in gill cells of Japanese eels (*Anguilla japonica*) in adaptation to water salinity changes. *Fish Shellfish Immunol.* **73**, 288–296.
- Guffey, S. C. and Goss, G. G.** (2014). Time course of the acute response of the North Pacific spiny dogfish shark (*Squalus suckleyi*) to low salinity. *Comp. Biochem. Physiol. Part A Mol. Integr. Physiol.* **171**, 9–15.
- Haas, B. J., Papanicolaou, A., Yassour, M., Grabherr, M., Philip, D., Bowden, J., Couger, M. B., Eccles, D., Li, B., Macmanes, M. D., et al.** (2013). De novo transcript sequence reconstruction from RNA-Seq: reference generation and analysis with Trinity. *Nat Protoc.* **8**, 1–43.
- Hall, A.** (1998). Rho GTPases and the Actin Cytoskeleton. *Science (80- )*. **279**, 509–514.
- Hammerschlag, N.** (2006). Osmoregulation in elasmobranchs: a review for fish biologists, behaviourists and ecologists. *Mar. Freshw. Behav. Physiol.* **39**, 209–228.
- Hazon, N., Wells, A., Pillans, R. D., Good, J. P., Anderson, W. G. and Franklin, C. E.** (2003). Urea based osmoregulation and endocrine control in elasmobranch fish with special reference to euryhalinity. *Comp. Biochem. Physiol. - B Biochem. Mol. Biol.* **136**, 685–700.
- Heather, J. M. and Chain, B.** (2016). The sequence of sequencers: The history of sequencing DNA. *Genomics* **107**, 1–8.
- Holmes, W. N. and Phillips, J. G.** (1985). The avian salt gland. *Biol. Rev.* **60**, 213–256.
- Houde, E. D. and Rutherford, E. S.** (1993). Recent Trends in Estuarine Fisheries: Predictions of Fish Production and Yield. *Estuaries* **16**, 161.
- Huang, D. W., Sherman, B. T. and Lempicki, R. A.** (2009a). Bioinformatics enrichment tools: Paths toward the comprehensive functional analysis of large gene lists. *Nucleic Acids Res.* **37**, 1–13.
- Huang, D. W., Sherman, B. T. and Lempicki, R. A.** (2009b). Systematic and integrative analysis of large gene lists using DAVID bioinformatics resources. *Nat. Protoc.* **4**, 44–57.
- Hyodo, S., Katoh, F., Kaneko, T. and Takei, Y.** (2004). A facilitative urea transporter is localized in the renal collecting tubule of the dogfish *Triakis scyllia*. *J. Exp. Biol.* **207**, 347–356.
- Hyodo, S., Kakumura, K., Takagi, W., Hasegawa, K., Yamaguchi, Y., Braasch, I., Guiguen, Y., Loker, R., Letaw, J. H., Ferrara, A., et al.** (2014). Morphological and functional characteristics of the kidney of cartilaginous fishes: with special reference to urea reabsorption. *Comp. Biochem. Physiol. C. Toxicol. Pharmacol.* **307**, R1381–R1395.
- Janech, M. G., Fitzgibbon, W. R., Chen, R., Nowak, M. W., Miller, D. H., Paul, R. V. and Ploth, D. W.** (2003). Molecular and functional characterization of a urea transporter from the kidney of the Atlantic stingray. *Am. J. Physiol. - Ren. Physiol.* **284**, F996–F1005.

- Kammerer, B. D. and Kültz, D.** (2009). Prolonged apoptosis in mitochondria-rich cells of tilapia (*Oreochromis mossambicus*) exposed to elevated salinity. *J. Comp. Physiol. B Biochem. Syst. Environ. Physiol.* **179**, 535–542.
- Kempton, R. T.** (1953). Studies on the elasmobranch kidney. II. Reabsorption of urea by the smooth dogfish, *Mustelus canis*. *Biol. Bull.* **104**, 45–46.
- Kim, K.** (2002). Multifunctional role of Fas-associated death domain protein in apoptosis. *J. Biochem. Mol. Biol.* **35**, 1–6.
- King, B. L., Gillis, J. A., Carlisle, H. R. and Dahn, R. D.** (2011). A natural deletion of the HoxC cluster in elasmobranch fishes. *Science.* **334**, 1517.
- Kirschner, L. B.** (1993). The energetics of osmotic regulation in ureotelic and hypoosmotic fishes. *J. Exp. Zool.* **267**, 19–26.
- Kolosov, D., Bui, P., Chasiotis, H. and Kelly, S. P.** (2013). Claudins in teleost fishes. *Tissue Barriers* **1**, e25391.
- Koussounadis, A., Langdon, S. P., Um, I. H., Harrison, D. J. and Smith, V. A.** (2015). Relationship between differentially expressed mRNA and mRNA-protein correlations in a xenograft model system. *Sci. Rep.* **5**, 1–9.
- Krause, G., Winkler, L., Mueller, S. L., Haseloff, R. F., Piontek, J. and Blasig, I. E.** (2008). Structure and function of claudins. *Biochim. Biophys. Acta - Biomembr.* **1778**, 631–645.
- Krishnaswamy Gopalan, T., Gururaj, P., Gupta, R., Gopal, D. R. a., Rajesh, P., Chidambaram, B., Kalyanasundaram, A. and Angamuthu, R.** (2014). Transcriptome profiling reveals higher vertebrate orthologous of intra-cytoplasmic pattern recognition receptors in grey bamboo shark. *PLoS One* **9**, e100018.
- Kültz, D.** (2015). Physiological mechanisms used by fish to cope with salinity stress. *J. Exp. Biol.* **218**, 1907–1914.
- Kültz, D., Chakravarty, D. and Adilakshmi, T.** (2001). A novel 14-3-3 gene is osmoregulated in gill epithelium of the euryhaline teleost *Fundulus heteroclitus*. *J. Exp. Biol.* **204**, 2975–85.
- Lacy, E. R. and Reale, E.** (1985). The elasmobranch kidney II. Sequence and structure of the nephrons. *Anat. Embryol. (Berl).* **173**, 163–186.
- Lacy, E. R. and Reale, E.** (1986). The elasmobranch kidney. III. Fine structure of the peritubular sheath. *Anat. Embryol. (Berl).* **173**, 299–305.
- Langmead, B. and Salzberg, S. L.** (2012). Fast gapped-read alignment with Bowtie 2. *Nat. Methods* **9**, 357–359.
- Laxson, C. J., Condon, N. E., Drazen, J. C. and Yancey, P. H.** (2011). Decreasing urea: trimethylamine N-oxide ratios with depth in chondrichthyes: a physiological depth limit? *Physiol. Biochem. Zool.* **84**, 494–505.
- Li, B. and Dewey, C. N.** (2011). RSEM: Accurate transcript quantification from RNA-Seq data with or without a reference genome. *BMC Bioinformatics* **12**, 323.
- Li, S., Kato, A., Takabe, S., Chen, A.-P., Romero, M. F., Umezawa, T., Nakada, T., Hyodo, S. and Hirose, S.** (2013). Expression of a novel isoform of Na<sup>+</sup>/H<sup>+</sup> exchanger 3 in the kidney and intestine of banded houndshark, *Triakis scyllium*. *AJP Regul. Integr. Comp. Physiol.* **304**, R865–R876.
- Liedtke, W., Choe, Y., Martí-Renom, M. A., Bell, A. M., Denis, C. S., AndrejŠali, Hudspeth, A. J., Friedman, J. M. and Heller, S.** (2000). Vanilloid receptor–related osmotically activated channel (VR-OAC), a candidate vertebrate osmoreceptor. *Cell* **103**, 525–535.

- Lopez-Bojorquez, L., Villalobos, P., Garcia-G., C., Orozco, A. and Valverde-R., C.** (2007). Functional identification of an osmotic response element (ORE) in the promoter region of the killifish deiodinase 2 gene (FhDio2). *J. Exp. Biol.* **210**, 3126–3132.
- Lovejoy, N. R., Bermingham, E. and Martin, A. P.** (1998). Marine incursion into South America. *Nature* **396**, 421–422.
- MacLellan, R. J., Tunnah, L., Barnett, D., Wright, P. A., MacCormack, T. and Currie, S.** (2015). Chaperone roles for TMAO and HSP70 during hyposmotic stress in the spiny dogfish shark (*Squalus acanthias*). *J. Comp. Physiol. B Biochem. Syst. Environ. Physiol.* **185**, 729–740.
- Maier, T., Güell, M. and Serrano, L.** (2009). Correlation of mRNA and protein in complex biological samples. *FEBS Lett.* **583**, 3966–3973.
- Marshall, W. S.** (2005). Hypotonic shock mediation by p38 MAPK, JNK, PKC, FAK, OSR1 and SPAK in osmosensing chloride secreting cells of killifish opercular epithelium. *J. Exp. Biol.* **208**, 1063–1077.
- Marshall, W. S., Breves, J. P., Doohan, E. M., Tipsmark, C. K., Kelly, S. P., Robertson, G. N. and Schulte, P. M.** (2018). *claudin-10* isoform expression and cation selectivity change with salinity in salt-secreting epithelia of *Fundulus heteroclitus*. *J. Exp. Biol.* **221**, jeb168906.
- Martin, R. A.** (2005). Conservation of freshwater and euryhaline elasmobranchs: a review. *J. Mar. Biol. Assoc. UK* **85**, 1049.
- Martini, F. H.** (1998). The Ecology of Hagfishes. In *The Biology of Hagfishes* (ed. Jorgensen, J. M., Lomholt, J. P., Weber, R. E., and Malte, H.), pp. 57–77. London: Chapman & Hall.
- Mazon, E., Puzzolo, D., Caputi, A. P. and Cuzzocrea, S.** (2002). Role of IL-10 in hepatocyte tight junction alteration in mouse model of experimental colitis. *Mol. Med.* **8**, 353–66.
- McCarthy, D. J., Chen, Y. and Smyth, G. K.** (2012). Differential expression analysis of multifactor RNA-Seq experiments with respect to biological variation. *Nucleic Acids Res.* **40**, 4288–4297.
- McMillan, D. G. and Morse, W. W.** (1999). Essential Fish Habitat Source Document: Spiny Dogfish, *Squalus acanthias*, Life History and Habitat Characteristics. *U.S. Dep. Commer. NOAA Tech. Memo. NMFS-NE-15*, 1–19.
- Metzger, D. C. H. and Schulte, P. M.** (2016). Maternal stress has divergent effects on gene expression patterns in the brains of male and female threespine stickleback. *Proc. R. Soc. London B Biol. Sci.* **283**,
- Mines, G. R.** (1912). On the relations to electrolytes of the hearts of different species of animals. *J. Physiol.* **43**, 467–506.
- Morash, A. J., Mackellar, S. R. C., Tunnah, L., Barnett, D. A., Stehfest, K. M., Semmens, J. M. and Currie, S.** (2016). Pass the salt: physiological consequences of ecologically relevant hyposmotic exposure in juvenile gummy sharks (*Mustelus antarcticus*) and school sharks (*Galeorhinus galeus*). *Conserv. Physiol.* **4**, cow036.
- Morgan, R. L.** (2003a). Urea transport in kidney brush-border membrane vesicles from an elasmobranch, *Raja erinacea*. *J. Exp. Biol.* **206**, 3293–3302.
- Morgan, R. L.** (2003b). Regulation of a renal urea transporter with reduced salinity in a marine elasmobranch, *Raja erinacea*. *J. Exp. Biol.* **206**, 3285–3292.
- Morrissey, J. F. and Gruber, S. H.** (1993). Habitat selection by juvenile lemon sharks, *Negaprion brevirostris*. *Environ. Biol. Fishes* **38**, 311–319.
- Mortazavi, A., Williams, B. A., McCue, K., Schaeffer, L. and Wold, B.** (2008). Mapping and

- quantifying mammalian transcriptomes by RNA-Seq. *Nat. Methods* **5**, 621–628.
- Mulley, J. F., Hargreaves, A. D., Hegarty, M. J., Heller, R. S. and Swain, M. T.** (2014). Transcriptomic analysis of the lesser spotted catshark (*Scyliorhinus canicula*) pancreas, liver and brain reveals molecular level conservation of vertebrate pancreas function. *BMC Genomics* **15**, 1–18.
- Nagalakshmi, U., Wang, Z., Waern, K., Shou, C., Raha, D., Gerstein, M. and Snyder, M.** (2008). The Transcriptional Landscape of the Yeast Genome Defined by RNA Sequencing. *Science* (80-. ). **320**, 1344–1349.
- Nakada, T., Westhoff, C. M., Yamaguchi, Y., Hyodo, S., Li, X., Muro, T., Kato, A., Nakamura, N. and Hirose, S.** (2010). Rhesus glycoprotein P2 (Rhp2) is a novel member of the Rh family of ammonia transporters highly expressed in shark kidney. *J. Biol. Chem.* **285**, 2653–2664.
- Naour, S., Espinoza, B. M., Aedo, J. E., Zuloaga, R., Maldonado, J., Bastias-molina, M., Silva, H., Meneses, C., Gallardo-escarate, C., Molina, A., et al.** (2017). Transcriptomic analysis of the hepatic response to stress in the red cusk-eel (*Genypterus chilensis*): Insights into lipid metabolism, oxidative stress and liver steatosis. *PLoS One* 1–18.
- Naylor, G. J. P., Caira, J. N., Jensen, K., Rosana, K. A. M., Straube, N. and Lakner, C.** (2012). *Biology of Sharks and Their Relatives*.
- Nguyen, T. V., Jung, H., Nguyen, T. M., Hurwood, D. and Mather, P.** (2016). Evaluation of potential candidate genes involved in salinity tolerance in striped catfish (*Pangasianodon hypophthalmus*) using an RNA-Seq approach. *Mar. Genomics* **25**, 75–88.
- Nilsson, G. E.** (2007). Gill remodeling in fish - a new fashion or an ancient secret? *J. Exp. Biol.* **210**, 2403–2409.
- Nilsson, G. E., Dymowska, A. and Stecyk, J. A. W.** (2012). New insights into the plasticity of gill structure. *Respir. Physiol. Neurobiol.* **184**, 214–222.
- Nishimura, O., Hara, Y. and Kuraku, S.** (2017). GVolante for standardizing completeness assessment of genome and transcriptome assemblies. *Bioinformatics* **33**, 3635–3637.
- Okoniewski, M. J. and Miller, C. J.** (2006). Hybridization interactions between probesets in short oligo microarrays lead to spurious correlations. *BMC Bioinformatics* **7**, 1–14.
- Payan, P., Goldstein, L. and Forster, R. P.** (1973). Gills and kidneys in ureosmotic regulation in euryhaline skates. *Am. J. Physiol.* **224**, 367–372.
- Rahmatullah, M. and Boyde, T. R. C.** (1980). Improvements in the determination of urea using diacetyl monoxime; methods with and without deproteinisation. *Clin. Chim. Acta* **107**, 3–9.
- Randall, D. J., Wood, C. M., Perry, S. F., Bergman, H., Maloiy, G. M., Mommsen, T. P. and Wright, P. A.** (1989). Urea excretion as a strategy for survival in a fish living in a very alkaline environment. *Nature* **337**, 165–166.
- Reilly, B. ., Cramp, R. L., Wilson, J. M., Campbell, H. A. and Franklin, C. E.** (2011). Branchial osmoregulation in the euryhaline bull shark, *Carcharhinus leucas*: a molecular analysis of ion transporters. *J. Exp. Biol.* **214**, 2883–2895.
- Ricciotti, E. and FitzGerald, G. .** (2011). Prostaglandins and Inflammation. *Arterioscler. Thromb. Vasc. Biol.* **31**, 986–1000.
- Richards, V. P., Suzuki, H., Stanhope, M. J. and Shivji, M. S.** (2013). Characterization of the heart transcriptome of the white shark (*Carcharodon carcharias*). *BMC Genomics* **14**, 1–14.
- Riedl, S. J. and Shi, Y.** (2004). Molecular mechanisms of caspase regulation during apoptosis. *Nat. Rev. Mol. Cell Biol.* **5**, 897–907.
- Robinson, M. D., McCarthy, D. J. and Smyth, G. K.** (2009). edgeR: A Bioconductor package

- for differential expression analysis of digital gene expression data. *Bioinformatics* **26**, 139–140.
- Samuelsson, B.** (1983). Leukotrienes: mediators of immediate hypersensitivity reactions and inflammation. *Science* **220**, 568–575.
- Sanger, F. and Coulson, A. R.** (1975). A rapid method for determining sequences in DNA by primed synthesis with DNA polymerase. *J. Mol. Biol.* **94**, 441–448.
- Sanger, F., Nicklen, S. and Coulson, A. R.** (1977). DNA sequencing with chain-terminating inhibitors. *Proc. Natl. Acad. Sci.* **74**, 5463–5467.
- Schmidt-Nielsen, B., Truniger, B. and Rabinowitz, L.** (1972). Sodium-linked urea transport by the renal tubule of the spiny dogfish *Squalus acanthias*. *Comp. Biochem. Physiol. - A Physiol.* **42**, 13–25.
- Schooler, J. M., Goldstein, L., Hartman, S. C. and Forster, R. P.** (1966). Pathways of urea synthesis in the elasmobranch, *Squalus acanthias*. *Comp. Biochem. Physiol.* **18**, 271–281.
- Schultz, E. T. and McCormick, S. D.** (2013). Evolution in an evolutionary context. In *Fish Physiology: Euryhaline Fishes* (ed. McCormick, S. D., Farrell, A. P., and Brauner, C. J.), pp. 477–533. Elsevier.
- Scott, G. R., Schulte, P. M. and Wood, C. M.** (2006). Plasticity of osmoregulatory function in the killifish intestine: drinking rates, salt and water transport, and gene expression after freshwater transfer. *J. Exp. Biol.* **209**, 4040–4050.
- Shendure, J. and Ji, H.** (2008). Next-generation DNA sequencing. *Nat. Biotechnol.* **26**, 1135–1145.
- Shivkamat, P. and Roy, R.** (2005). Regulation of membrane lipid bilayer structure during salinity adaptation: A study with the gill epithelial cell membranes of *Oreochromis niloticus*. *Comp. Biochem. Physiol. - B Biochem. Mol. Biol.* **142**, 28–36.
- Shoemaker, V. H. and Nagy, K. A.** (1977). Osmoregulation in amphibians and reptiles. *Annu. Rev. Physiol.* **37**, 365–377.
- Silva, P., Stoff, J., Field, M., Fine, L., Forrest, J. N. and Epstein, F. H.** (1977). Mechanism of active chloride secretion by shark rectal gland: role of Na-K-ATPase in chloride transport. *Am. J. Physiol.* **233**, F298–306.
- Simpfendorfer, C. A., Freitas, G. G., Wiley, T. R. and Heupel, M. R.** (2005). Distribution and habitat partitioning of immature bull sharks (*Carcharhinus leucas*) in a Southwest Florida estuary. *Estuaries* **28**, 78–85.
- Simpson, W. W. and Ogden, E.** (1932). The physiological significance of urea. *J. Exp. Biol.* **9**, 1–5.
- Singer, D., Camargo, S. M. R., Huggel, K., Romeo, E., Danilczyk, U., Kuba, K., Chesnov, S., Caron, M. G., Penninger, J. M. and Verrey, F.** (2009). Orphan transporter SLC6A18 is renal neutral amino acid transporter B0AT3. *J. Biol. Chem.* **284**, 19953–19960.
- Smith, H. W.** (1936). The retention and physiological role of urea in the Elasmobranchii. *Biol. Rev.* **11**, 49–82.
- Song, X., Hu, X., Sun, B., Bo, Y., Wu, K., Xiao, L. and Gong, C.** (2017). A transcriptome analysis focusing on inflammation-related genes of grass carp intestines following infection with *Aeromonas hydrophila*. *Sci. Rep.* **7**, 1–12.
- Starokadomskyy, P., Gluck, N., Li, H., Chen, B., Wallis, M., Maine, G. N., Mao, X., Zaidi, I. W., Hein, M. Y., McDonald, F. J., et al.** (2013). CCDC22 deficiency in humans blunts activation of proinflammatory NF- $\kappa$ B signaling. *J. Clin. Invest.* **123**, 2244–2256.
- Steele, S. L., Yancey, P. H. and Wright, P. A.** (2005). The little skate *Raja erinacea* exhibits an

- extrahepatic ornithine urea cycle in the muscle and modulates nitrogen metabolism during low-salinity challenge. *Physiol. Biochem. Zool.* **78**, 216–26.
- Street, T. O., Bolen, D. W. and Rose, G. D.** (2006). A molecular mechanism for osmolyte-induced protein stability. *Proc. Natl. Academy Sci.* **103**, 13997–14002.
- Supek, F., Bošnjak, M., Škunca, N. and Šmuc, T.** (2011). REVIGO summarizes and visualizes long lists of gene ontology terms. *PLoS One* **6**, e21800.
- Suyama, M. and Tokuhira, T.** (1954). Urea content and ammonia formation of the muscle of cartilaginous fishes: the distribution of urea and trimethylamine oxide in different parts of the body. *Bull. Japanese Soc. Sci. Fish.* **19**, 1003–1006.
- Takabe, S., Inokuchi, M., Yamaguchi, Y. and Hyodo, S.** (2016). Distribution and dynamics of branchial ionocytes in houndshark reared in full-strength and diluted seawater environments. *Comp. Biochem. Physiol. - A Mol. Integr. Physiol.* **198**, 22–32.
- Tanaka, K.** (2009). The proteasome: Overview of structure and functions. *Proc. Japan Acad. Ser. B* **85**, 12–36.
- Tarca, A. L., Romero, R. and Draghici, S.** (2006). Analysis of microarray experiments of gene expression profiling. *Am. J. Obstet. Gynecol.* **195**, 373–388.
- Tomalty, K. M. H., Meek, M. H., Stephens, M. R., Rincón, G., Fangué, N. A., May, B. P. and Baerwald, M. R.** (2015). Transcriptional Response to Acute Thermal Exposure in Juvenile Chinook Salmon Determined by RNAseq. *G3 Genes, Genomes, Genet.* **5**, 1335–1349.
- Tse, W. K. F.** (2014). The role of osmotic stress transcription factor 1 in fishes. *Front. Zool.* **11**, 86.
- Ubeda, A. J., Simpfendorfer, C. A. and Heupel, M. R.** (2009). Movements of bonnetheads, *Sphyrna tiburo*, as a response to salinity change in a Florida estuary. *Environ. Biol. Fishes* **84**, 293–303.
- Wang, X. and Kültz, D.** (2017). Osmolality/salinity-responsive enhancers (OSREs) control induction of osmoprotective genes in euryhaline fish. *Proc. Natl. Acad. Sci.* **114**, E2729–E2738.
- Wang, Z., Gerstein, M. and Snyder, M.** (2009). RNA-Seq: a revolutionary tool for transcriptomics. *Nat. Rev. Genet.* **10**, 57–63.
- Wells, A., Anderson, W. G., Cains, J. E., Cooper, M. W. and Hazon, N.** (2006). Effects of angiotensin II and C-type natriuretic peptide on the in situ perfused trunk preparation of the dogfish, *Scyliorhinus canicula*. *Gen. Comp. Endocrinol.* **145**, 109–115.
- Wilson, J. M., Morgan, J. D., Vogl, a. W. and Randall, D. J.** (2002). Branchial mitochondria-rich cells in the dogfish *Squalus acanthias*. *Comp. Biochem. Physiol. - A Mol. Integr. Physiol.* **132**, 365–374.
- Wong, T. M. and Chan, D. K.** (1977). Physiological adjustments to dilution of the external medium in the Lip-shark *Hemiscyllium plagiolum* (Bennett). *J. Exp. Zool. Part A Ecol. Genet. Physiol.* **200**, 85–95.
- Wood, C. M. and Giacomini, M.** (2016). Feeding through your gills and turning a toxicant into a resource: how the dogfish shark scavenges ammonia from its environment. *J. Exp. Biol.* **219**, 3218–3226.
- Wood, C., Part, P. and Wright, P.** (1995). Ammonia and urea metabolism in relation to gill function and acid-base balance in a marine elasmobranch, the spiny dogfish (*Squalus acanthias*). *J. Exp. Biol.* **198**, 1545–58.
- Wood, C. M., Liew, H. J., De Boeck, G. and Walsh, P. J.** (2013). A perfusion study of the

- handling of urea and urea analogues by the gills of the dogfish shark (*Squalus acanthias*). *PeerJ* **1**, e33.
- Wright, P. A. and Wood, C. M.** (2015). Regulation of Ions, Acid–Base, and Nitrogenous Wastes in Elasmobranchs. In *Elasmobranch Fishes: Internal Processes* (ed. Shadwick, R. E.), Farrell, A. P.), and Brauner, C. J.), pp. 279–345. Elsevier Inc.
- Yamaguchi, Y., Takaki, S. and Hyodo, S.** (2009). Subcellular distribution of urea transporter in the collecting tubule of shark kidney is dependent on environmental salinity. *J. Exp. Zool. Part A Ecol. Genet. Physiol.* **311**, 705–718.
- Yancey, P. H.** (2015). Organic Osmolytes in Elasmobranchs. In *Physiology of Elasmobranch fishes: Internal Processes* (ed. Shadwick, R. E., Farrell, A. P., and Brauner, C. J.), pp. 221–277. Elsevier Inc.
- Yancey, P. H. and Somero, G. N.** (1979). Counteraction of urea destabilization of protein structure by methylamine osmoregulatory compounds of elasmobranch fishes. *Biochem. J.* **183**, 317–323.
- Yancey, P. H. and Somero, G. N.** (1980). Methylamine osmoregulatory solutes of elasmobranch fishes counteract urea inhibition of enzymes. *J. Exp. Zool.* **212**, 205–213.
- Young, M. D., Wakefield, M. J., Smyth, G. K. and Oshlack, A.** (2010). Gene ontology analysis for RNA-seq: accounting for selection bias. *Genome Biol.* **11**, R14.
- Zhang, X., Wen, H., Wang, H., Ren, Y., Zhao, J. and Li, Y.** (2017a). RNA-Seq analysis of salinity stress-responsive transcriptome in the liver of spotted sea bass (*Lateolabrax maculatus*). *PLoS One* **12**, 1–18.
- Zhang, Z., Zheng, Z., Cai, J., Liu, Q., Yang, J., Gong, Y., Wu, M., Shen, Q. and Xu, S.** (2017b). Effect of cadmium on oxidative stress and immune function of common carp (*Cyprinus carpio* L.) by transcriptome analysis. *Aquat. Toxicol.* **192**, 171–177.
- Zimmer, A. M. and Wood, C. M.** (2014). Exposure to Acute Severe Hypoxia Leads to Increased Urea Loss and Disruptions in Acid-Base and Ionoregulatory Balance in Dogfish Sharks (*Squalus acanthias*). *Physiol Biochem Zool* **87**, 623–639.
- Zou, Q., Habermann-Rottinghaus, S. M. and Murphy, K. P.** (1998). Urea effects on protein stability: hydrogen bonding and the hydrophobic effect. *PROTEINS Struct. Funct. Genet.* **31**, 107–115.

## Appendix

**Table S1.** Complete list of the differentially expressed transcripts following 65% SW exposure. Differential expression analysis at the transcript level was performed using the edgeR software within the Trinity pipeline and annotation was performed using Trinotate. Log<sub>2</sub>FC represent fold change of time point B relative to time point A. P-values were adjusted using the Benjamin-Hochberg correction for multiple comparisons. The annotation provided states the UniProt protein identifier followed by the species.

Trinity ID	Time point A	Time point B	Log <sub>2</sub> FC	P <sub>adj</sub> Value	Annotation
TRINITY_DN161214_c0_g1_i1	0hr	12hr	3.27	3.05E-03	JUN_SERCA
TRINITY_DN168738_c0_g1_i1	0hr	12hr	-5.85	4.37E-02	NA
TRINITY_DN169657_c0_g2_i1	0hr	12hr	-7.82	1.11E-02	NA
TRINITY_DN170805_c0_g1_i5	0hr	12hr	-8.31	1.02E-02	NA
TRINITY_DN170964_c0_g1_i1	0hr	12hr	2.89	4.78E-02	NA
TRINITY_DN171293_c0_g1_i4	0hr	12hr	-9.68	3.38E-02	CC124_DANRE
TRINITY_DN171894_c0_g1_i1	0hr	12hr	-10.97	9.74E-06	NA
TRINITY_DN172243_c1_g1_i3	0hr	12hr	-10.28	2.37E-02	NA
TRINITY_DN172243_c1_g1_i4	0hr	12hr	10.79	1.13E-02	NA
TRINITY_DN172243_c1_g1_i5	0hr	12hr	9.44	2.76E-02	NA
TRINITY_DN172328_c0_g1_i3	0hr	12hr	7.87	4.93E-02	SPDYA_HUMAN
TRINITY_DN172329_c12_g1_i2	0hr	12hr	9.24	5.65E-03	IMP3_HUMAN
TRINITY_DN172721_c0_g1_i5	0hr	12hr	-7.64	4.32E-02	NA
TRINITY_DN172829_c0_g3_i4	0hr	12hr	4.76	7.68E-03	CCL20_MOUSE
TRINITY_DN173383_c0_g1_i4	0hr	12hr	6.78	4.30E-02	VAOD2_XENTR
TRINITY_DN173409_c9_g2_i1	0hr	12hr	-10.82	1.91E-02	NA
TRINITY_DN173696_c3_g1_i8	0hr	12hr	10.39	1.58E-02	FKBP3_HUMAN
TRINITY_DN174167_c7_g1_i1	0hr	12hr	7.84	4.95E-02	NUP50_HUMAN
TRINITY_DN174372_c5_g1_i11	0hr	12hr	-7.70	2.12E-02	SNF8_HUMAN
TRINITY_DN174388_c0_g1_i27	0hr	12hr	-8.62	7.85E-07	IL10_HORSE
TRINITY_DN174630_c11_g1_i8	0hr	12hr	8.23	1.74E-02	NA
TRINITY_DN174812_c1_g2_i1	0hr	12hr	8.58	4.18E-02	NA
TRINITY_DN174877_c7_g1_i1	0hr	12hr	3.88	1.26E-02	NA
TRINITY_DN175212_c7_g1_i4	0hr	12hr	7.58	1.26E-03	LENG1_BOVIN
TRINITY_DN175500_c9_g1_i11	0hr	12hr	8.98	3.78E-02	WDR13_PANTR

TRINITY_DN175607_c11_g2_i5	Ohr	12hr	-5.87	1.86E-02	MAAI_RAT
TRINITY_DN175704_c12_g2_i1	Ohr	12hr	-10.15	3.06E-03	MAP2_HUMAN
TRINITY_DN176050_c7_g1_i6	Ohr	12hr	-9.70	7.70E-03	TMUB2_RAT
TRINITY_DN176101_c6_g1_i16	Ohr	12hr	9.02	3.78E-02	NA
TRINITY_DN176101_c6_g1_i22	Ohr	12hr	8.16	1.22E-03	NA
TRINITY_DN176101_c6_g1_i6	Ohr	12hr	8.34	4.95E-02	NA
TRINITY_DN176117_c6_g1_i2	Ohr	12hr	7.78	1.07E-02	NA
TRINITY_DN176144_c11_g1_i4	Ohr	12hr	-7.36	2.30E-02	NA
TRINITY_DN176147_c8_g1_i6	Ohr	12hr	6.88	1.00E-02	RS17_COTJA
TRINITY_DN176194_c4_g1_i3	Ohr	12hr	-9.14	5.79E-03	DEXI_DANRE
TRINITY_DN176221_c3_g2_i9	Ohr	12hr	-9.11	8.49E-03	LOX5_HUMAN
TRINITY_DN176293_c4_g2_i1	Ohr	12hr	-9.02	5.55E-04	NA
TRINITY_DN176620_c5_g3_i11	Ohr	12hr	-7.33	2.66E-02	LFG1_HUMAN
TRINITY_DN176754_c12_g1_i10	Ohr	12hr	8.32	1.15E-02	SURF4_TAKRU
TRINITY_DN176862_c5_g1_i5	Ohr	12hr	8.52	3.59E-02	MEPCE_HUMAN
TRINITY_DN177277_c9_g2_i1	Ohr	12hr	-6.82	3.59E-02	NOP56_MACFA
TRINITY_DN177280_c9_g1_i3	Ohr	12hr	9.58	3.89E-02	FBXW7_HUMAN
TRINITY_DN177281_c3_g3_i3	Ohr	12hr	8.47	1.11E-02	NA
TRINITY_DN177301_c1_g2_i7	Ohr	12hr	10.73	1.72E-09	HEX11_RAT
TRINITY_DN177451_c12_g4_i4	Ohr	12hr	-7.23	4.23E-02	NA
TRINITY_DN177452_c9_g4_i2	Ohr	12hr	9.15	3.72E-02	NA
TRINITY_DN177492_c5_g1_i13	Ohr	12hr	9.64	3.24E-02	CNO10_HUMAN
TRINITY_DN177675_c0_g1_i7	Ohr	12hr	-8.80	4.44E-02	LATS1_HUMAN
TRINITY_DN177848_c4_g1_i16	Ohr	12hr	8.32	4.48E-02	BL1S6_BOVIN
TRINITY_DN177915_c12_g3_i6	Ohr	12hr	8.16	4.48E-02	NA
TRINITY_DN178035_c5_g1_i4	Ohr	12hr	8.71	7.03E-03	NA
TRINITY_DN178035_c5_g1_i8	Ohr	12hr	8.67	9.51E-03	NA
TRINITY_DN178379_c10_g7_i1	Ohr	12hr	4.48	4.16E-02	NA
TRINITY_DN178442_c1_g2_i5	Ohr	12hr	-8.19	4.87E-02	UBE2T_XENLA
TRINITY_DN178549_c16_g1_i6	Ohr	12hr	-8.95	4.48E-02	UCHL5_PIG
TRINITY_DN178559_c4_g1_i6	Ohr	12hr	9.11	3.65E-02	NA
TRINITY_DN178610_c8_g2_i9	Ohr	12hr	-7.10	4.26E-02	NA
TRINITY_DN178768_c4_g1_i5	Ohr	12hr	8.61	3.54E-02	PRPF3_CHICK
TRINITY_DN178814_c12_g1_i5	Ohr	12hr	-8.93	1.91E-07	S2533_DANRE
TRINITY_DN178862_c11_g2_i3	Ohr	12hr	-8.35	1.13E-02	DNAI2_HUMAN
TRINITY_DN179152_c1_g1_i10	Ohr	12hr	7.41	2.27E-02	NA
TRINITY_DN179242_c5_g2_i8	Ohr	12hr	-6.89	4.87E-02	EFHC2_DANRE
TRINITY_DN179243_c7_g1_i12	Ohr	12hr	-10.39	2.30E-05	VWA3A_HUMAN
TRINITY_DN179282_c15_g1_i4	Ohr	12hr	5.48	1.00E-02	NA

TRINITY_DN179328_c8_g2_i2	Ohr	12hr	8.38	1.13E-02	NA
TRINITY_DN179384_c0_g4_i4	Ohr	12hr	9.19	3.02E-02	TSAP1_HUMAN
TRINITY_DN179559_c21_g2_i1	Ohr	12hr	-5.85	1.91E-02	NA
TRINITY_DN179662_c3_g2_i4	Ohr	12hr	-8.56	4.95E-02	IF2_DESHY
TRINITY_DN179664_c5_g5_i2	Ohr	12hr	10.24	3.25E-04	NA
TRINITY_DN179816_c0_g2_i16	Ohr	12hr	4.49	2.71E-02	NA
TRINITY_DN179843_c1_g2_i8	Ohr	12hr	7.62	3.16E-03	NA
TRINITY_DN180125_c12_g1_i3	Ohr	12hr	-7.37	5.46E-03	NA
TRINITY_DN180265_c9_g1_i5	Ohr	12hr	6.63	4.34E-02	NA
TRINITY_DN180330_c2_g1_i1	Ohr	12hr	-7.60	5.83E-04	NA
TRINITY_DN180368_c7_g1_i9	Ohr	12hr	7.92	4.82E-02	ZMY12_HUMAN
TRINITY_DN180393_c6_g1_i2	Ohr	12hr	7.73	2.55E-03	NA
TRINITY_DN180424_c1_g1_i17	Ohr	12hr	7.45	2.02E-03	AAK1_MOUSE
TRINITY_DN180712_c6_g1_i2	Ohr	12hr	7.94	4.48E-02	PDLI2_BOVIN
TRINITY_DN180817_c8_g1_i4	Ohr	12hr	2.74	3.18E-02	PGH2_RABIT
TRINITY_DN180862_c3_g1_i16	Ohr	12hr	9.75	1.37E-04	TCPB_BOVIN
TRINITY_DN180862_c3_g1_i18	Ohr	12hr	-8.87	4.26E-02	TCPB_BOVIN
TRINITY_DN180862_c3_g1_i19	Ohr	12hr	-11.06	1.30E-02	TCPB_BOVIN
TRINITY_DN180862_c3_g1_i21	Ohr	12hr	12.35	9.47E-11	TCPB_RAT
TRINITY_DN180930_c6_g1_i1	Ohr	12hr	-9.34	4.48E-02	NA
TRINITY_DN181003_c4_g1_i1	Ohr	12hr	-10.37	2.61E-05	TF2AA_HUMAN
TRINITY_DN181077_c0_g1_i5	Ohr	12hr	-9.96	3.83E-03	NA
TRINITY_DN181104_c1_g1_i3	Ohr	12hr	8.41	3.06E-03	IDLC_RAT
TRINITY_DN181210_c11_g1_i4	Ohr	12hr	-6.86	4.07E-02	NA
TRINITY_DN181351_c0_g1_i15	Ohr	12hr	5.72	2.83E-02	NA
TRINITY_DN181351_c0_g1_i2	Ohr	12hr	7.34	4.66E-02	ART2_YEAST
TRINITY_DN181407_c0_g1_i11	Ohr	12hr	-7.51	1.76E-03	PICK1_MOUSE
TRINITY_DN181453_c7_g1_i1	Ohr	12hr	3.63	1.74E-06	RN186_BOVIN
TRINITY_DN181463_c5_g1_i3	Ohr	12hr	9.61	2.94E-02	SYEM_CHICK
TRINITY_DN181725_c0_g1_i4	Ohr	12hr	8.66	2.38E-03	RRT15_YEAST
TRINITY_DN181725_c0_g1_i7	Ohr	12hr	5.89	2.56E-02	NA
TRINITY_DN181760_c5_g5_i2	Ohr	12hr	-8.42	1.56E-02	NA
TRINITY_DN181892_c9_g3_i4	Ohr	12hr	9.74	4.52E-03	NA
TRINITY_DN182342_c0_g1_i2	Ohr	12hr	-10.67	3.39E-02	ARC1B_RAT
TRINITY_DN182445_c4_g2_i7	Ohr	12hr	8.19	4.48E-02	NA
TRINITY_DN182642_c3_g1_i2	Ohr	12hr	8.97	3.88E-02	NA
TRINITY_DN182642_c3_g1_i4	Ohr	12hr	10.49	2.41E-02	NA
TRINITY_DN182642_c3_g1_i9	Ohr	12hr	9.42	2.79E-02	NA
TRINITY_DN182727_c2_g1_i8	Ohr	12hr	-5.17	3.78E-02	WWP2_HUMAN

TRINITY_DN182752_c9_g1_i2	Ohr	12hr	7.11	4.41E-02	NA
TRINITY_DN182955_c3_g1_i3	Ohr	12hr	-11.04	8.89E-04	NA
TRINITY_DN183286_c1_g2_i3	Ohr	12hr	6.78	1.62E-02	NA
TRINITY_DN183387_c0_g1_i13	Ohr	12hr	8.24	3.02E-02	YL154_YEAST
TRINITY_DN183387_c0_g1_i14	Ohr	12hr	7.01	4.44E-02	YL154_YEAST
TRINITY_DN183387_c0_g1_i5	Ohr	12hr	6.00	1.91E-02	YL154_YEAST
TRINITY_DN183486_c1_g1_i1	Ohr	12hr	6.16	2.43E-02	YL154_YEAST
TRINITY_DN183499_c7_g1_i2	Ohr	12hr	-8.69	4.48E-02	NA
TRINITY_DN183586_c6_g1_i1	Ohr	12hr	-9.21	1.89E-02	TM213_HUMAN
TRINITY_DN183625_c5_g1_i9	Ohr	12hr	9.21	1.68E-04	SCAM3_BOVIN
TRINITY_DN183700_c0_g1_i1	Ohr	12hr	3.21	4.66E-02	ATS1_HUMAN
TRINITY_DN183700_c0_g1_i10	Ohr	12hr	9.60	5.41E-04	ATS1_HUMAN
TRINITY_DN183700_c0_g1_i6	Ohr	12hr	4.78	2.09E-02	ATS1_HUMAN
TRINITY_DN183830_c5_g3_i1	Ohr	12hr	7.15	1.90E-02	ITAM_MOUSE
TRINITY_DN184111_c7_g3_i8	Ohr	12hr	7.16	4.48E-02	NA
TRINITY_DN184298_c0_g1_i2	Ohr	12hr	-9.47	3.62E-02	NA
TRINITY_DN184485_c4_g1_i2	Ohr	12hr	7.08	4.91E-04	NA
TRINITY_DN184671_c4_g1_i2	Ohr	12hr	-8.83	4.42E-02	NA
TRINITY_DN184759_c9_g1_i7	Ohr	12hr	-7.99	4.95E-02	COIL_XENLA
TRINITY_DN184862_c6_g1_i1	Ohr	12hr	7.38	2.70E-02	BANP_XENTR
TRINITY_DN185152_c7_g1_i1	Ohr	12hr	7.51	3.24E-02	NA
TRINITY_DN185152_c7_g1_i5	Ohr	12hr	11.06	9.55E-03	PLLP_BOVIN
TRINITY_DN185220_c1_g1_i3	Ohr	12hr	-9.28	5.55E-04	DLP1_HUMAN
TRINITY_DN185241_c5_g1_i17	Ohr	12hr	-8.95	4.89E-04	CHMP7_HUMAN
TRINITY_DN185445_c0_g2_i3	Ohr	12hr	4.60	5.79E-03	NOS2_HUMAN
TRINITY_DN185464_c6_g1_i10	Ohr	12hr	-9.07	2.96E-04	GFI1_CANFA
TRINITY_DN185588_c3_g1_i2	Ohr	12hr	-6.80	1.37E-02	TOPK_MOUSE
TRINITY_DN185602_c11_g2_i1	Ohr	12hr	-5.53	3.49E-02	Tm1
TRINITY_DN185645_c0_g2_i1	Ohr	12hr	10.01	2.11E-02	NA
TRINITY_DN185653_c1_g1_i15	Ohr	12hr	8.87	3.29E-02	COPD_PONAB
TRINITY_DN185704_c6_g1_i4	Ohr	12hr	-8.93	4.52E-02	CEP68_MOUSE
TRINITY_DN185752_c2_g1_i3	Ohr	12hr	-8.55	9.51E-03	DMAP1_HUMAN
TRINITY_DN185816_c4_g1_i8	Ohr	12hr	-7.26	2.98E-02	GPR39_PIG
TRINITY_DN186127_c2_g1_i2	Ohr	12hr	-7.83	1.37E-02	NA
TRINITY_DN186170_c4_g1_i3	Ohr	12hr	-8.25	9.17E-03	GOLP3_RAT
TRINITY_DN186334_c0_g1_i2	Ohr	12hr	-9.45	4.01E-02	NA
TRINITY_DN186353_c6_g3_i1	Ohr	12hr	-8.93	1.18E-02	NA
TRINITY_DN186412_c13_g1_i5	Ohr	12hr	-9.09	2.86E-03	NA
TRINITY_DN186497_c3_g1_i7	Ohr	12hr	6.25	1.88E-02	KAT5_RAT

TRINITY_DN186707_c7_g1_i3	Ohr	12hr	7.18	4.19E-03	NA
TRINITY_DN186770_c7_g1_i3	Ohr	12hr	-8.42	4.93E-02	ISOC2_XENLA
TRINITY_DN186803_c6_g1_i2	Ohr	12hr	-7.73	2.22E-02	ARP2B_XENLA
TRINITY_DN186863_c4_g1_i11	Ohr	12hr	-8.71	1.67E-02	HDA1B_XENLA
TRINITY_DN186867_c4_g2_i2	Ohr	12hr	4.39	7.87E-04	NA
TRINITY_DN187108_c7_g6_i1	Ohr	12hr	6.11	2.28E-02	NA
TRINITY_DN187306_c1_g1_i4	Ohr	12hr	-7.42	3.03E-02	RN112_BOVIN
TRINITY_DN187344_c0_g1_i3	Ohr	12hr	5.26	3.59E-02	NA
TRINITY_DN187491_c0_g3_i2	Ohr	12hr	-9.94	3.44E-03	WBP11_MOUSE
TRINITY_DN187760_c2_g1_i10	Ohr	12hr	-9.85	6.45E-03	TSN3_PONAB
TRINITY_DN187835_c1_g1_i23	Ohr	12hr	-8.14	9.18E-03	ERGI3_DANRE
TRINITY_DN187851_c12_g1_i3	Ohr	12hr	-10.24	2.43E-02	HAUS1_HUMAN
TRINITY_DN187940_c6_g2_i2	Ohr	12hr	10.21	2.10E-03	TAF11_MOUSE
TRINITY_DN187989_c6_g2_i14	Ohr	12hr	7.84	2.13E-06	EK11_MOUSE
TRINITY_DN188228_c12_g1_i4	Ohr	12hr	7.35	8.80E-03	MTNA_HUMAN
TRINITY_DN188367_c9_g3_i3	Ohr	12hr	6.83	2.69E-02	NA
TRINITY_DN188555_c2_g1_i3	Ohr	12hr	7.73	5.68E-04	NALP3_HUMAN
TRINITY_DN188558_c11_g3_i3	Ohr	12hr	-5.83	9.05E-03	CCNK_MOUSE
TRINITY_DN188563_c2_g2_i10	Ohr	12hr	-9.34	4.23E-02	STXB4_HUMAN
TRINITY_DN188563_c2_g2_i7	Ohr	12hr	8.71	4.59E-04	STXB4_HUMAN
TRINITY_DN188607_c1_g3_i6	Ohr	12hr	10.07	2.56E-02	BAG4_MOUSE
TRINITY_DN188825_c21_g1_i2	Ohr	12hr	-8.50	3.25E-04	NA
TRINITY_DN188980_c1_g1_i14	Ohr	12hr	7.66	2.28E-03	JTB_HUMAN
TRINITY_DN189033_c10_g1_i2	Ohr	12hr	6.91	7.40E-03	NA
TRINITY_DN189168_c4_g2_i2	Ohr	12hr	-10.63	3.34E-03	PLCA_HUMAN
TRINITY_DN189262_c16_g1_i13	Ohr	12hr	8.47	3.65E-02	NA
TRINITY_DN189283_c5_g2_i12	Ohr	12hr	9.91	3.59E-02	XBP1_BOVIN
TRINITY_DN189453_c2_g1_i16	Ohr	12hr	8.54	7.62E-03	WDR73_XENLA
TRINITY_DN189605_c14_g1_i5	Ohr	12hr	9.61	1.27E-03	CD53_HUMAN
TRINITY_DN189618_c10_g3_i1	Ohr	12hr	-8.42	4.49E-02	NA
TRINITY_DN189678_c9_g3_i2	Ohr	12hr	-5.55	4.18E-02	FACR1_CHICK
TRINITY_DN189869_c2_g1_i11	Ohr	12hr	-8.09	1.36E-02	TM138_HUMAN
TRINITY_DN190057_c5_g1_i1	Ohr	12hr	-7.30	2.62E-02	NA
TRINITY_DN190067_c3_g1_i1	Ohr	12hr	-8.10	3.00E-02	CDO1_BOVIN
TRINITY_DN190317_c0_g1_i29	Ohr	12hr	-8.94	2.38E-03	FXDC2_MACFA
TRINITY_DN190443_c0_g2_i16	Ohr	12hr	-10.66	5.81E-04	VATB2_PONAB
TRINITY_DN190592_c0_g1_i6	Ohr	12hr	9.10	3.24E-02	PPAC2_DANRE
TRINITY_DN190648_c0_g1_i12	Ohr	12hr	-8.11	1.90E-02	NA
TRINITY_DN190775_c2_g3_i6	Ohr	12hr	-11.12	9.31E-04	CISY_DANRE

TRINITY_DN190963_c18_g1_i2	Ohr	12hr	-5.78	3.99E-02	NA
TRINITY_DN191006_c4_g1_i4	Ohr	12hr	9.84	3.24E-02	ERP29_MOUSE
TRINITY_DN191009_c0_g8_i5	Ohr	12hr	-12.00	1.48E-07	RM09_HUMAN
TRINITY_DN191102_c3_g1_i16	Ohr	12hr	-8.70	1.07E-02	ALKMO_XENTR
TRINITY_DN191143_c7_g1_i1	Ohr	12hr	-6.80	4.65E-02	NA
TRINITY_DN191143_c7_g1_i4	Ohr	12hr	-9.98	3.84E-03	NA
TRINITY_DN191150_c6_g2_i2	Ohr	12hr	-7.94	5.41E-04	NA
TRINITY_DN191303_c2_g2_i19	Ohr	12hr	8.13	6.98E-03	IF4G1_MOUSE
TRINITY_DN191303_c2_g2_i21	Ohr	12hr	7.80	1.44E-02	IF4G1_MOUSE
TRINITY_DN191360_c1_g1_i9	Ohr	12hr	-9.19	3.96E-02	SPT2_HUMAN
TRINITY_DN191458_c8_g1_i2	Ohr	12hr	7.42	2.15E-02	NA
TRINITY_DN191491_c5_g3_i3	Ohr	12hr	-7.06	1.07E-02	NA
TRINITY_DN191516_c0_g1_i2	Ohr	12hr	-7.93	1.11E-02	NA
TRINITY_DN191967_c1_g1_i11	Ohr	12hr	9.12	4.37E-02	LRCH3_MOUSE
TRINITY_DN192046_c4_g1_i2	Ohr	12hr	-9.83	6.14E-03	RFA3_HUMAN
TRINITY_DN192084_c3_g2_i4	Ohr	12hr	-8.21	5.29E-04	TF2H4_MOUSE
TRINITY_DN192255_c1_g1_i2	Ohr	12hr	-8.49	8.41E-03	NA
TRINITY_DN192369_c5_g1_i23	Ohr	12hr	-8.94	1.69E-03	CD82_RAT
TRINITY_DN192384_c2_g2_i9	Ohr	12hr	-9.40	4.42E-02	DX39B_CANFA
TRINITY_DN192389_c1_g2_i2	Ohr	12hr	-5.41	2.96E-03	NA
TRINITY_DN192395_c10_g1_i2	Ohr	12hr	-8.59	4.44E-02	NA
TRINITY_DN192433_c4_g7_i1	Ohr	12hr	7.49	2.93E-02	CTF2_MOUSE
TRINITY_DN192952_c6_g1_i1	Ohr	12hr	5.78	3.05E-02	NA
TRINITY_DN192991_c9_g1_i1	Ohr	12hr	3.67	2.27E-02	NA
TRINITY_DN193142_c5_g9_i2	Ohr	12hr	7.33	6.27E-03	NA
TRINITY_DN193166_c1_g1_i3	Ohr	12hr	4.42	5.79E-03	B2L14_RAT
TRINITY_DN193277_c6_g1_i1	Ohr	12hr	-8.58	4.52E-02	HYAL_CROAD
TRINITY_DN193366_c2_g3_i3	Ohr	12hr	-9.24	6.27E-03	STAR3_HUMAN
TRINITY_DN193366_c2_g6_i10	Ohr	12hr	8.78	7.70E-03	RRP8_HUMAN
TRINITY_DN193515_c0_g2_i12	Ohr	12hr	-10.35	2.28E-02	AKIR1_XENTR
TRINITY_DN193544_c13_g1_i3	Ohr	12hr	-8.13	1.69E-02	NA
TRINITY_DN193599_c9_g1_i8	Ohr	12hr	-10.35	2.40E-03	AGK_HUMAN
TRINITY_DN193766_c4_g4_i2	Ohr	12hr	9.58	3.24E-02	NA
TRINITY_DN193809_c1_g2_i10	Ohr	12hr	-11.09	1.37E-02	UQCC3_DANRE
TRINITY_DN193830_c8_g1_i1	Ohr	12hr	6.33	1.91E-02	NA
TRINITY_DN193872_c7_g2_i4	Ohr	12hr	-8.86	4.48E-02	NA
TRINITY_DN193931_c6_g3_i5	Ohr	12hr	7.89	4.35E-04	RBBP6_HUMAN
TRINITY_DN194002_c3_g1_i8	Ohr	12hr	-10.06	3.14E-02	ZN217_HUMAN
TRINITY_DN194082_c6_g2_i3	Ohr	12hr	-8.05	1.48E-02	NA

TRINITY_DN194161_c8_g2_i1	Ohr	12hr	8.00	1.11E-02	NA
TRINITY_DN194177_c0_g2_i13	Ohr	12hr	-7.46	3.16E-03	U5S1_CHICK
TRINITY_DN194215_c0_g1_i1	Ohr	12hr	4.89	1.68E-02	NA
TRINITY_DN194297_c0_g1_i1	Ohr	12hr	9.50	4.48E-02	NA
TRINITY_DN194297_c0_g7_i1	Ohr	12hr	4.53	1.56E-02	NA
TRINITY_DN194352_c0_g1_i3	Ohr	12hr	10.95	2.44E-06	NDK3_HUMAN
TRINITY_DN194404_c3_g2_i2	Ohr	12hr	9.19	4.73E-03	ARMC6_MOUSE
TRINITY_DN194482_c5_g1_i5	Ohr	12hr	8.96	3.78E-02	GATL1_XENLA
TRINITY_DN194537_c0_g2_i4	Ohr	12hr	-8.85	3.34E-04	NA
TRINITY_DN194537_c0_g2_i5	Ohr	12hr	9.19	7.03E-03	NA
TRINITY_DN194578_c9_g2_i4	Ohr	12hr	-6.99	3.59E-02	UBC12_XENTR
TRINITY_DN194663_c2_g2_i11	Ohr	12hr	8.52	4.87E-02	NA
TRINITY_DN194663_c2_g2_i12	Ohr	12hr	5.10	3.97E-02	NA
TRINITY_DN194663_c2_g2_i13	Ohr	12hr	5.93	9.44E-03	NA
TRINITY_DN194663_c2_g2_i9	Ohr	12hr	5.41	2.29E-02	NA
TRINITY_DN194679_c1_g2_i5	Ohr	12hr	8.56	4.17E-02	NA
TRINITY_DN194693_c2_g1_i13	Ohr	12hr	-8.73	1.47E-06	GCP3_HUMAN
TRINITY_DN194698_c0_g1_i3	Ohr	12hr	-8.43	1.13E-03	PARP3_HUMAN
TRINITY_DN194702_c2_g3_i1	Ohr	12hr	5.86	3.00E-02	NA
TRINITY_DN194725_c4_g1_i7	Ohr	12hr	8.43	4.34E-02	S22A2_HUMAN
TRINITY_DN194769_c6_g4_i3	Ohr	12hr	6.81	4.12E-02	VAV_BOVIN
TRINITY_DN195027_c5_g1_i10	Ohr	12hr	5.44	2.02E-03	STYK1_HUMAN
TRINITY_DN195035_c2_g1_i4	Ohr	12hr	-10.53	2.00E-02	PARK7_CHICK
TRINITY_DN195196_c5_g4_i3	Ohr	12hr	-6.85	1.38E-02	NA
TRINITY_DN195262_c3_g1_i4	Ohr	12hr	8.43	1.90E-02	NA
TRINITY_DN195262_c3_g1_i6	Ohr	12hr	5.25	3.24E-02	NA
TRINITY_DN195422_c3_g4_i4	Ohr	12hr	10.07	3.59E-03	EYA3_HUMAN
TRINITY_DN195428_c4_g1_i10	Ohr	12hr	-7.61	1.57E-02	SMIM4_MOUSE
TRINITY_DN195428_c4_g1_i7	Ohr	12hr	-7.18	4.48E-02	SMIM4_MOUSE
TRINITY_DN195508_c0_g2_i11	Ohr	12hr	5.14	4.98E-02	STK24_HUMAN
TRINITY_DN195675_c9_g3_i3	Ohr	12hr	-3.97	1.69E-02	NA
TRINITY_DN195723_c8_g2_i1	Ohr	12hr	-8.68	9.51E-03	SHPK_HUMAN
TRINITY_DN195837_c0_g1_i12	Ohr	12hr	8.63	4.34E-02	CSK21_CHICK
TRINITY_DN195837_c1_g1_i1	Ohr	12hr	9.60	3.75E-03	NA
TRINITY_DN196032_c4_g1_i10	Ohr	12hr	8.60	1.55E-05	ORN_BOVIN
TRINITY_DN196125_c2_g2_i1	Ohr	12hr	-6.42	1.65E-02	NA
TRINITY_DN196194_c1_g6_i11	Ohr	12hr	-6.75	3.48E-03	NA
TRINITY_DN196194_c1_g6_i5	Ohr	12hr	-5.50	9.05E-03	NA
TRINITY_DN196335_c1_g1_i12	Ohr	12hr	11.62	1.55E-07	MICU1_XENTR

TRINITY_DN196728_c6_g1_i9	Ohr	12hr	8.60	3.54E-02	NA
TRINITY_DN196908_c8_g1_i2	Ohr	12hr	8.25	4.48E-02	NA
TRINITY_DN196927_c3_g2_i2	Ohr	12hr	6.46	4.44E-02	TNF6B_HUMAN
TRINITY_DN196987_c5_g2_i2	Ohr	12hr	-8.76	9.05E-03	NA
TRINITY_DN197051_c7_g2_i2	Ohr	12hr	-7.85	4.44E-03	NA
TRINITY_DN197070_c5_g3_i2	Ohr	12hr	-9.43	4.07E-02	NA
TRINITY_DN197105_c8_g1_i1	Ohr	12hr	9.75	1.16E-03	NA
TRINITY_DN197105_c8_g1_i7	Ohr	12hr	9.84	3.25E-03	NA
TRINITY_DN197130_c1_g1_i12	Ohr	12hr	-7.18	4.07E-02	RSU1_BOVIN
TRINITY_DN197183_c11_g1_i1	Ohr	12hr	-8.64	4.95E-02	NA
TRINITY_DN197236_c2_g2_i5	Ohr	12hr	-9.07	4.26E-02	NA
TRINITY_DN197456_c2_g1_i8	Ohr	12hr	8.72	4.66E-02	SPCS1_MOUSE
TRINITY_DN197587_c3_g1_i1	Ohr	12hr	9.35	3.43E-02	CASP6_MOUSE
TRINITY_DN197617_c0_g1_i1	Ohr	12hr	7.91	4.27E-02	RTN4_MOUSE
TRINITY_DN197874_c2_g1_i10	Ohr	12hr	-6.85	4.44E-02	NA
TRINITY_DN197876_c8_g4_i3	Ohr	12hr	-8.84	8.38E-03	NA
TRINITY_DN198029_c8_g1_i2	Ohr	12hr	9.78	3.02E-02	NA
TRINITY_DN198069_c4_g1_i1	Ohr	12hr	-8.83	4.32E-02	CNPY4_DANRE
TRINITY_DN198072_c3_g1_i5	Ohr	12hr	-9.66	4.32E-03	CHMP3_DANRE
TRINITY_DN198093_c11_g1_i10	Ohr	12hr	-8.83	4.89E-04	TAF3_CHICK
TRINITY_DN198111_c4_g2_i29	Ohr	12hr	5.06	4.75E-02	GRN_HUMAN
TRINITY_DN198309_c11_g3_i3	Ohr	12hr	-8.63	1.06E-02	PCID2_HUMAN
TRINITY_DN198516_c4_g2_i12	Ohr	12hr	-9.36	4.07E-02	SEPT7_XENLA
TRINITY_DN198536_c10_g3_i2	Ohr	12hr	-10.03	4.07E-02	NA
TRINITY_DN198561_c1_g1_i3	Ohr	12hr	2.71	1.20E-03	PDPFL_HUMAN
TRINITY_DN198669_c2_g1_i14	Ohr	12hr	10.73	1.58E-02	S2536_CHICK
TRINITY_DN198753_c0_g1_i4	Ohr	12hr	9.25	3.24E-02	BECN1_MOUSE
TRINITY_DN198858_c2_g1_i8	Ohr	12hr	9.20	2.17E-04	HGS_MOUSE
TRINITY_DN198932_c13_g2_i2	Ohr	12hr	-7.01	3.60E-02	NA
TRINITY_DN198961_c1_g2_i4	Ohr	12hr	-4.83	1.60E-03	GALK1_BOVIN
TRINITY_DN198991_c3_g1_i8	Ohr	12hr	-10.15	2.55E-03	LEO1_DANRE
TRINITY_DN199121_c0_g1_i3	Ohr	12hr	9.42	6.45E-03	CNO6L_HUMAN
TRINITY_DN199217_c21_g1_i7	Ohr	12hr	10.12	1.91E-02	5HT2B_HUMAN
TRINITY_DN199222_c1_g2_i9	Ohr	12hr	-7.85	3.44E-03	CW15A_XENLA
TRINITY_DN199506_c3_g1_i3	Ohr	12hr	-7.22	4.48E-02	MMP25_HUMAN
TRINITY_DN199526_c1_g2_i1	Ohr	12hr	-8.11	1.88E-02	NA
TRINITY_DN199545_c8_g1_i5	Ohr	12hr	8.56	4.34E-02	NA
TRINITY_DN199834_c3_g3_i2	Ohr	12hr	-8.08	3.15E-02	NA
TRINITY_DN199952_c6_g1_i2	Ohr	12hr	10.31	1.72E-09	NA

TRINITY_DN200253_c6_g2_i1	Ohr	12hr	6.39	3.78E-02	NA
TRINITY_DN200339_c2_g2_i11	Ohr	12hr	-4.53	4.34E-02	IMA1_MOUSE
TRINITY_DN200423_c2_g1_i9	Ohr	12hr	11.27	2.28E-03	TPIS_MACMU
TRINITY_DN200449_c3_g1_i17	Ohr	12hr	8.94	9.86E-03	S6A18_RAT
TRINITY_DN200454_c8_g4_i3	Ohr	12hr	-10.44	2.17E-03	EIF3I_TAEGU
TRINITY_DN200711_c6_g2_i7	Ohr	12hr	-7.67	1.52E-02	NA
TRINITY_DN200823_c5_g1_i8	Ohr	12hr	8.40	1.17E-02	UEVLD_HUMAN
TRINITY_DN200886_c5_g1_i6	Ohr	12hr	-7.94	7.46E-05	RF1ML_BOVIN
TRINITY_DN200898_c1_g1_i4	Ohr	12hr	-10.72	1.73E-02	S14L1_HUMAN
TRINITY_DN200898_c1_g1_i7	Ohr	12hr	-9.51	3.59E-02	S14L1_HUMAN
TRINITY_DN200951_c3_g1_i14	Ohr	12hr	-7.87	1.88E-02	MTF2_PONAB
TRINITY_DN201083_c8_g2_i2	Ohr	12hr	7.40	2.20E-02	NA
TRINITY_DN201155_c7_g1_i3	Ohr	12hr	-10.53	2.10E-03	MXI1_MOUSE
TRINITY_DN201341_c7_g1_i1	Ohr	12hr	8.81	4.01E-02	SL9A9_HUMAN
TRINITY_DN201348_c1_g1_i18	Ohr	12hr	8.58	8.30E-03	SSUH2_HUMAN
TRINITY_DN201467_c2_g1_i5	Ohr	12hr	-8.84	4.66E-02	NA
TRINITY_DN201487_c0_g2_i7	Ohr	12hr	-7.81	1.13E-02	NA
TRINITY_DN201652_c6_g1_i3	Ohr	12hr	-9.55	4.19E-02	GANAB_MACFA
TRINITY_DN201658_c3_g1_i16	Ohr	12hr	9.66	2.76E-02	NA
TRINITY_DN201837_c2_g1_i9	Ohr	12hr	-4.93	1.30E-02	HGFL_BOVIN
TRINITY_DN202066_c3_g3_i10	Ohr	12hr	-9.18	1.13E-02	DCAM_MESAU
TRINITY_DN202139_c11_g1_i3	Ohr	12hr	8.60	1.02E-02	ERCC3_BOVIN
TRINITY_DN202160_c4_g1_i2	Ohr	12hr	5.62	4.87E-02	NA
TRINITY_DN202160_c4_g2_i2	Ohr	12hr	4.96	4.37E-02	NA
TRINITY_DN202160_c4_g3_i1	Ohr	12hr	5.09	1.67E-02	HS30C_XENLA
TRINITY_DN202160_c4_g5_i1	Ohr	12hr	6.61	3.96E-02	HSP30_ONCTS
TRINITY_DN202178_c3_g1_i1	Ohr	12hr	-9.83	1.75E-05	NA
TRINITY_DN202301_c10_g1_i3	Ohr	12hr	7.43	2.59E-02	CCNL1_HUMAN
TRINITY_DN202355_c2_g2_i4	Ohr	12hr	8.89	4.21E-02	TNF6B_HUMAN
TRINITY_DN202466_c2_g2_i2	Ohr	12hr	9.93	3.13E-03	MERL_HUMAN
TRINITY_DN202479_c1_g4_i1	Ohr	12hr	-6.12	4.68E-02	NA
TRINITY_DN202495_c0_g3_i10	Ohr	12hr	-9.66	4.07E-02	DC1I2_BOVIN
TRINITY_DN202536_c4_g1_i3	Ohr	12hr	8.03	1.94E-05	NA
TRINITY_DN202608_c11_g1_i2	Ohr	12hr	-8.53	4.95E-02	NA
TRINITY_DN202788_c2_g2_i8	Ohr	12hr	8.74	4.66E-02	AHSA1_HUMAN
TRINITY_DN202842_c5_g1_i7	Ohr	12hr	8.15	4.52E-02	TSSP_MOUSE
TRINITY_DN202855_c5_g1_i3	Ohr	12hr	-8.45	1.29E-02	WDR46_HUMAN
TRINITY_DN203067_c3_g1_i7	Ohr	12hr	-9.78	6.24E-08	P4R3A_MOUSE
TRINITY_DN203262_c6_g3_i2	Ohr	12hr	-6.84	1.39E-03	PIEZ2_MOUSE

TRINITY_DN203280_c14_g2_i7	Ohr	12hr	-7.98	4.67E-04	LGMN_BOVIN
TRINITY_DN203497_c1_g1_i3	Ohr	12hr	6.48	4.71E-02	NA
TRINITY_DN203597_c4_g2_i1	Ohr	12hr	-12.51	3.20E-04	CAB45_XENTR
TRINITY_DN203691_c3_g2_i2	Ohr	12hr	-9.85	6.13E-03	ZN711_HUMAN
TRINITY_DN203818_c2_g2_i1	Ohr	12hr	-10.45	3.18E-02	SNX4_BOVIN
TRINITY_DN203839_c8_g2_i1	Ohr	12hr	8.85	5.53E-04	CLCC1_BOVIN
TRINITY_DN203880_c16_g1_i10	Ohr	12hr	10.05	1.28E-02	NA
TRINITY_DN203913_c2_g1_i23	Ohr	12hr	-10.20	3.16E-03	SYQ_BOVIN
TRINITY_DN204052_c1_g1_i3	Ohr	12hr	-8.63	1.62E-02	NA
TRINITY_DN204052_c1_g1_i4	Ohr	12hr	-5.92	4.82E-02	NA
TRINITY_DN204150_c4_g2_i4	Ohr	12hr	-9.89	3.24E-02	BICD2_HUMAN
TRINITY_DN204168_c2_g1_i3	Ohr	12hr	9.31	4.83E-04	TM50A_MOUSE
TRINITY_DN204200_c1_g2_i2	Ohr	12hr	8.31	4.46E-02	QORX_HUMAN
TRINITY_DN204263_c5_g1_i1	Ohr	12hr	6.82	4.01E-02	NA
TRINITY_DN204304_c8_g1_i13	Ohr	12hr	-9.89	4.32E-03	NA
TRINITY_DN204350_c0_g1_i6	Ohr	12hr	9.49	3.24E-02	CL004_MOUSE
TRINITY_DN204447_c1_g1_i11	Ohr	12hr	-8.77	1.58E-02	ESPN_MOUSE
TRINITY_DN204464_c1_g1_i9	Ohr	12hr	6.75	4.18E-02	TAR1_YEAST
TRINITY_DN204772_c9_g1_i2	Ohr	12hr	7.55	3.25E-04	IRG1_HUMAN
TRINITY_DN204835_c4_g8_i1	Ohr	12hr	6.78	3.24E-02	NA
TRINITY_DN204985_c12_g1_i2	Ohr	12hr	-5.80	3.39E-02	NA
TRINITY_DN204994_c4_g2_i3	Ohr	12hr	8.64	4.07E-02	NA
TRINITY_DN205185_c13_g1_i24	Ohr	12hr	6.55	6.55E-03	NA
TRINITY_DN205185_c13_g1_i9	Ohr	12hr	-7.20	2.55E-03	NA
TRINITY_DN205218_c1_g2_i12	Ohr	12hr	9.73	2.46E-02	MBB1A_DANRE
TRINITY_DN205237_c4_g2_i7	Ohr	12hr	10.13	2.55E-03	NA
TRINITY_DN205251_c3_g2_i2	Ohr	12hr	-8.45	4.64E-02	NA
TRINITY_DN205449_c1_g2_i21	Ohr	12hr	8.93	3.97E-02	NA
TRINITY_DN205510_c2_g1_i3	Ohr	12hr	-6.33	3.62E-02	NA
TRINITY_DN205553_c10_g1_i3	Ohr	12hr	9.07	3.25E-04	FKRP_HUMAN
TRINITY_DN205641_c1_g2_i2	Ohr	12hr	6.95	4.42E-02	NA
TRINITY_DN205643_c3_g2_i4	Ohr	12hr	-9.86	3.44E-02	IFFO2_HUMAN
TRINITY_DN205792_c5_g1_i3	Ohr	12hr	6.93	3.25E-04	I20RB_HUMAN
TRINITY_DN205823_c2_g2_i3	Ohr	12hr	-8.88	4.48E-02	VPS36_HUMAN
TRINITY_DN205825_c3_g1_i10	Ohr	12hr	10.64	1.22E-03	PDC6I_HUMAN
TRINITY_DN205837_c2_g2_i4	Ohr	12hr	-10.29	2.44E-02	NGBR_DANRE
TRINITY_DN205951_c3_g2_i14	Ohr	12hr	-8.18	4.89E-04	NA
TRINITY_DN205963_c5_g2_i21	Ohr	12hr	-9.23	3.88E-02	DHSO_CHICK
TRINITY_DN206140_c2_g2_i3	Ohr	12hr	8.55	3.59E-02	NA

TRINITY_DN206147_c8_g1_i2	Ohr	12hr	-8.00	1.04E-02	NA
TRINITY_DN206203_c5_g2_i14	Ohr	12hr	-7.26	6.60E-03	NA
TRINITY_DN206386_c6_g1_i2	Ohr	12hr	-12.52	1.57E-04	NA
TRINITY_DN206414_c2_g2_i3	Ohr	12hr	-6.75	3.24E-02	NA
TRINITY_DN206439_c4_g2_i3	Ohr	12hr	-8.21	5.55E-04	NA
TRINITY_DN206535_c4_g1_i6	Ohr	12hr	5.41	2.56E-02	NA
TRINITY_DN206561_c0_g1_i13	Ohr	12hr	-5.73	2.29E-02	PRP8_HUMAN
TRINITY_DN206564_c0_g1_i4	Ohr	12hr	10.29	5.29E-04	NA
TRINITY_DN206641_c8_g1_i1	Ohr	12hr	8.02	2.12E-02	RVT_1
TRINITY_DN206707_c4_g1_i4	Ohr	12hr	9.63	1.45E-04	PICAL_RAT
TRINITY_DN206739_c5_g1_i1	Ohr	12hr	-11.62	4.15E-04	NA
TRINITY_DN206810_c4_g1_i6	Ohr	12hr	8.32	4.66E-02	BTK_MOUSE
TRINITY_DN206898_c2_g1_i2	Ohr	12hr	-9.06	4.12E-02	EHD1_PONAB
TRINITY_DN206993_c3_g5_i1	Ohr	12hr	5.37	2.35E-02	NA
TRINITY_DN206993_c3_g5_i3	Ohr	12hr	5.13	1.60E-02	SC6A5_HUMAN
TRINITY_DN207030_c1_g2_i6	Ohr	12hr	-9.83	4.32E-03	EXOC3_BOVIN
TRINITY_DN207129_c0_g1_i9	Ohr	12hr	-8.85	1.76E-02	NA
TRINITY_DN207140_c4_g1_i9	Ohr	12hr	-10.30	1.06E-02	DNSL3_HUMAN
TRINITY_DN207157_c3_g1_i5	Ohr	12hr	7.80	4.66E-02	KTNB1_DANRE
TRINITY_DN207167_c5_g1_i9	Ohr	12hr	-6.91	9.23E-03	NA
TRINITY_DN207291_c3_g1_i2	Ohr	12hr	-9.50	7.83E-03	BCAP_CHICK
TRINITY_DN207363_c9_g1_i15	Ohr	12hr	9.90	2.68E-02	FBXW9_BOVIN
TRINITY_DN207363_c9_g1_i16	Ohr	12hr	9.33	3.59E-02	FBXW9_BOVIN
TRINITY_DN207382_c3_g1_i3	Ohr	12hr	-9.95	5.55E-04	EPT1_MOUSE
TRINITY_DN207446_c3_g3_i2	Ohr	12hr	6.66	4.48E-02	SRRM1_CHICK
TRINITY_DN207551_c18_g1_i5	Ohr	12hr	9.03	3.87E-02	NA
TRINITY_DN207571_c3_g3_i9	Ohr	12hr	7.53	2.29E-02	ECHD2_BOVIN
TRINITY_DN207597_c3_g1_i5	Ohr	12hr	-8.86	4.89E-04	UHRF1_DANRE
TRINITY_DN207654_c11_g1_i2	Ohr	12hr	6.62	4.44E-02	SP20H_CHICK
TRINITY_DN207763_c6_g1_i10	Ohr	12hr	-8.39	4.95E-02	K0020_RAT
TRINITY_DN207865_c0_g2_i2	Ohr	12hr	9.15	4.48E-02	NA
TRINITY_DN207885_c1_g2_i8	Ohr	12hr	9.22	7.83E-03	NA
TRINITY_DN207887_c8_g3_i3	Ohr	12hr	6.46	3.15E-02	NA
TRINITY_DN208061_c4_g1_i13	Ohr	12hr	4.75	4.08E-02	ANXA5_MOUSE
TRINITY_DN208164_c8_g1_i12	Ohr	12hr	8.25	3.98E-02	IF6_DANRE
TRINITY_DN208164_c8_g1_i16	Ohr	12hr	11.33	3.54E-04	IF6_DANRE
TRINITY_DN208164_c8_g1_i19	Ohr	12hr	9.69	4.32E-03	IF6_DANRE
TRINITY_DN208177_c2_g5_i4	Ohr	12hr	-8.20	1.02E-02	NA
TRINITY_DN208272_c4_g3_i5	Ohr	12hr	8.46	3.66E-02	NA

TRINITY_DN208373_c1_g4_i7	Ohr	12hr	-11.44	7.85E-07	ANM5_HUMAN
TRINITY_DN208421_c0_g1_i1	Ohr	12hr	5.31	4.48E-02	NA
TRINITY_DN208421_c0_g1_i18	Ohr	12hr	9.57	2.41E-02	NA
TRINITY_DN208421_c0_g1_i4	Ohr	12hr	3.67	2.56E-02	NA
TRINITY_DN208421_c0_g1_i7	Ohr	12hr	8.90	3.24E-02	NA
TRINITY_DN208501_c12_g1_i13	Ohr	12hr	8.20	2.26E-03	PPIE_HUMAN
TRINITY_DN208578_c1_g4_i10	Ohr	12hr	7.48	2.18E-02	NA
TRINITY_DN208630_c2_g1_i1	Ohr	12hr	-8.65	4.76E-02	NA
TRINITY_DN208651_c2_g1_i15	Ohr	12hr	-8.87	4.48E-02	AL1L1_XENLA
TRINITY_DN208674_c2_g1_i3	Ohr	12hr	-6.82	4.66E-02	NA
TRINITY_DN208697_c1_g2_i1	Ohr	12hr	4.42	2.44E-02	HSP71_RAT
TRINITY_DN208697_c1_g3_i1	Ohr	12hr	5.83	3.07E-02	HSP70_XENLA
TRINITY_DN208697_c1_g5_i1	Ohr	12hr	6.85	4.66E-02	HS71A_MOUSE
TRINITY_DN208756_c8_g3_i6	Ohr	12hr	-9.61	4.15E-04	NA
TRINITY_DN208771_c6_g1_i2	Ohr	12hr	-8.45	9.52E-03	NA
TRINITY_DN208892_c4_g6_i6	Ohr	12hr	8.09	6.98E-03	NA
TRINITY_DN209024_c13_g1_i2	Ohr	12hr	6.98	3.65E-02	NA
TRINITY_DN209102_c3_g2_i6	Ohr	12hr	-10.66	2.86E-04	NA
TRINITY_DN209205_c9_g1_i2	Ohr	12hr	-8.62	4.42E-02	NA
TRINITY_DN209249_c7_g1_i9	Ohr	12hr	-10.86	1.59E-03	NA
TRINITY_DN209298_c7_g1_i9	Ohr	12hr	-12.82	1.09E-02	CN159_MOUSE
TRINITY_DN209307_c5_g5_i4	Ohr	12hr	8.05	4.93E-02	NA
TRINITY_DN209318_c1_g1_i2	Ohr	12hr	-10.18	3.02E-02	MYOF_MOUSE
TRINITY_DN209428_c1_g1_i4	Ohr	12hr	9.18	1.13E-03	NOXO1_HUMAN
TRINITY_DN209428_c1_g1_i6	Ohr	12hr	4.88	2.76E-02	NA
TRINITY_DN209461_c3_g2_i1	Ohr	12hr	-11.06	2.12E-02	NA
TRINITY_DN209485_c0_g1_i2	Ohr	12hr	9.09	3.77E-02	SES2_BOVIN
TRINITY_DN209563_c5_g2_i4	Ohr	12hr	-8.62	9.44E-03	NA
TRINITY_DN209579_c1_g1_i9	Ohr	12hr	-10.09	1.90E-03	DPYL3_HUMAN
TRINITY_DN209612_c11_g2_i13	Ohr	12hr	10.47	1.90E-02	YKT6_BOVIN
TRINITY_DN209905_c4_g1_i1	Ohr	12hr	10.01	2.68E-02	LAMC3_HUMAN
TRINITY_DN210043_c6_g1_i7	Ohr	12hr	9.99	2.63E-02	AP4E1_HUMAN
TRINITY_DN210148_c2_g1_i8	Ohr	12hr	9.05	8.56E-03	MYBPH_CHICK
TRINITY_DN210149_c0_g2_i20	Ohr	12hr	11.90	5.87E-07	DIC_HUMAN
TRINITY_DN210149_c0_g2_i4	Ohr	12hr	11.48	1.73E-16	DIC_HUMAN
TRINITY_DN210163_c1_g2_i11	Ohr	12hr	-7.39	2.51E-02	SPP2B_CHICK
TRINITY_DN210172_c2_g1_i2	Ohr	12hr	6.53	4.61E-02	NA
TRINITY_DN210197_c5_g1_i10	Ohr	12hr	-9.22	4.32E-02	MDR1_CRIGR
TRINITY_DN210270_c8_g1_i1	Ohr	12hr	-7.86	8.26E-03	NA

TRINITY_DN210309_c1_g1_i3	Ohr	12hr	5.08	1.44E-02	NA
TRINITY_DN210383_c0_g1_i1	Ohr	12hr	4.82	3.78E-02	HSP71_ORYLA
TRINITY_DN210383_c0_g3_i1	Ohr	12hr	4.41	3.65E-02	HSP70_XENLA
TRINITY_DN210383_c0_g5_i2	Ohr	12hr	6.44	4.48E-02	HS71L_BOVIN
TRINITY_DN210414_c7_g3_i9	Ohr	12hr	-7.29	6.27E-03	NA
TRINITY_DN210447_c2_g1_i6	Ohr	12hr	-7.10	7.18E-03	NA
TRINITY_DN210526_c6_g1_i5	Ohr	12hr	7.17	2.41E-02	S2538_XENTR
TRINITY_DN210639_c3_g1_i15	Ohr	12hr	4.89	1.34E-02	NA
TRINITY_DN210734_c2_g1_i1	Ohr	12hr	5.98	3.58E-02	LV601_HUMAN
TRINITY_DN210838_c6_g1_i12	Ohr	12hr	-6.77	4.82E-02	NA
TRINITY_DN210848_c9_g2_i8	Ohr	12hr	-9.58	3.96E-02	PISD_CRIGR
TRINITY_DN210873_c2_g6_i2	Ohr	12hr	-7.92	1.20E-02	NA
TRINITY_DN210887_c7_g1_i1	Ohr	12hr	-8.61	4.72E-02	NA
TRINITY_DN211003_c4_g1_i7	Ohr	12hr	-7.70	2.71E-02	NA
TRINITY_DN211114_c3_g1_i1	Ohr	12hr	11.91	5.87E-07	NA
TRINITY_DN211114_c3_g1_i4	Ohr	12hr	12.05	7.76E-09	NA
TRINITY_DN211119_c7_g2_i1	Ohr	12hr	-10.37	3.44E-02	NA
TRINITY_DN211226_c5_g3_i3	Ohr	12hr	8.71	3.47E-02	NA
TRINITY_DN211239_c2_g3_i15	Ohr	12hr	4.11	2.09E-02	PAR3L_HUMAN
TRINITY_DN211272_c5_g1_i2	Ohr	12hr	9.38	2.09E-04	NDUA7_PONPY
TRINITY_DN211334_c8_g1_i6	Ohr	12hr	-7.11	4.18E-02	PLBL2_HUMAN
TRINITY_DN211445_c4_g1_i19	Ohr	12hr	8.65	4.36E-04	IQUB_HUMAN
TRINITY_DN211503_c5_g1_i4	Ohr	12hr	9.45	3.59E-02	RWDD1_RAT
TRINITY_DN211514_c4_g1_i5	Ohr	12hr	-8.39	1.49E-03	NA
TRINITY_DN211653_c9_g1_i1	Ohr	12hr	2.73	3.49E-02	H32_CRILO
TRINITY_DN211671_c2_g1_i8	Ohr	12hr	8.73	2.61E-05	PLXB2_MOUSE
TRINITY_DN211703_c3_g2_i18	Ohr	12hr	7.73	2.76E-02	RAC1_RAT
TRINITY_DN211819_c6_g2_i5	Ohr	12hr	-13.40	9.55E-03	IF5A1_RABIT
TRINITY_DN211927_c2_g1_i9	Ohr	12hr	-10.26	2.46E-02	ITB2_HUMAN
TRINITY_DN211982_c2_g1_i9	Ohr	12hr	8.44	9.31E-04	IF44L_HUMAN
TRINITY_DN212057_c0_g2_i4	Ohr	12hr	-7.90	1.30E-02	NA
TRINITY_DN212085_c0_g1_i16	Ohr	12hr	-5.77	3.59E-02	CIB1_RAT
TRINITY_DN212085_c0_g1_i7	Ohr	12hr	-10.41	2.49E-02	CIB1_RAT
TRINITY_DN212122_c8_g1_i3	Ohr	12hr	5.09	2.27E-02	TRFM_RABIT
TRINITY_DN212136_c5_g2_i7	Ohr	12hr	4.66	1.74E-02	HSP30_ONCTS
TRINITY_DN212136_c5_g3_i1	Ohr	12hr	3.91	1.00E-02	NA
TRINITY_DN212136_c5_g4_i3	Ohr	12hr	4.63	2.55E-02	NA
TRINITY_DN212402_c2_g1_i2	Ohr	12hr	9.11	3.14E-02	CYGB2_DANRE
TRINITY_DN212659_c3_g3_i1	Ohr	12hr	-8.88	1.56E-02	PSA7_BOVIN

TRINITY_DN212659_c3_g3_i2	Ohr	12hr	-11.38	1.45E-04	PSA7_BOVIN
TRINITY_DN212762_c4_g1_i21	Ohr	12hr	7.95	4.95E-02	MP2K5_RAT
TRINITY_DN212800_c3_g1_i2	Ohr	12hr	8.78	1.54E-07	NA
TRINITY_DN212862_c11_g2_i2	Ohr	12hr	7.01	4.82E-02	NA
TRINITY_DN212862_c12_g1_i15	Ohr	12hr	8.63	1.06E-02	NA
TRINITY_DN212864_c3_g2_i4	Ohr	12hr	-7.24	2.76E-02	NLRC3_HUMAN
TRINITY_DN165995_c0_g1_i4	Ohr	48hr	-7.04	3.72E-02	NA
TRINITY_DN168738_c0_g1_i1	Ohr	48hr	-6.56	3.11E-02	NA
TRINITY_DN168766_c0_g1_i3	Ohr	48hr	-6.31	2.26E-03	NA
TRINITY_DN170805_c0_g1_i8	Ohr	48hr	8.43	5.54E-03	NA
TRINITY_DN171092_c0_g1_i2	Ohr	48hr	7.55	1.94E-02	NA
TRINITY_DN171237_c0_g1_i3	Ohr	48hr	6.22	6.57E-04	TBB3_MACFA
TRINITY_DN171293_c0_g1_i4	Ohr	48hr	-9.44	4.17E-02	CC124_DANRE
TRINITY_DN171894_c0_g1_i1	Ohr	48hr	-10.73	8.98E-05	NA
TRINITY_DN172197_c0_g1_i2	Ohr	48hr	-5.02	3.88E-02	NA
TRINITY_DN173068_c0_g1_i3	Ohr	48hr	7.90	9.87E-03	NA
TRINITY_DN173097_c10_g1_i4	Ohr	48hr	7.64	1.01E-02	ZDHC3_HUMAN
TRINITY_DN173324_c0_g1_i2	Ohr	48hr	-9.26	4.48E-02	Tm1
TRINITY_DN173533_c0_g1_i1	Ohr	48hr	-4.57	3.66E-02	NR4A2_MOUSE
TRINITY_DN173533_c0_g1_i6	Ohr	48hr	-4.16	4.50E-03	NR4A2_MOUSE
TRINITY_DN173533_c0_g1_i7	Ohr	48hr	-3.77	2.09E-02	NR4A2_XENTR
TRINITY_DN173696_c3_g1_i6	Ohr	48hr	9.43	2.53E-02	FKBP3_HUMAN
TRINITY_DN173696_c3_g1_i8	Ohr	48hr	9.60	2.52E-02	FKBP3_HUMAN
TRINITY_DN174045_c8_g1_i2	Ohr	48hr	3.49	4.16E-02	DKK1_HUMAN
TRINITY_DN174045_c8_g1_i3	Ohr	48hr	3.79	3.88E-03	DKK1_HUMAN
TRINITY_DN174906_c3_g1_i2	Ohr	48hr	4.22	3.11E-02	NA
TRINITY_DN175027_c12_g1_i1	Ohr	48hr	5.01	3.22E-02	NA
TRINITY_DN175047_c10_g4_i7	Ohr	48hr	4.65	4.32E-02	NA
TRINITY_DN175085_c4_g2_i5	Ohr	48hr	-10.06	1.60E-02	ACADL_RAT
TRINITY_DN175100_c7_g1_i5	Ohr	48hr	6.92	4.77E-02	NECP1_MOUSE
TRINITY_DN175185_c10_g1_i3	Ohr	48hr	-9.34	4.75E-02	OLFM4_MOUSE
TRINITY_DN175323_c8_g1_i2	Ohr	48hr	-8.21	1.90E-02	NA
TRINITY_DN175437_c8_g3_i10	Ohr	48hr	-11.50	5.44E-05	KLF13_HUMAN
TRINITY_DN175437_c8_g3_i2	Ohr	48hr	-9.23	6.75E-03	KLF13_HUMAN
TRINITY_DN175491_c12_g3_i1	Ohr	48hr	-3.27	2.53E-02	NA
TRINITY_DN175865_c3_g4_i3	Ohr	48hr	-7.21	3.16E-02	MYG1_MOUSE
TRINITY_DN175945_c6_g2_i2	Ohr	48hr	-5.55	1.02E-02	NA
TRINITY_DN176101_c6_g1_i16	Ohr	48hr	8.44	3.11E-02	NA
TRINITY_DN176117_c6_g1_i2	Ohr	48hr	7.11	2.36E-03	NA

TRINITY_DN176442_c12_g6_i1	Ohr	48hr	3.54	3.48E-02	NA
TRINITY_DN176560_c7_g3_i1	Ohr	48hr	-8.37	1.20E-02	NA
TRINITY_DN176621_c10_g1_i2	Ohr	48hr	-8.86	1.64E-02	EI2BE_RABIT
TRINITY_DN176676_c3_g1_i11	Ohr	48hr	-9.99	3.81E-02	TB10A_HUMAN
TRINITY_DN176732_c3_g1_i1	Ohr	48hr	-9.22	1.52E-03	UAP1L_XENTR
TRINITY_DN176870_c1_g2_i3	Ohr	48hr	-5.89	3.25E-02	ASTER_CHICK
TRINITY_DN176996_c7_g1_i6	Ohr	48hr	8.77	4.22E-02	NA
TRINITY_DN177280_c9_g1_i3	Ohr	48hr	9.28	3.63E-02	FBXW7_HUMAN
TRINITY_DN177301_c1_g2_i7	Ohr	48hr	10.03	2.53E-03	HEX11_RAT
TRINITY_DN177810_c2_g1_i7	Ohr	48hr	7.50	2.48E-02	CD82_RAT
TRINITY_DN177877_c14_g1_i2	Ohr	48hr	7.27	3.54E-02	TEC_HUMAN
TRINITY_DN177915_c12_g3_i6	Ohr	48hr	7.23	2.79E-02	NA
TRINITY_DN177926_c5_g1_i6	Ohr	48hr	-9.37	4.75E-02	SUGP2_HUMAN
TRINITY_DN177926_c5_g1_i8	Ohr	48hr	-7.69	3.66E-02	SUGP1_HUMAN
TRINITY_DN178035_c5_g1_i8	Ohr	48hr	7.89	2.00E-02	NA
TRINITY_DN178151_c0_g1_i3	Ohr	48hr	9.95	1.93E-02	LV107_HUMAN
TRINITY_DN178356_c0_g1_i13	Ohr	48hr	-6.10	4.44E-02	NA
TRINITY_DN178389_c1_g1_i6	Ohr	48hr	-9.26	1.17E-02	RAB7A_CANFA
TRINITY_DN178441_c11_g1_i1	Ohr	48hr	-8.72	4.21E-02	NPDC1_HUMAN
TRINITY_DN178441_c11_g1_i6	Ohr	48hr	-9.95	1.71E-02	NPDC1_HUMAN
TRINITY_DN178546_c4_g1_i12	Ohr	48hr	-7.10	2.26E-03	PCKGC_MOUSE
TRINITY_DN178641_c5_g3_i10	Ohr	48hr	9.05	2.18E-02	RAB2A_CHICK
TRINITY_DN178885_c5_g2_i6	Ohr	48hr	7.53	4.18E-02	MOB1A_RAT
TRINITY_DN179066_c9_g3_i4	Ohr	48hr	-9.62	3.84E-02	ES1_RAT
TRINITY_DN179066_c9_g3_i7	Ohr	48hr	-8.57	2.19E-02	ES1_RAT
TRINITY_DN179215_c9_g1_i3	Ohr	48hr	-10.02	5.48E-03	PAPS2_MOUSE
TRINITY_DN179473_c4_g1_i1	Ohr	48hr	-8.65	5.45E-03	C1QBP_RAT
TRINITY_DN180042_c9_g1_i3	Ohr	48hr	-8.33	1.60E-02	TM100_HUMAN
TRINITY_DN180125_c12_g1_i3	Ohr	48hr	-7.13	2.79E-02	NA
TRINITY_DN180324_c8_g1_i2	Ohr	48hr	-7.59	4.21E-02	NA
TRINITY_DN180393_c6_g1_i2	Ohr	48hr	7.97	1.97E-03	NA
TRINITY_DN180424_c1_g1_i17	Ohr	48hr	6.50	3.81E-02	AAK1_MOUSE
TRINITY_DN180670_c1_g1_i7	Ohr	48hr	-9.33	1.02E-02	TSN5_BOVIN
TRINITY_DN180862_c3_g1_i16	Ohr	48hr	9.31	1.99E-02	TCPB_BOVIN
TRINITY_DN180862_c3_g1_i21	Ohr	48hr	11.52	3.83E-03	TCPB_RAT
TRINITY_DN180949_c1_g1_i1	Ohr	48hr	10.18	3.20E-02	RNF13_CHICK
TRINITY_DN181003_c4_g1_i1	Ohr	48hr	-10.13	2.31E-04	TF2AA_HUMAN
TRINITY_DN181104_c1_g1_i3	Ohr	48hr	7.82	4.47E-02	IDLC_RAT
TRINITY_DN181104_c1_g1_i8	Ohr	48hr	-8.32	3.83E-03	IDLC_RAT

TRINITY_DN181112_c2_g1_i2	Ohr	48hr	8.71	3.62E-04	NA
TRINITY_DN181132_c7_g1_i1	Ohr	48hr	8.18	3.88E-02	NA
TRINITY_DN181407_c0_g1_i11	Ohr	48hr	-7.27	1.04E-02	PICK1_MOUSE
TRINITY_DN181453_c7_g1_i1	Ohr	48hr	3.27	5.15E-05	RN186_BOVIN
TRINITY_DN181542_c2_g1_i7	Ohr	48hr	8.80	2.48E-02	TM244_HUMAN
TRINITY_DN181569_c14_g1_i5	Ohr	48hr	-8.26	2.15E-03	NA
TRINITY_DN181837_c4_g3_i4	Ohr	48hr	-10.87	1.60E-03	NA
TRINITY_DN181938_c1_g1_i4	Ohr	48hr	-9.21	4.65E-02	NA
TRINITY_DN182005_c7_g1_i9	Ohr	48hr	-9.59	1.25E-03	NEDD8_RAT
TRINITY_DN182320_c5_g2_i7	Ohr	48hr	4.53	2.52E-02	Tm1
TRINITY_DN182445_c4_g2_i7	Ohr	48hr	7.58	1.17E-02	NA
TRINITY_DN182571_c5_g3_i2	Ohr	48hr	-8.99	2.01E-03	NA
TRINITY_DN182624_c11_g1_i1	Ohr	48hr	9.60	5.83E-03	UBE2C_XENLA
TRINITY_DN182766_c5_g2_i16	Ohr	48hr	8.72	3.95E-02	NA
TRINITY_DN182847_c8_g1_i8	Ohr	48hr	-9.96	5.54E-03	NA
TRINITY_DN182896_c1_g6_i2	Ohr	48hr	-7.10	3.82E-02	NA
TRINITY_DN182955_c3_g1_i3	Ohr	48hr	-10.79	1.52E-03	NA
TRINITY_DN183183_c22_g1_i2	Ohr	48hr	10.38	2.52E-02	PCOC2_HUMAN
TRINITY_DN183248_c2_g1_i4	Ohr	48hr	-7.85	1.27E-04	ANR10_HUMAN
TRINITY_DN183269_c9_g3_i6	Ohr	48hr	9.39	1.02E-02	SCG1_PIG
TRINITY_DN183286_c1_g2_i3	Ohr	48hr	6.99	2.79E-02	NA
TRINITY_DN183395_c3_g1_i4	Ohr	48hr	-8.54	1.25E-02	NA
TRINITY_DN183527_c9_g1_i11	Ohr	48hr	-10.10	1.30E-02	APMAP_HUMAN
TRINITY_DN183580_c1_g3_i1	Ohr	48hr	-4.40	8.63E-03	NA
TRINITY_DN183586_c6_g1_i1	Ohr	48hr	-8.96	2.48E-02	TM213_HUMAN
TRINITY_DN183659_c7_g1_i8	Ohr	48hr	5.45	1.64E-02	NA
TRINITY_DN183700_c0_g1_i10	Ohr	48hr	6.63	3.54E-02	ATS1_HUMAN
TRINITY_DN183830_c5_g3_i1	Ohr	48hr	7.49	1.91E-02	ITAM_MOUSE
TRINITY_DN183858_c11_g1_i23	Ohr	48hr	-4.64	2.94E-02	ADK_HUMAN
TRINITY_DN183916_c14_g1_i1	Ohr	48hr	-3.28	3.39E-02	NA
TRINITY_DN184224_c0_g1_i26	Ohr	48hr	-7.57	5.35E-03	SARDH_MOUSE
TRINITY_DN184353_c0_g1_i5	Ohr	48hr	4.99	4.12E-02	NA
TRINITY_DN184448_c11_g2_i1	Ohr	48hr	7.57	2.19E-02	NA
TRINITY_DN184485_c4_g1_i2	Ohr	48hr	6.42	6.39E-03	NA
TRINITY_DN184603_c1_g1_i2	Ohr	48hr	-7.42	2.94E-02	PIM3_COTJA
TRINITY_DN184968_c4_g1_i3	Ohr	48hr	-2.68	2.48E-02	NA
TRINITY_DN185010_c10_g3_i3	Ohr	48hr	7.39	4.75E-02	NA
TRINITY_DN185152_c7_g1_i1	Ohr	48hr	7.52	1.60E-03	NA
TRINITY_DN185263_c2_g1_i9	Ohr	48hr	-3.90	3.81E-02	PNPT1_HUMAN

TRINITY_DN185653_c1_g1_i15	Ohr	48hr	11.67	2.34E-04	COPD_PONAB
TRINITY_DN185821_c6_g1_i8	Ohr	48hr	8.58	1.12E-02	SNR25_HUMAN
TRINITY_DN186140_c7_g2_i4	Ohr	48hr	-7.70	3.60E-02	GALA_DANRE
TRINITY_DN186286_c1_g1_i3	Ohr	48hr	-7.80	4.04E-03	RND1_HUMAN
TRINITY_DN186437_c11_g4_i3	Ohr	48hr	7.88	2.15E-02	NA
TRINITY_DN186559_c0_g2_i6	Ohr	48hr	-5.86	4.55E-04	NA
TRINITY_DN186707_c7_g1_i3	Ohr	48hr	6.97	2.09E-02	NA
TRINITY_DN186803_c6_g1_i2	Ohr	48hr	-7.48	3.46E-02	ARP2B_XENLA
TRINITY_DN186804_c9_g1_i2	Ohr	48hr	-8.06	3.32E-02	NA
TRINITY_DN186882_c7_g1_i3	Ohr	48hr	-9.24	1.11E-02	CALR_RABIT
TRINITY_DN186925_c3_g1_i11	Ohr	48hr	10.68	1.63E-02	BCCIP_BOVIN
TRINITY_DN187068_c5_g1_i1	Ohr	48hr	9.45	4.32E-02	BAP29_MOUSE
TRINITY_DN187137_c0_g1_i9	Ohr	48hr	-6.19	5.04E-03	ABCE1_MOUSE
TRINITY_DN187433_c0_g4_i12	Ohr	48hr	-8.29	1.79E-04	CCD22_DANRE
TRINITY_DN187491_c0_g3_i2	Ohr	48hr	-9.69	5.61E-03	WBP11_MOUSE
TRINITY_DN187835_c1_g1_i7	Ohr	48hr	-9.07	1.40E-03	ERGI3_XENLA
TRINITY_DN187920_c1_g1_i4	Ohr	48hr	9.91	4.54E-05	NA
TRINITY_DN187940_c6_g2_i2	Ohr	48hr	10.11	5.15E-05	TAF11_MOUSE
TRINITY_DN187989_c6_g2_i14	Ohr	48hr	7.49	9.61E-04	EKI1_MOUSE
TRINITY_DN188262_c7_g1_i5	Ohr	48hr	-2.62	1.91E-02	NA
TRINITY_DN188278_c9_g1_i1	Ohr	48hr	-7.78	5.35E-03	NA
TRINITY_DN188316_c3_g2_i8	Ohr	48hr	-5.04	2.53E-02	NA
TRINITY_DN188378_c6_g2_i5	Ohr	48hr	-4.92	4.99E-03	NA
TRINITY_DN188435_c0_g1_i1	Ohr	48hr	8.87	2.97E-02	NEK2_HUMAN
TRINITY_DN188484_c0_g3_i3	Ohr	48hr	5.05	3.99E-02	PTSS2_CRIGR
TRINITY_DN188525_c12_g2_i1	Ohr	48hr	10.30	2.15E-02	PKHA1_HUMAN
TRINITY_DN188555_c2_g1_i3	Ohr	48hr	7.33	3.72E-04	NALP3_HUMAN
TRINITY_DN188607_c1_g3_i6	Ohr	48hr	9.66	1.71E-02	BAG4_MOUSE
TRINITY_DN188759_c5_g2_i2	Ohr	48hr	-8.46	2.15E-02	CEBPA_HUMAN
TRINITY_DN188980_c1_g1_i14	Ohr	48hr	7.30	5.61E-03	JTB_HUMAN
TRINITY_DN189114_c6_g2_i1	Ohr	48hr	-5.22	3.54E-02	FKB1A_RABIT
TRINITY_DN189165_c6_g1_i17	Ohr	48hr	4.64	2.29E-02	RANB3_PONAB
TRINITY_DN189168_c4_g2_i2	Ohr	48hr	-10.38	5.54E-03	PLCA_HUMAN
TRINITY_DN189196_c4_g1_i3	Ohr	48hr	-10.54	6.59E-04	NA
TRINITY_DN189221_c3_g1_i4	Ohr	48hr	-6.24	3.56E-03	NA
TRINITY_DN189252_c6_g1_i4	Ohr	48hr	-7.59	4.01E-02	NA
TRINITY_DN189283_c5_g2_i12	Ohr	48hr	8.65	2.68E-02	XBP1_BOVIN
TRINITY_DN189453_c2_g1_i16	Ohr	48hr	7.86	3.43E-02	WDR73_XENLA
TRINITY_DN189678_c9_g3_i2	Ohr	48hr	-7.60	1.84E-02	FACR1_CHICK

TRINITY_DN189740_c11_g1_i2	Ohr	48hr	-6.97	4.34E-02	NA
TRINITY_DN189869_c2_g1_i11	Ohr	48hr	-7.86	2.16E-02	TM138_HUMAN
TRINITY_DN190057_c5_g1_i1	Ohr	48hr	-7.06	3.81E-02	NA
TRINITY_DN190325_c3_g2_i3	Ohr	48hr	-10.08	3.83E-03	NA
TRINITY_DN190692_c1_g3_i13	Ohr	48hr	-9.57	6.46E-04	TAOK2_XENLA
TRINITY_DN190773_c13_g3_i2	Ohr	48hr	-7.89	2.29E-02	NA
TRINITY_DN190787_c6_g1_i3	Ohr	48hr	7.15	5.54E-03	NA
TRINITY_DN190906_c2_g3_i1	Ohr	48hr	-8.80	1.25E-03	Tm1
TRINITY_DN190906_c2_g6_i1	Ohr	48hr	-9.18	8.26E-03	NA
TRINITY_DN191040_c6_g1_i3	Ohr	48hr	-9.33	1.23E-02	FUMH_DANRE
TRINITY_DN191190_c7_g5_i1	Ohr	48hr	8.10	3.66E-02	NA
TRINITY_DN191260_c8_g1_i1	Ohr	48hr	-9.55	6.46E-03	NA
TRINITY_DN191516_c0_g1_i5	Ohr	48hr	-7.96	3.33E-02	NA
TRINITY_DN191624_c11_g1_i1	Ohr	48hr	11.33	3.38E-03	SCG1_HUMAN
TRINITY_DN191624_c11_g1_i2	Ohr	48hr	8.95	1.08E-02	SCG1_HUMAN
TRINITY_DN191704_c7_g2_i4	Ohr	48hr	-9.12	1.60E-02	FGFR3_CHICK
TRINITY_DN191720_c5_g1_i1	Ohr	48hr	-2.83	1.53E-02	GTR11_HUMAN
TRINITY_DN191850_c5_g1_i2	Ohr	48hr	-9.52	3.99E-02	NA
TRINITY_DN191903_c0_g2_i2	Ohr	48hr	8.90	3.10E-03	NA
TRINITY_DN191911_c3_g2_i10	Ohr	48hr	8.97	2.29E-02	RHOA_PONAB
TRINITY_DN192102_c5_g2_i4	Ohr	48hr	-9.60	1.95E-02	NA
TRINITY_DN192102_c5_g2_i7	Ohr	48hr	9.64	7.44E-03	NA
TRINITY_DN192255_c1_g1_i2	Ohr	48hr	-8.26	1.34E-02	NA
TRINITY_DN192259_c7_g1_i1	Ohr	48hr	8.45	3.88E-02	Tm1
TRINITY_DN192447_c3_g1_i2	Ohr	48hr	-7.45	2.48E-02	GPM6B_MOUSE
TRINITY_DN192450_c8_g3_i2	Ohr	48hr	-8.17	9.03E-03	GHR_COLLI
TRINITY_DN192607_c0_g2_i12	Ohr	48hr	-7.58	4.19E-02	TM55B_HUMAN
TRINITY_DN192960_c12_g1_i1	Ohr	48hr	-7.68	3.81E-02	NA
TRINITY_DN193103_c0_g1_i13	Ohr	48hr	6.68	3.81E-02	HA1F_CHICK
TRINITY_DN193230_c5_g1_i3	Ohr	48hr	9.63	1.90E-02	3HAO_XENTR
TRINITY_DN193242_c0_g1_i5	Ohr	48hr	-10.50	3.51E-02	ARF4_BOVIN
TRINITY_DN193515_c0_g2_i12	Ohr	48hr	-10.11	2.94E-02	AKIR1_XENTR
TRINITY_DN193600_c10_g1_i2	Ohr	48hr	-5.74	1.76E-02	NA
TRINITY_DN193653_c8_g1_i6	Ohr	48hr	5.77	8.13E-03	NA
TRINITY_DN193687_c6_g1_i3	Ohr	48hr	6.81	3.01E-02	GDPD3_HUMAN
TRINITY_DN193809_c1_g2_i10	Ohr	48hr	-10.84	1.92E-02	UQCC3_DANRE
TRINITY_DN193809_c1_g2_i2	Ohr	48hr	-9.81	1.30E-02	UQCC3_DANRE
TRINITY_DN194036_c0_g1_i6	Ohr	48hr	-10.46	2.97E-02	NA
TRINITY_DN194294_c1_g2_i10	Ohr	48hr	-7.94	2.15E-02	PRP31_XENTR

TRINITY_DN194306_c10_g1_i3	Ohr	48hr	8.15	4.09E-02	NA
TRINITY_DN194337_c9_g1_i8	Ohr	48hr	8.60	1.57E-03	HYI_XENLA
TRINITY_DN194362_c1_g2_i8	Ohr	48hr	-7.81	2.15E-02	TNPO1_HUMAN
TRINITY_DN194537_c0_g2_i4	Ohr	48hr	-8.60	2.15E-03	NA
TRINITY_DN194557_c5_g1_i2	Ohr	48hr	-9.90	5.38E-03	RAE1L_XENTR
TRINITY_DN194658_c4_g1_i1	Ohr	48hr	4.42	4.33E-02	NA
TRINITY_DN194679_c1_g2_i5	Ohr	48hr	9.46	1.92E-02	NA
TRINITY_DN194716_c1_g2_i5	Ohr	48hr	-5.43	3.81E-02	B4GT7_HUMAN
TRINITY_DN194875_c9_g1_i2	Ohr	48hr	9.31	1.99E-02	NA
TRINITY_DN195035_c2_g1_i4	Ohr	48hr	-10.28	2.65E-02	PARK7_CHICK
TRINITY_DN195064_c5_g2_i4	Ohr	48hr	8.00	2.15E-02	VRK1_BOVIN
TRINITY_DN195422_c3_g4_i4	Ohr	48hr	9.50	1.90E-02	EYA3_HUMAN
TRINITY_DN195493_c11_g1_i4	Ohr	48hr	2.77	4.84E-02	NA
TRINITY_DN195498_c0_g2_i11	Ohr	48hr	-8.59	1.07E-02	MIC60_HUMAN
TRINITY_DN195573_c4_g1_i2	Ohr	48hr	6.13	3.66E-02	NA
TRINITY_DN195678_c9_g1_i8	Ohr	48hr	-9.20	7.98E-03	NA
TRINITY_DN195750_c4_g2_i8	Ohr	48hr	2.14	2.52E-02	CYR61_CHICK
TRINITY_DN195953_c12_g1_i3	Ohr	48hr	5.07	3.84E-02	CCND1_CHICK
TRINITY_DN196032_c4_g1_i10	Ohr	48hr	9.68	1.57E-03	ORN_BOVIN
TRINITY_DN196293_c0_g1_i8	Ohr	48hr	-8.20	2.06E-02	FADD_MOUSE
TRINITY_DN196335_c1_g1_i12	Ohr	48hr	10.61	8.24E-03	MICU1_XENTR
TRINITY_DN196567_c6_g1_i6	Ohr	48hr	8.26	8.94E-03	GPN1_HUMAN
TRINITY_DN196658_c4_g3_i3	Ohr	48hr	-9.18	1.25E-03	NA
TRINITY_DN196695_c0_g1_i8	Ohr	48hr	-8.95	1.19E-02	SRS12_HUMAN
TRINITY_DN196728_c6_g1_i9	Ohr	48hr	9.62	3.86E-07	NA
TRINITY_DN197062_c0_g1_i10	Ohr	48hr	4.55	6.75E-03	NA
TRINITY_DN197062_c0_g1_i18	Ohr	48hr	3.56	2.83E-02	NA
TRINITY_DN197105_c8_g1_i1	Ohr	48hr	10.17	1.18E-02	NA
TRINITY_DN197105_c8_g1_i7	Ohr	48hr	9.55	1.90E-02	NA
TRINITY_DN197261_c10_g1_i1	Ohr	48hr	-9.57	1.26E-06	NA
TRINITY_DN197388_c0_g4_i1	Ohr	48hr	4.28	2.78E-02	NA
TRINITY_DN197456_c2_g1_i8	Ohr	48hr	9.41	1.91E-02	SPCS1_MOUSE
TRINITY_DN197518_c6_g1_i6	Ohr	48hr	-9.62	7.29E-03	ILEU_HORSE
TRINITY_DN197587_c3_g1_i1	Ohr	48hr	9.24	2.52E-02	CASP6_MOUSE
TRINITY_DN197728_c11_g1_i5	Ohr	48hr	8.14	1.14E-02	YAF2_MOUSE
TRINITY_DN197774_c4_g1_i12	Ohr	48hr	-9.77	6.92E-04	VPS8_HUMAN
TRINITY_DN197779_c0_g1_i3	Ohr	48hr	7.57	4.44E-02	GELS_CHICK
TRINITY_DN197822_c4_g1_i1	Ohr	48hr	8.71	2.90E-02	DGKE_HUMAN
TRINITY_DN197876_c8_g4_i3	Ohr	48hr	-8.61	1.17E-02	NA

TRINITY_DN198251_c10_g1_i4	Ohr	48hr	-6.84	2.48E-02	NDUB9_MOUSE
TRINITY_DN198480_c6_g1_i2	Ohr	48hr	-7.75	3.35E-02	NA
TRINITY_DN198572_c8_g3_i1	Ohr	48hr	-9.15	4.23E-03	NA
TRINITY_DN198772_c14_g1_i7	Ohr	48hr	8.14	1.02E-02	ENT1_SCHPO
TRINITY_DN198958_c6_g1_i1	Ohr	48hr	10.05	2.79E-02	REEP5_HUMAN
TRINITY_DN198994_c6_g1_i1	Ohr	48hr	6.54	4.63E-02	NA
TRINITY_DN199121_c0_g1_i25	Ohr	48hr	7.91	3.54E-02	CNO6L_HUMAN
TRINITY_DN199121_c0_g1_i3	Ohr	48hr	7.06	2.18E-02	CNO6L_HUMAN
TRINITY_DN199220_c2_g1_i12	Ohr	48hr	-8.06	1.92E-02	PCBP4_MOUSE
TRINITY_DN199227_c4_g1_i2	Ohr	48hr	-8.51	1.91E-02	I17RA_MOUSE
TRINITY_DN199235_c10_g1_i1	Ohr	48hr	9.88	7.59E-05	NA
TRINITY_DN199286_c1_g1_i12	Ohr	48hr	8.79	8.10E-03	XCT_MOUSE
TRINITY_DN199359_c3_g1_i5	Ohr	48hr	8.26	2.94E-02	NA
TRINITY_DN199456_c4_g1_i1	Ohr	48hr	10.41	1.24E-02	NA
TRINITY_DN199481_c5_g1_i7	Ohr	48hr	9.88	2.75E-02	SF3B3_HUMAN
TRINITY_DN199501_c2_g2_i1	Ohr	48hr	8.31	2.90E-02	COPT1_HUMAN
TRINITY_DN199526_c1_g2_i2	Ohr	48hr	-7.92	3.57E-02	NA
TRINITY_DN199586_c4_g1_i6	Ohr	48hr	10.16	1.58E-02	CPT2_XENTR
TRINITY_DN199596_c7_g1_i1	Ohr	48hr	7.88	1.71E-02	NA
TRINITY_DN199634_c3_g1_i5	Ohr	48hr	-9.45	1.57E-03	KAT7_HUMAN
TRINITY_DN199655_c10_g2_i2	Ohr	48hr	-3.82	4.38E-02	NA
TRINITY_DN199952_c6_g1_i2	Ohr	48hr	9.13	9.19E-05	NA
TRINITY_DN200152_c1_g1_i3	Ohr	48hr	6.26	2.75E-02	NA
TRINITY_DN200423_c2_g1_i9	Ohr	48hr	9.69	2.12E-02	TPIS_MACCMU
TRINITY_DN200454_c8_g4_i3	Ohr	48hr	-10.19	3.83E-03	EIF3I_TAEGU
TRINITY_DN200487_c0_g2_i16	Ohr	48hr	6.92	4.67E-02	CPZIP_MOUSE
TRINITY_DN200615_c9_g2_i3	Ohr	48hr	9.12	2.66E-02	WDR26_XENTR
TRINITY_DN200835_c1_g1_i7	Ohr	48hr	-5.46	4.00E-02	ITM2A_MOUSE
TRINITY_DN200874_c11_g1_i1	Ohr	48hr	-6.90	2.83E-02	NA
TRINITY_DN200898_c1_g1_i7	Ohr	48hr	-9.26	4.45E-02	S14L1_HUMAN
TRINITY_DN200951_c3_g1_i14	Ohr	48hr	-7.63	2.94E-02	MTF2_PONAB
TRINITY_DN201061_c1_g1_i11	Ohr	48hr	-7.78	2.02E-02	ZFAN4_MOUSE
TRINITY_DN201093_c0_g1_i11	Ohr	48hr	-6.47	2.97E-02	NA
TRINITY_DN201149_c7_g1_i1	Ohr	48hr	-7.82	3.48E-02	NA
TRINITY_DN201165_c0_g1_i1	Ohr	48hr	-3.64	4.39E-02	NA
TRINITY_DN201264_c1_g2_i1	Ohr	48hr	-5.74	5.48E-03	PCY2_BOVIN
TRINITY_DN201313_c6_g1_i8	Ohr	48hr	9.64	2.17E-02	NA
TRINITY_DN201348_c1_g1_i18	Ohr	48hr	7.65	3.75E-02	SSUH2_HUMAN
TRINITY_DN201427_c10_g1_i2	Ohr	48hr	7.68	5.15E-05	NA

TRINITY_DN201586_c9_g1_i12	Ohr	48hr	-10.66	2.49E-03	GPC5B_HUMAN
TRINITY_DN201658_c3_g1_i16	Ohr	48hr	9.32	2.59E-02	NA
TRINITY_DN202019_c0_g1_i20	Ohr	48hr	-10.42	3.19E-03	TRAF7_HUMAN
TRINITY_DN202041_c10_g2_i3	Ohr	48hr	7.17	4.81E-02	NA
TRINITY_DN202055_c0_g1_i11	Ohr	48hr	-6.39	4.67E-02	PIGT_MOUSE
TRINITY_DN202139_c11_g1_i3	Ohr	48hr	9.23	3.19E-03	ERCC3_BOVIN
TRINITY_DN202139_c11_g1_i4	Ohr	48hr	-8.43	1.20E-02	ERCC3_BOVIN
TRINITY_DN202155_c0_g2_i11	Ohr	48hr	10.15	1.20E-02	VAMP4_HUMAN
TRINITY_DN202397_c8_g2_i6	Ohr	48hr	-8.31	2.75E-02	NA
TRINITY_DN202515_c3_g1_i4	Ohr	48hr	-7.95	3.30E-02	F120B_HUMAN
TRINITY_DN202536_c4_g1_i3	Ohr	48hr	6.81	4.48E-02	NA
TRINITY_DN202580_c4_g2_i4	Ohr	48hr	-2.76	3.01E-02	GTR11_HUMAN
TRINITY_DN202605_c0_g1_i11	Ohr	48hr	8.88	4.21E-02	HMR1_PANTR
TRINITY_DN202646_c0_g1_i2	Ohr	48hr	-10.07	2.98E-02	SMIM7_BOVIN
TRINITY_DN202818_c1_g1_i12	Ohr	48hr	-9.84	5.79E-03	GCC2_MOUSE
TRINITY_DN202939_c0_g3_i3	Ohr	48hr	-6.99	4.63E-02	NA
TRINITY_DN203164_c6_g1_i1	Ohr	48hr	-7.88	3.64E-03	THOC2_RHIFE
TRINITY_DN203176_c2_g1_i2	Ohr	48hr	-7.14	3.99E-02	NA
TRINITY_DN203262_c6_g3_i2	Ohr	48hr	-6.27	7.86E-03	PIEZ2_MOUSE
TRINITY_DN203280_c14_g2_i7	Ohr	48hr	-7.75	4.23E-03	LGMN_BOVIN
TRINITY_DN203355_c0_g2_i32	Ohr	48hr	5.69	3.88E-02	SEM3F_MOUSE
TRINITY_DN203355_c0_g2_i5	Ohr	48hr	-9.36	4.28E-02	SEM3F_MOUSE
TRINITY_DN203614_c5_g1_i5	Ohr	48hr	-4.22	8.93E-03	NA
TRINITY_DN203680_c0_g1_i2	Ohr	48hr	11.68	4.54E-03	NA
TRINITY_DN203771_c2_g1_i3	Ohr	48hr	-7.97	2.09E-02	HNRPQ_MOUSE
TRINITY_DN203841_c2_g1_i13	Ohr	48hr	2.68	4.87E-02	XPO1_MOUSE
TRINITY_DN203880_c16_g1_i13	Ohr	48hr	-9.62	1.01E-02	NA
TRINITY_DN203913_c2_g1_i23	Ohr	48hr	-9.96	4.75E-03	SYQ_BOVIN
TRINITY_DN203914_c1_g6_i3	Ohr	48hr	-9.47	1.14E-02	NA
TRINITY_DN203960_c8_g1_i5	Ohr	48hr	9.48	2.29E-04	OSBL9_HUMAN
TRINITY_DN204026_c10_g1_i3	Ohr	48hr	3.66	1.25E-03	NA
TRINITY_DN204054_c2_g1_i11	Ohr	48hr	-10.80	6.06E-05	S19A3_MACFA
TRINITY_DN204058_c0_g1_i4	Ohr	48hr	-7.71	3.81E-02	Tm1
TRINITY_DN204108_c2_g3_i10	Ohr	48hr	-7.72	3.99E-02	CTR3_HUMAN
TRINITY_DN204168_c2_g1_i3	Ohr	48hr	9.05	1.53E-02	TM50A_MOUSE
TRINITY_DN204304_c8_g1_i13	Ohr	48hr	-9.64	5.99E-03	NA
TRINITY_DN204320_c4_g1_i7	Ohr	48hr	11.36	7.83E-04	OSTF1_XENLA
TRINITY_DN204456_c4_g1_i1	Ohr	48hr	-9.42	1.01E-02	TECR_HUMAN
TRINITY_DN204480_c9_g1_i3	Ohr	48hr	8.02	1.13E-02	NA

TRINITY_DN204630_c2_g2_i9	Ohr	48hr	6.06	2.48E-02	NA
TRINITY_DN204676_c3_g2_i2	Ohr	48hr	-11.53	6.46E-04	MAL2_BOVIN
TRINITY_DN204737_c14_g1_i2	Ohr	48hr	-9.36	4.31E-02	NA
TRINITY_DN204830_c2_g1_i2	Ohr	48hr	-8.07	1.90E-02	LANC2_HUMAN
TRINITY_DN204848_c7_g2_i5	Ohr	48hr	-9.42	1.90E-02	YRDC_RAT
TRINITY_DN204937_c4_g2_i4	Ohr	48hr	-8.93	2.71E-02	MBRL_MOUSE
TRINITY_DN204990_c4_g1_i1	Ohr	48hr	-2.86	3.52E-02	NA
TRINITY_DN205185_c13_g1_i9	Ohr	48hr	-6.96	1.90E-02	NA
TRINITY_DN205237_c4_g2_i7	Ohr	48hr	10.57	6.87E-10	NA
TRINITY_DN205449_c1_g2_i22	Ohr	48hr	-8.79	2.41E-03	NA
TRINITY_DN205666_c5_g1_i5	Ohr	48hr	-9.79	3.54E-02	NA
TRINITY_DN205773_c2_g3_i2	Ohr	48hr	7.75	4.52E-02	NA
TRINITY_DN205800_c6_g1_i16	Ohr	48hr	-9.25	4.94E-02	BMS1_HUMAN
TRINITY_DN205800_c6_g1_i17	Ohr	48hr	10.36	1.31E-02	BMS1_HUMAN
TRINITY_DN205825_c3_g1_i10	Ohr	48hr	8.59	1.91E-02	PDC6I_HUMAN
TRINITY_DN205837_c2_g2_i4	Ohr	48hr	-10.06	3.11E-02	NGBR_DANRE
TRINITY_DN205912_c0_g1_i10	Ohr	48hr	9.28	1.01E-02	SNX14_PONAB
TRINITY_DN205919_c3_g2_i2	Ohr	48hr	7.64	3.80E-02	SQSTM_MOUSE
TRINITY_DN205951_c3_g2_i14	Ohr	48hr	-7.94	3.83E-03	NA
TRINITY_DN205990_c1_g1_i4	Ohr	48hr	-8.23	1.57E-02	MSH2_CHLAE
TRINITY_DN206054_c6_g1_i4	Ohr	48hr	7.30	3.54E-02	FAD_binding_3
TRINITY_DN206111_c5_g2_i1	Ohr	48hr	8.57	4.58E-05	GBG5_RAT
TRINITY_DN206236_c0_g2_i10	Ohr	48hr	6.18	4.22E-02	HMR1_HUMAN
TRINITY_DN206375_c10_g1_i4	Ohr	48hr	-8.26	1.38E-02	RL27_RAT
TRINITY_DN206564_c0_g1_i4	Ohr	48hr	7.05	4.02E-02	NA
TRINITY_DN206727_c7_g1_i2	Ohr	48hr	-9.49	6.57E-04	CLD10_BOVIN
TRINITY_DN206739_c5_g1_i1	Ohr	48hr	-11.37	6.57E-04	NA
TRINITY_DN206770_c4_g1_i10	Ohr	48hr	8.55	5.61E-03	PFD2_HUMAN
TRINITY_DN206814_c2_g4_i1	Ohr	48hr	-7.38	1.57E-03	NA
TRINITY_DN206991_c0_g1_i9	Ohr	48hr	-11.10	8.51E-03	RNF10_HUMAN
TRINITY_DN207017_c1_g1_i18	Ohr	48hr	-7.03	4.22E-02	NA
TRINITY_DN207129_c0_g1_i12	Ohr	48hr	9.48	1.43E-02	NA
TRINITY_DN207173_c6_g1_i4	Ohr	48hr	8.39	3.66E-02	3BP5_RAT
TRINITY_DN207234_c9_g1_i5	Ohr	48hr	8.37	2.58E-02	CTDSL_CHICK
TRINITY_DN207291_c3_g1_i2	Ohr	48hr	-9.26	1.05E-02	BCAP_CHICK
TRINITY_DN207446_c3_g3_i2	Ohr	48hr	9.30	2.10E-02	SRRM1_CHICK
TRINITY_DN207557_c8_g1_i22	Ohr	48hr	-7.44	1.20E-02	TTC25_DANRE
TRINITY_DN207619_c2_g1_i4	Ohr	48hr	-10.83	1.57E-03	IF2A_CHICK
TRINITY_DN207711_c2_g1_i8	Ohr	48hr	6.45	3.16E-02	CTL3_HUMAN

TRINITY_DN207763_c6_g1_i18	Ohr	48hr	9.45	1.91E-02	K0020_RAT
TRINITY_DN207790_c4_g1_i3	Ohr	48hr	-7.62	2.79E-02	TE2IP_HUMAN
TRINITY_DN207838_c1_g2_i1	Ohr	48hr	-10.78	2.39E-02	F210B_MOUSE
TRINITY_DN208122_c5_g3_i1	Ohr	48hr	-10.12	3.11E-02	POPD2_MOUSE
TRINITY_DN208164_c8_g1_i12	Ohr	48hr	9.29	2.00E-02	IF6_DANRE
TRINITY_DN208164_c8_g1_i16	Ohr	48hr	9.68	1.84E-02	IF6_DANRE
TRINITY_DN208177_c2_g5_i4	Ohr	48hr	-7.95	3.43E-02	NA
TRINITY_DN208205_c1_g7_i1	Ohr	48hr	6.35	2.66E-02	NA
TRINITY_DN208293_c8_g3_i2	Ohr	48hr	-9.30	4.56E-02	FGF2_SHEEP
TRINITY_DN208299_c4_g1_i11	Ohr	48hr	-7.74	3.66E-02	M3K15_HUMAN
TRINITY_DN208325_c6_g1_i3	Ohr	48hr	7.87	3.66E-02	NA
TRINITY_DN208357_c3_g2_i3	Ohr	48hr	-7.06	1.60E-02	NA
TRINITY_DN208373_c1_g4_i1	Ohr	48hr	-8.21	2.26E-02	ANM5_PONAB
TRINITY_DN208415_c4_g1_i5	Ohr	48hr	8.86	4.31E-03	CALX_RAT
TRINITY_DN208519_c5_g1_i3	Ohr	48hr	5.60	1.52E-03	MLRM_CHICK
TRINITY_DN208522_c3_g5_i1	Ohr	48hr	-2.86	1.01E-02	NA
TRINITY_DN208572_c5_g1_i2	Ohr	48hr	-10.39	1.05E-04	CATIN_HUMAN
TRINITY_DN208572_c5_g1_i23	Ohr	48hr	10.10	5.62E-05	CATIN_DANRE
TRINITY_DN208594_c3_g1_i1	Ohr	48hr	-8.14	8.94E-03	BL1S3_HUMAN
TRINITY_DN208651_c2_g1_i3	Ohr	48hr	-9.99	5.47E-05	AL1L1_XENLA
TRINITY_DN208735_c2_g1_i1	Ohr	48hr	-10.71	7.24E-05	AT2C1_HUMAN
TRINITY_DN208771_c6_g1_i2	Ohr	48hr	-8.20	3.06E-02	NA
TRINITY_DN208809_c1_g1_i9	Ohr	48hr	-10.96	1.33E-03	DDX18_HUMAN
TRINITY_DN208822_c8_g1_i4	Ohr	48hr	-8.22	1.76E-02	NA
TRINITY_DN208822_c8_g1_i6	Ohr	48hr	7.73	3.57E-02	NA
TRINITY_DN209034_c4_g1_i12	Ohr	48hr	-9.16	4.77E-02	DSC3_BOVIN
TRINITY_DN209076_c1_g1_i11	Ohr	48hr	-7.95	3.54E-02	TRXR1_RAT
TRINITY_DN209081_c3_g3_i7	Ohr	48hr	-10.66	1.74E-03	UDB10_HUMAN
TRINITY_DN209090_c2_g1_i23	Ohr	48hr	8.04	4.21E-02	GRB7_HUMAN
TRINITY_DN209090_c2_g1_i32	Ohr	48hr	8.49	2.84E-02	GRB10_HUMAN
TRINITY_DN209090_c2_g1_i34	Ohr	48hr	-9.39	1.39E-02	GRB10_HUMAN
TRINITY_DN209201_c4_g1_i6	Ohr	48hr	-9.04	1.23E-02	ADDA_HUMAN
TRINITY_DN209256_c3_g1_i3	Ohr	48hr	8.98	1.45E-02	FITM2_MOUSE
TRINITY_DN209256_c3_g1_i6	Ohr	48hr	-9.45	1.93E-02	FITM2_MOUSE
TRINITY_DN209290_c0_g1_i1	Ohr	48hr	-9.97	3.30E-02	NA
TRINITY_DN209298_c7_g1_i9	Ohr	48hr	-12.57	1.60E-02	CN159_MOUSE
TRINITY_DN209451_c1_g2_i2	Ohr	48hr	-10.08	2.98E-02	NOL8_HUMAN
TRINITY_DN209461_c3_g2_i1	Ohr	48hr	-10.81	2.48E-02	NA
TRINITY_DN209476_c1_g3_i2	Ohr	48hr	-3.75	4.55E-02	AFG32_BOVIN

TRINITY_DN209549_c9_g2_i1	Ohr	48hr	-8.71	1.01E-02	NA
TRINITY_DN209608_c2_g2_i3	Ohr	48hr	-8.26	2.01E-02	CACO1_RAT
TRINITY_DN209612_c11_g2_i13	Ohr	48hr	9.80	1.59E-02	YKT6_BOVIN
TRINITY_DN209612_c11_g2_i3	Ohr	48hr	-9.74	5.91E-03	YKT6_BOVIN
TRINITY_DN209642_c7_g1_i8	Ohr	48hr	11.48	8.94E-03	COX5A_PONPY
TRINITY_DN209667_c6_g4_i1	Ohr	48hr	6.64	5.48E-03	NA
TRINITY_DN209870_c1_g3_i7	Ohr	48hr	-9.07	1.76E-03	STOM_HUMAN
TRINITY_DN210133_c5_g2_i14	Ohr	48hr	-9.32	7.61E-03	PTBP2_RAT
TRINITY_DN210149_c0_g2_i20	Ohr	48hr	11.56	3.62E-04	DIC_HUMAN
TRINITY_DN210149_c0_g2_i4	Ohr	48hr	10.29	2.13E-03	DIC_HUMAN
TRINITY_DN210172_c2_g1_i2	Ohr	48hr	7.15	1.71E-02	NA
TRINITY_DN210246_c9_g1_i4	Ohr	48hr	6.10	3.81E-02	F195A_BOVIN
TRINITY_DN210258_c5_g3_i3	Ohr	48hr	10.82	1.91E-02	FOXK1_MOUSE
TRINITY_DN210309_c1_g1_i3	Ohr	48hr	5.32	1.91E-02	NA
TRINITY_DN210389_c1_g1_i14	Ohr	48hr	-10.01	4.08E-04	TLN1_CHICK
TRINITY_DN210601_c0_g1_i12	Ohr	48hr	-6.86	4.41E-02	RBM10_RAT
TRINITY_DN210873_c2_g6_i2	Ohr	48hr	-7.69	4.08E-02	NA
TRINITY_DN211003_c4_g1_i7	Ohr	48hr	-7.47	3.67E-02	NA
TRINITY_DN211062_c4_g1_i8	Ohr	48hr	-10.39	2.22E-07	CADH1_CHICK
TRINITY_DN211114_c3_g1_i1	Ohr	48hr	12.35	3.38E-04	NA
TRINITY_DN211114_c3_g1_i2	Ohr	48hr	-8.28	4.34E-02	NA
TRINITY_DN211114_c3_g1_i4	Ohr	48hr	11.65	1.64E-05	NA
TRINITY_DN211165_c4_g1_i5	Ohr	48hr	-8.09	4.93E-02	SF3B1_HUMAN
TRINITY_DN211219_c2_g2_i7	Ohr	48hr	-4.94	5.54E-03	AL3A1_HUMAN
TRINITY_DN211226_c5_g3_i3	Ohr	48hr	7.38	3.59E-02	NA
TRINITY_DN211238_c9_g1_i6	Ohr	48hr	-10.95	3.08E-02	NA
TRINITY_DN211239_c2_g3_i15	Ohr	48hr	5.36	1.02E-03	PAR3L_HUMAN
TRINITY_DN211240_c3_g2_i5	Ohr	48hr	-7.31	3.46E-02	VWA7_MOUSE
TRINITY_DN211364_c3_g1_i6	Ohr	48hr	-4.56	4.82E-02	SORL_HUMAN
TRINITY_DN211442_c0_g2_i2	Ohr	48hr	-10.57	1.97E-03	NA
TRINITY_DN211445_c4_g1_i19	Ohr	48hr	9.86	1.34E-04	IQUB_HUMAN
TRINITY_DN211526_c9_g1_i13	Ohr	48hr	11.43	4.23E-03	HGD_PONAB
TRINITY_DN211557_c0_g1_i32	Ohr	48hr	-10.58	1.36E-04	AOXA_HUMAN
TRINITY_DN211583_c1_g1_i1	Ohr	48hr	7.61	1.52E-03	SGK1_MOUSE
TRINITY_DN211594_c13_g1_i4	Ohr	48hr	-5.55	2.88E-02	FTCD_PIG
TRINITY_DN211618_c1_g1_i1	Ohr	48hr	-7.96	2.18E-02	NA
TRINITY_DN211671_c2_g1_i30	Ohr	48hr	-10.13	2.94E-02	PLXB2_HUMAN
TRINITY_DN211671_c2_g1_i35	Ohr	48hr	-9.56	4.21E-02	PLXB2_MOUSE
TRINITY_DN211671_c2_g1_i8	Ohr	48hr	6.64	3.54E-02	PLXB2_MOUSE

TRINITY_DN211914_c3_g4_i3	0hr	48hr	-6.75	3.48E-02	NA
TRINITY_DN211915_c8_g1_i3	0hr	48hr	-9.83	4.98E-03	IKBP1_HUMAN
TRINITY_DN211922_c10_g1_i11	0hr	48hr	-7.40	2.77E-02	VMA5A_MOUSE
TRINITY_DN211982_c2_g1_i9	0hr	48hr	7.32	1.84E-02	IF44L_HUMAN
TRINITY_DN212155_c1_g1_i3	0hr	48hr	-9.53	6.31E-03	NA
TRINITY_DN212439_c11_g1_i1	0hr	48hr	-2.99	1.38E-02	NA
TRINITY_DN212719_c4_g1_i2	0hr	48hr	3.27	1.84E-02	NA
TRINITY_DN212800_c3_g1_i2	0hr	48hr	8.18	3.88E-03	NA
TRINITY_DN212884_c17_g1_i1	0hr	48hr	9.09	6.57E-04	RPTOR_MOUSE
TRINITY_DN212884_c17_g1_i6	0hr	48hr	-10.23	3.19E-03	RPTOR_MOUSE
TRINITY_DN160434_c0_g1_i1	12hr	48hr	6.14	5.23E-03	MOG2A_XENLA
TRINITY_DN166426_c0_g1_i3	12hr	48hr	7.97	4.04E-02	TIM10_RAT
TRINITY_DN168766_c0_g1_i3	12hr	48hr	-6.02	4.17E-02	NA
TRINITY_DN169657_c0_g2_i1	12hr	48hr	7.80	4.00E-02	NA
TRINITY_DN170873_c0_g1_i3	12hr	48hr	-8.20	1.57E-02	NA
TRINITY_DN171092_c0_g1_i2	12hr	48hr	7.46	2.00E-02	NA
TRINITY_DN172243_c1_g1_i4	12hr	48hr	-10.46	2.04E-02	NA
TRINITY_DN172518_c0_g1_i7	12hr	48hr	4.77	2.82E-02	PRG4_MOUSE
TRINITY_DN172829_c0_g3_i2	12hr	48hr	-7.01	3.87E-02	CCL20_MOUSE
TRINITY_DN172829_c0_g3_i3	12hr	48hr	-7.27	2.07E-02	CCL20_MOUSE
TRINITY_DN172829_c0_g3_i4	12hr	48hr	-4.43	1.39E-02	CCL20_MOUSE
TRINITY_DN173068_c0_g1_i3	12hr	48hr	5.89	2.14E-02	NA
TRINITY_DN173409_c9_g2_i1	12hr	48hr	9.33	4.42E-02	NA
TRINITY_DN173520_c0_g2_i1	12hr	48hr	6.91	1.95E-02	ZBT46_MOUSE
TRINITY_DN173696_c3_g1_i6	12hr	48hr	9.34	2.49E-02	FKBP3_HUMAN
TRINITY_DN174311_c2_g2_i4	12hr	48hr	8.26	6.70E-04	RAPA_DIPOM
TRINITY_DN174659_c4_g1_i7	12hr	48hr	7.27	1.51E-02	IMPA1_PONAB
TRINITY_DN174884_c1_g1_i1	12hr	48hr	8.23	1.39E-02	KXDL1_XENTR
TRINITY_DN175027_c12_g1_i1	12hr	48hr	6.10	3.88E-02	NA
TRINITY_DN175047_c10_g4_i7	12hr	48hr	5.14	1.88E-02	NA
TRINITY_DN175148_c10_g1_i2	12hr	48hr	9.09	2.16E-02	NA
TRINITY_DN175277_c13_g1_i2	12hr	48hr	7.29	2.70E-02	NA
TRINITY_DN175437_c8_g3_i10	12hr	48hr	-10.07	2.70E-02	KLF13_HUMAN
TRINITY_DN175437_c8_g3_i9	12hr	48hr	9.08	6.70E-03	KLF13_HUMAN
TRINITY_DN175704_c12_g2_i1	12hr	48hr	8.64	3.41E-02	MAP2_HUMAN
TRINITY_DN176144_c11_g1_i4	12hr	48hr	7.67	7.08E-03	NA
TRINITY_DN176194_c4_g1_i3	12hr	48hr	7.91	3.60E-02	DEXI_DANRE
TRINITY_DN176221_c3_g2_i9	12hr	48hr	9.94	5.33E-03	LOX5_HUMAN
TRINITY_DN176293_c4_g2_i1	12hr	48hr	8.64	6.13E-03	NA

TRINITY_DN176604_c9_g1_i4	12hr	48hr	9.07	4.00E-02	CTU2_DANRE
TRINITY_DN176668_c10_g2_i6	12hr	48hr	8.96	4.33E-02	SH3L3_PONAB
TRINITY_DN176676_c3_g1_i11	12hr	48hr	-10.56	1.98E-02	TB10A_HUMAN
TRINITY_DN176732_c3_g1_i1	12hr	48hr	-9.37	1.02E-03	UAP1L_XENTR
TRINITY_DN176908_c4_g5_i2	12hr	48hr	7.06	1.39E-02	NA
TRINITY_DN177712_c5_g1_i1	12hr	48hr	-6.50	3.06E-02	RTBS_DROME
TRINITY_DN177788_c9_g1_i1	12hr	48hr	3.82	2.21E-02	NA
TRINITY_DN177926_c5_g1_i8	12hr	48hr	-7.39	2.27E-02	SUGP1_HUMAN
TRINITY_DN178424_c6_g2_i5	12hr	48hr	-5.32	2.97E-02	MED8_DANRE
TRINITY_DN178442_c1_g2_i5	12hr	48hr	7.80	4.81E-02	UBE2T_XENLA
TRINITY_DN179054_c10_g1_i6	12hr	48hr	-7.17	3.87E-02	NPRL2_BOVIN
TRINITY_DN179066_c9_g3_i4	12hr	48hr	-9.17	4.55E-02	ES1_RAT
TRINITY_DN179215_c9_g1_i3	12hr	48hr	-8.12	4.51E-03	PAPS2_MOUSE
TRINITY_DN179450_c4_g2_i5	12hr	48hr	-9.76	3.48E-02	P53_ONCMY
TRINITY_DN179559_c21_g2_i1	12hr	48hr	4.99	2.90E-02	NA
TRINITY_DN179606_c7_g1_i11	12hr	48hr	-7.68	1.71E-02	KBP_CHICK
TRINITY_DN180215_c6_g3_i3	12hr	48hr	6.53	1.37E-02	CMGA_PIG
TRINITY_DN180235_c11_g6_i2	12hr	48hr	-6.12	4.82E-02	NA
TRINITY_DN180392_c3_g3_i5	12hr	48hr	8.41	6.62E-04	MLF2_HUMAN
TRINITY_DN180670_c1_g1_i7	12hr	48hr	-7.22	2.59E-02	TSN5_BOVIN
TRINITY_DN180862_c3_g1_i19	12hr	48hr	11.54	1.08E-02	TCPB_BOVIN
TRINITY_DN180949_c1_g1_i1	12hr	48hr	10.09	3.22E-02	RNF13_CHICK
TRINITY_DN181012_c15_g1_i2	12hr	48hr	-7.76	2.04E-02	NA
TRINITY_DN181044_c4_g1_i2	12hr	48hr	8.86	6.56E-03	NA
TRINITY_DN181104_c1_g1_i8	12hr	48hr	-8.29	1.25E-02	IDLC_RAT
TRINITY_DN181210_c11_g1_i4	12hr	48hr	7.14	3.33E-02	NA
TRINITY_DN181463_c5_g1_i3	12hr	48hr	-9.27	4.62E-02	SYEM_CHICK
TRINITY_DN181760_c5_g5_i2	12hr	48hr	6.89	3.50E-02	NA
TRINITY_DN181823_c2_g1_i23	12hr	48hr	-9.12	4.55E-02	NA
TRINITY_DN182005_c7_g1_i9	12hr	48hr	-9.37	1.62E-03	NEDD8_RAT
TRINITY_DN182642_c3_g1_i4	12hr	48hr	-10.15	2.70E-02	NA
TRINITY_DN182727_c2_g1_i8	12hr	48hr	6.05	1.19E-02	WWP2_HUMAN
TRINITY_DN182736_c5_g1_i1	12hr	48hr	7.20	1.51E-02	RHG32_XENLA
TRINITY_DN182766_c5_g2_i16	12hr	48hr	8.63	4.19E-02	NA
TRINITY_DN183104_c11_g1_i5	12hr	48hr	-8.22	1.20E-02	THRB_HUMAN
TRINITY_DN183248_c2_g1_i4	12hr	48hr	-7.78	4.93E-03	ANR10_HUMAN
TRINITY_DN183269_c9_g3_i6	12hr	48hr	9.10	1.24E-02	SCG1_PIG
TRINITY_DN183286_c1_g1_i21	12hr	48hr	-8.44	2.00E-02	NA
TRINITY_DN183486_c1_g1_i1	12hr	48hr	-6.23	2.25E-02	YL154_YEAST

TRINITY_DN183527_c9_g1_i11	12hr	48hr	-9.34	1.50E-03	APMAP_HUMAN
TRINITY_DN183625_c5_g1_i9	12hr	48hr	-8.88	1.42E-03	SCAM3_BOVIN
TRINITY_DN183804_c12_g2_i4	12hr	48hr	8.03	3.41E-02	TSR1_XENLA
TRINITY_DN184008_c5_g1_i8	12hr	48hr	8.85	4.41E-04	NUD24_ARATH
TRINITY_DN184224_c0_g1_i26	12hr	48hr	-6.52	2.06E-02	SARDH_MOUSE
TRINITY_DN184298_c0_g1_i2	12hr	48hr	8.20	3.62E-02	NA
TRINITY_DN184393_c3_g1_i5	12hr	48hr	-8.28	2.26E-02	UB2J1_MOUSE
TRINITY_DN184531_c8_g2_i2	12hr	48hr	-3.67	4.81E-02	NA
TRINITY_DN184603_c1_g1_i2	12hr	48hr	-7.92	2.61E-02	PIM3_COTJA
TRINITY_DN185220_c1_g1_i3	12hr	48hr	9.58	2.87E-05	DLP1_HUMAN
TRINITY_DN185241_c5_g1_i17	12hr	48hr	9.06	8.12E-03	CHMP7_HUMAN
TRINITY_DN185464_c6_g1_i10	12hr	48hr	7.68	4.66E-02	GFI1_CANFA
TRINITY_DN185525_c0_g1_i8	12hr	48hr	-10.42	1.57E-02	NA
TRINITY_DN185602_c11_g2_i1	12hr	48hr	5.18	4.02E-02	Tm1
TRINITY_DN185645_c0_g2_i1	12hr	48hr	-9.67	3.35E-02	NA
TRINITY_DN185752_c2_g1_i3	12hr	48hr	7.22	2.04E-02	DMAP1_HUMAN
TRINITY_DN185801_c0_g2_i16	12hr	48hr	5.60	4.81E-02	MET17_BOVIN
TRINITY_DN185957_c10_g1_i14	12hr	48hr	-9.11	8.19E-03	ACLY_MOUSE
TRINITY_DN186140_c7_g2_i4	12hr	48hr	-7.14	2.82E-02	GALA_DANRE
TRINITY_DN186334_c0_g1_i2	12hr	48hr	8.09	3.93E-02	NA
TRINITY_DN186725_c7_g1_i2	12hr	48hr	9.91	1.59E-05	NA
TRINITY_DN186726_c5_g1_i15	12hr	48hr	-3.83	4.70E-02	NA
TRINITY_DN186752_c2_g1_i6	12hr	48hr	8.13	3.14E-02	NA
TRINITY_DN187108_c7_g6_i1	12hr	48hr	-6.40	1.89E-02	NA
TRINITY_DN187127_c6_g1_i1	12hr	48hr	4.84	3.41E-02	GBRA5_HUMAN
TRINITY_DN187454_c8_g1_i5	12hr	48hr	-7.31	1.50E-03	CTL5_XENTR
TRINITY_DN187585_c6_g1_i3	12hr	48hr	-8.95	8.54E-03	SYS1_MOUSE
TRINITY_DN187760_c2_g1_i10	12hr	48hr	9.57	3.93E-03	TSN3_PONAB
TRINITY_DN187833_c1_g1_i20	12hr	48hr	-6.63	4.34E-02	NA
TRINITY_DN187835_c1_g1_i7	12hr	48hr	-9.27	8.68E-04	ERGI3_XENLA
TRINITY_DN187885_c1_g1_i4	12hr	48hr	-4.33	4.84E-03	COQ4_HUMAN
TRINITY_DN187935_c6_g1_i1	12hr	48hr	7.81	1.65E-02	DCTP1_RAT
TRINITY_DN188411_c11_g1_i2	12hr	48hr	2.54	3.01E-03	NA
TRINITY_DN188435_c0_g1_i1	12hr	48hr	8.78	3.10E-02	NEK2_HUMAN
TRINITY_DN188525_c12_g2_i1	12hr	48hr	10.20	2.12E-02	PKHA1_HUMAN
TRINITY_DN188564_c3_g1_i4	12hr	48hr	7.20	4.54E-02	PPM1H_HUMAN
TRINITY_DN188596_c2_g1_i7	12hr	48hr	-8.83	2.00E-03	GP146_XENLA
TRINITY_DN188604_c1_g1_i6	12hr	48hr	-8.02	1.48E-02	TAP26_HUMAN
TRINITY_DN188701_c4_g4_i1	12hr	48hr	-6.47	6.97E-03	CDC73_MOUSE

TRINITY_DN188755_c0_g1_i9	12hr	48hr	5.85	1.51E-02	IFI27_HUMAN
TRINITY_DN188759_c5_g2_i1	12hr	48hr	-8.13	1.37E-02	CEBPA_RAT
TRINITY_DN189044_c0_g2_i5	12hr	48hr	7.59	8.12E-03	PLEC_MOUSE
TRINITY_DN189196_c4_g1_i3	12hr	48hr	-8.69	8.62E-04	NA
TRINITY_DN189208_c6_g1_i2	12hr	48hr	8.12	8.28E-04	NA
TRINITY_DN189221_c3_g1_i4	12hr	48hr	-5.21	5.21E-03	NA
TRINITY_DN189262_c16_g1_i5	12hr	48hr	8.16	5.08E-03	NA
TRINITY_DN189723_c6_g4_i6	12hr	48hr	-9.80	4.96E-03	UFSP1_MOUSE
TRINITY_DN190182_c6_g1_i3	12hr	48hr	-8.15	3.01E-03	NA
TRINITY_DN190316_c8_g1_i5	12hr	48hr	7.73	1.45E-02	TPC_BOVIN
TRINITY_DN190317_c0_g1_i5	12hr	48hr	8.91	4.54E-02	FXDC2_HUMAN
TRINITY_DN190325_c3_g2_i3	12hr	48hr	-10.77	2.87E-05	NA
TRINITY_DN190443_c0_g2_i16	12hr	48hr	10.06	3.87E-03	VATB2_PONAB
TRINITY_DN190692_c1_g3_i13	12hr	48hr	-8.16	2.68E-03	TAOK2_XENLA
TRINITY_DN190773_c13_g3_i2	12hr	48hr	-8.74	1.08E-02	NA
TRINITY_DN190906_c2_g3_i1	12hr	48hr	-7.35	6.17E-03	Tm1
TRINITY_DN190906_c2_g6_i1	12hr	48hr	-8.18	1.51E-02	NA
TRINITY_DN191006_c4_g1_i4	12hr	48hr	-9.50	4.34E-02	ERP29_MOUSE
TRINITY_DN191009_c0_g8_i5	12hr	48hr	10.52	9.61E-04	RM09_HUMAN
TRINITY_DN191143_c7_g1_i7	12hr	48hr	4.80	1.08E-02	NA
TRINITY_DN191190_c7_g5_i1	12hr	48hr	8.02	3.97E-02	NA
TRINITY_DN191360_c1_g1_i9	12hr	48hr	10.06	8.28E-05	SPT2_HUMAN
TRINITY_DN191458_c8_g1_i2	12hr	48hr	-7.09	3.45E-02	NA
TRINITY_DN191491_c5_g3_i3	12hr	48hr	6.23	3.20E-02	NA
TRINITY_DN191516_c0_g1_i2	12hr	48hr	8.46	5.23E-03	NA
TRINITY_DN191516_c0_g1_i5	12hr	48hr	-7.45	1.99E-02	NA
TRINITY_DN191580_c3_g1_i43	12hr	48hr	7.69	3.94E-02	RPC9_BOVIN
TRINITY_DN191624_c11_g1_i1	12hr	48hr	9.38	8.12E-03	SCG1_HUMAN
TRINITY_DN191624_c11_g1_i2	12hr	48hr	13.08	1.07E-03	SCG1_HUMAN
TRINITY_DN191743_c0_g2_i2	12hr	48hr	7.63	7.23E-03	NA
TRINITY_DN191743_c0_g2_i7	12hr	48hr	7.16	8.28E-04	NA
TRINITY_DN191911_c3_g2_i10	12hr	48hr	8.89	2.31E-02	RHOA_PONAB
TRINITY_DN192046_c4_g1_i2	12hr	48hr	10.13	1.39E-02	RFA3_HUMAN
TRINITY_DN192102_c5_g2_i4	12hr	48hr	-10.92	3.21E-03	NA
TRINITY_DN192263_c10_g2_i3	12hr	48hr	-7.73	1.85E-02	NA
TRINITY_DN192367_c5_g1_i5	12hr	48hr	8.44	1.08E-02	FCL_CRIGR
TRINITY_DN192369_c5_g1_i23	12hr	48hr	8.18	3.11E-02	CD82_RAT
TRINITY_DN192389_c1_g2_i2	12hr	48hr	5.87	2.22E-02	NA
TRINITY_DN192450_c8_g3_i2	12hr	48hr	-8.91	1.34E-04	GHR_COLLI

TRINITY_DN192607_c0_g2_i12	12hr	48hr	-7.45	1.20E-02	TM55B_HUMAN
TRINITY_DN193304_c2_g1_i16	12hr	48hr	-6.40	2.43E-02	CTNS_HUMAN
TRINITY_DN193366_c2_g3_i3	12hr	48hr	8.42	1.11E-02	STAR3_HUMAN
TRINITY_DN193544_c13_g1_i3	12hr	48hr	7.78	8.19E-03	NA
TRINITY_DN193599_c9_g1_i8	12hr	48hr	9.78	1.50E-03	AGK_HUMAN
TRINITY_DN193600_c10_g1_i2	12hr	48hr	-6.10	3.74E-03	NA
TRINITY_DN193687_c6_g1_i16	12hr	48hr	-8.76	1.80E-02	GDPD1_HUMAN
TRINITY_DN193830_c8_g1_i1	12hr	48hr	-6.43	2.52E-02	NA
TRINITY_DN193872_c7_g2_i3	12hr	48hr	-8.73	1.01E-02	NA
TRINITY_DN193931_c6_g3_i5	12hr	48hr	-7.55	4.69E-03	RBBP6_HUMAN
TRINITY_DN194002_c3_g1_i8	12hr	48hr	8.47	3.66E-02	ZN217_HUMAN
TRINITY_DN194021_c1_g1_i17	12hr	48hr	-8.79	1.45E-02	STAP1_HUMAN
TRINITY_DN194177_c0_g2_i9	12hr	48hr	-8.65	2.21E-02	USS1_CHICK
TRINITY_DN194279_c6_g1_i3	12hr	48hr	5.71	2.22E-02	SNX6_MOUSE
TRINITY_DN194306_c10_g1_i3	12hr	48hr	8.06	4.51E-02	NA
TRINITY_DN194353_c6_g1_i11	12hr	48hr	-4.08	1.90E-02	NA
TRINITY_DN194362_c1_g2_i8	12hr	48hr	-8.56	1.20E-02	TNPO1_HUMAN
TRINITY_DN194658_c4_g1_i1	12hr	48hr	4.40	3.22E-02	NA
TRINITY_DN194658_c6_g1_i1	12hr	48hr	7.56	4.81E-02	CPLX2_RAT
TRINITY_DN194663_c2_g2_i13	12hr	48hr	-5.63	3.50E-02	NA
TRINITY_DN194693_c2_g1_i13	12hr	48hr	7.69	1.76E-03	GCP3_HUMAN
TRINITY_DN194776_c2_g2_i4	12hr	48hr	-10.24	8.28E-05	LA_HUMAN
TRINITY_DN194907_c0_g1_i2	12hr	48hr	8.42	6.56E-03	S40A1_DANRE
TRINITY_DN194907_c0_g1_i5	12hr	48hr	-10.00	4.14E-03	S40A1_HUMAN
TRINITY_DN194986_c1_g1_i2	12hr	48hr	-7.95	3.93E-03	FBX36_MOUSE
TRINITY_DN195658_c10_g1_i1	12hr	48hr	-7.69	1.37E-02	FGF23_HUMAN
TRINITY_DN195679_c18_g1_i3	12hr	48hr	8.06	4.05E-02	NA
TRINITY_DN195696_c7_g7_i1	12hr	48hr	-9.16	4.57E-02	NA
TRINITY_DN195723_c8_g2_i1	12hr	48hr	8.59	7.07E-04	SHPK_HUMAN
TRINITY_DN195923_c1_g2_i6	12hr	48hr	6.26	7.73E-04	NA
TRINITY_DN195965_c7_g1_i6	12hr	48hr	-8.23	3.50E-02	NA
TRINITY_DN196567_c6_g1_i6	12hr	48hr	6.83	2.13E-02	GPN1_HUMAN
TRINITY_DN196695_c0_g1_i8	12hr	48hr	-8.47	1.14E-02	SRS12_HUMAN
TRINITY_DN196987_c5_g2_i2	12hr	48hr	7.99	1.50E-03	NA
TRINITY_DN197004_c0_g1_i11	12hr	48hr	8.77	2.58E-02	TEX9_HUMAN
TRINITY_DN197051_c7_g2_i2	12hr	48hr	6.87	4.19E-02	NA
TRINITY_DN197550_c3_g2_i5	12hr	48hr	-7.00	2.43E-02	NA
TRINITY_DN197774_c4_g1_i12	12hr	48hr	-8.58	1.08E-02	VPS8_HUMAN
TRINITY_DN197779_c0_g1_i3	12hr	48hr	7.49	4.82E-02	GELS_CHICK

TRINITY_DN197812_c8_g2_i3	12hr	48hr	-9.95	3.02E-02	NA
TRINITY_DN197822_c4_g1_i1	12hr	48hr	8.63	3.09E-02	DGKE_HUMAN
TRINITY_DN197822_c4_g1_i7	12hr	48hr	9.26	2.00E-02	DGKE_HUMAN
TRINITY_DN197874_c2_g1_i5	12hr	48hr	6.64	1.49E-02	NA
TRINITY_DN198029_c8_g1_i2	12hr	48hr	-9.44	4.04E-02	NA
TRINITY_DN198092_c12_g1_i1	12hr	48hr	12.07	3.71E-04	TMED2_CRIGR
TRINITY_DN198372_c13_g4_i1	12hr	48hr	-5.07	2.13E-02	NA
TRINITY_DN198480_c6_g1_i2	12hr	48hr	-7.82	2.01E-02	NA
TRINITY_DN198494_c11_g2_i3	12hr	48hr	-9.89	3.20E-04	NA
TRINITY_DN198550_c1_g2_i2	12hr	48hr	7.31	2.48E-02	NA
TRINITY_DN198669_c2_g1_i14	12hr	48hr	-10.39	2.17E-02	S2536_CHICK
TRINITY_DN198669_c2_g1_i2	12hr	48hr	9.76	5.33E-03	S2536_DANRE
TRINITY_DN198874_c2_g4_i4	12hr	48hr	-7.93	1.39E-02	INSI1_XENTR
TRINITY_DN198877_c3_g1_i13	12hr	48hr	9.05	7.93E-03	ZO1_CANFA
TRINITY_DN198932_c13_g2_i2	12hr	48hr	9.78	1.96E-03	NA
TRINITY_DN198958_c6_g1_i1	12hr	48hr	9.96	2.79E-02	REEP5_HUMAN
TRINITY_DN198961_c1_g2_i4	12hr	48hr	4.14	2.26E-02	GALK1_BOVIN
TRINITY_DN198985_c3_g2_i13	12hr	48hr	-5.50	3.23E-02	HXK1_HUMAN
TRINITY_DN198991_c3_g1_i8	12hr	48hr	10.09	9.67E-06	LEO1_DANRE
TRINITY_DN199019_c1_g1_i1	12hr	48hr	-8.81	1.32E-02	NA
TRINITY_DN199121_c0_g1_i25	12hr	48hr	7.82	3.97E-02	CNO6L_HUMAN
TRINITY_DN199217_c21_g1_i7	12hr	48hr	-9.78	3.14E-02	5HT2B_HUMAN
TRINITY_DN199222_c1_g2_i10	12hr	48hr	-7.32	3.51E-03	CW15A_XENLA
TRINITY_DN199222_c1_g2_i9	12hr	48hr	7.38	1.37E-02	CW15A_XENLA
TRINITY_DN199246_c11_g1_i4	12hr	48hr	-7.81	1.56E-02	NA
TRINITY_DN199286_c1_g1_i12	12hr	48hr	8.70	8.38E-03	XCT_MOUSE
TRINITY_DN199359_c3_g1_i5	12hr	48hr	8.17	3.11E-02	NA
TRINITY_DN199450_c0_g1_i18	12hr	48hr	8.18	2.04E-02	DRA_MACMU
TRINITY_DN199456_c4_g1_i1	12hr	48hr	10.32	1.24E-02	NA
TRINITY_DN199481_c5_g1_i7	12hr	48hr	9.79	2.71E-02	SF3B3_HUMAN
TRINITY_DN199586_c4_g1_i6	12hr	48hr	10.07	1.47E-02	CPT2_XENTR
TRINITY_DN199834_c3_g3_i2	12hr	48hr	8.97	1.89E-02	NA
TRINITY_DN199835_c2_g1_i3	12hr	48hr	8.69	3.11E-02	NA
TRINITY_DN200132_c6_g2_i1	12hr	48hr	-8.05	4.14E-03	NA
TRINITY_DN200177_c2_g1_i6	12hr	48hr	-9.17	4.55E-02	NA
TRINITY_DN200507_c2_g2_i5	12hr	48hr	7.78	4.48E-02	NA
TRINITY_DN200875_c6_g1_i1	12hr	48hr	8.68	9.10E-04	KLHL7_HUMAN
TRINITY_DN200886_c5_g1_i6	12hr	48hr	7.85	1.86E-02	RF1ML_BOVIN
TRINITY_DN200893_c5_g1_i1	12hr	48hr	9.48	1.83E-02	NA

TRINITY_DN200898_c1_g1_i4	12hr	48hr	11.39	9.90E-03	S14L1_HUMAN
TRINITY_DN200902_c0_g2_i1	12hr	48hr	-7.48	2.90E-02	STRAP_MOUSE
TRINITY_DN201061_c1_g1_i11	12hr	48hr	-6.97	4.05E-02	ZFAN4_MOUSE
TRINITY_DN201155_c7_g1_i3	12hr	48hr	9.72	2.87E-05	MXI1_MOUSE
TRINITY_DN201177_c2_g1_i8	12hr	48hr	-2.62	3.51E-02	BICR1_HUMAN
TRINITY_DN201264_c1_g2_i6	12hr	48hr	-8.21	1.47E-02	PCY2_BOVIN
TRINITY_DN201467_c2_g1_i8	12hr	48hr	-6.23	3.94E-02	NA
TRINITY_DN201652_c6_g1_i3	12hr	48hr	9.64	1.96E-03	GANAB_MACFA
TRINITY_DN201652_c6_g1_i7	12hr	48hr	-6.37	2.31E-02	GANAB_MACFA
TRINITY_DN202019_c0_g1_i20	12hr	48hr	-9.45	4.09E-02	TRAF7_HUMAN
TRINITY_DN202155_c0_g2_i11	12hr	48hr	10.05	1.21E-02	VAMP4_HUMAN
TRINITY_DN202377_c3_g1_i1	12hr	48hr	7.38	7.32E-03	NA
TRINITY_DN202445_c2_g1_i3	12hr	48hr	-9.16	7.96E-03	NA
TRINITY_DN202466_c2_g2_i2	12hr	48hr	-9.60	5.62E-03	MERL_HUMAN
TRINITY_DN202495_c0_g3_i10	12hr	48hr	9.29	4.46E-02	DC112_BOVIN
TRINITY_DN202499_c9_g1_i3	12hr	48hr	8.73	2.48E-02	LYG_CASCA
TRINITY_DN202516_c3_g1_i7	12hr	48hr	8.43	4.85E-02	ESYT3_XENTR
TRINITY_DN202566_c3_g1_i9	12hr	48hr	8.16	1.57E-02	OTUL_MOUSE
TRINITY_DN202646_c0_g1_i2	12hr	48hr	-10.08	6.90E-03	SMIM7_BOVIN
TRINITY_DN202750_c3_g1_i6	12hr	48hr	8.15	3.84E-02	ZFN2B_RAT
TRINITY_DN202814_c15_g3_i3	12hr	48hr	8.65	1.83E-04	NA
TRINITY_DN202842_c5_g1_i11	12hr	48hr	8.51	2.72E-02	TSSP_MOUSE
TRINITY_DN202842_c5_g2_i6	12hr	48hr	7.20	3.06E-02	TSSP_HUMAN
TRINITY_DN202981_c2_g1_i2	12hr	48hr	-7.40	7.08E-03	NA
TRINITY_DN203067_c3_g1_i7	12hr	48hr	8.19	7.16E-03	P4R3A_MOUSE
TRINITY_DN203176_c2_g1_i2	12hr	48hr	-7.58	2.12E-02	NA
TRINITY_DN203176_c2_g1_i4	12hr	48hr	8.04	1.96E-03	NA
TRINITY_DN203235_c5_g1_i2	12hr	48hr	-9.37	4.11E-02	NA
TRINITY_DN203247_c12_g1_i9	12hr	48hr	-9.03	3.31E-03	NA
TRINITY_DN203553_c15_g2_i1	12hr	48hr	-7.81	1.48E-02	G6PC_CANFA
TRINITY_DN203680_c0_g1_i2	12hr	48hr	11.60	4.93E-03	NA
TRINITY_DN203818_c2_g2_i1	12hr	48hr	8.85	3.31E-02	SNX4_BOVIN
TRINITY_DN203880_c16_g1_i13	12hr	48hr	-8.88	3.25E-03	NA
TRINITY_DN203995_c0_g2_i2	12hr	48hr	-8.81	9.84E-03	BRE1B_RAT
TRINITY_DN204052_c1_g1_i3	12hr	48hr	8.32	4.34E-02	NA
TRINITY_DN204054_c2_g1_i11	12hr	48hr	-10.19	3.21E-03	S19A3_MACFA
TRINITY_DN204108_c2_g3_i10	12hr	48hr	-10.67	3.47E-04	CTR3_HUMAN
TRINITY_DN204737_c14_g1_i3	12hr	48hr	9.87	4.66E-03	NA
TRINITY_DN204772_c9_g1_i2	12hr	48hr	-5.33	4.07E-02	IRG1_HUMAN

TRINITY_DN204790_c2_g4_i1	12hr	48hr	-8.03	2.59E-02	PURA2_MOUSE
TRINITY_DN204835_c4_g8_i1	12hr	48hr	-6.07	4.82E-02	NA
TRINITY_DN204937_c4_g2_i4	12hr	48hr	-7.60	1.34E-04	MBRL_MOUSE
TRINITY_DN205218_c1_g2_i12	12hr	48hr	-9.39	3.94E-02	MBB1A_DANRE
TRINITY_DN205218_c1_g2_i6	12hr	48hr	-10.24	1.48E-02	MBB1A_DANRE
TRINITY_DN205229_c5_g1_i4	12hr	48hr	7.44	1.16E-02	NA
TRINITY_DN205377_c3_g2_i19	12hr	48hr	10.86	3.19E-15	GTPB2_MOUSE
TRINITY_DN205474_c2_g1_i20	12hr	48hr	2.45	3.97E-02	FA49B_HUMAN
TRINITY_DN205535_c1_g1_i10	12hr	48hr	9.03	2.72E-02	CLAP2_HUMAN
TRINITY_DN205552_c8_g1_i1	12hr	48hr	3.56	3.85E-02	Tm1
TRINITY_DN205666_c5_g1_i5	12hr	48hr	-9.14	4.62E-02	NA
TRINITY_DN205773_c2_g3_i2	12hr	48hr	7.66	4.85E-02	NA
TRINITY_DN205800_c6_g1_i17	12hr	48hr	10.26	1.32E-02	BMS1_HUMAN
TRINITY_DN205823_c2_g2_i3	12hr	48hr	7.88	4.62E-02	VPS36_HUMAN
TRINITY_DN205912_c0_g1_i10	12hr	48hr	9.19	1.02E-02	SNX14_PONAB
TRINITY_DN205963_c5_g2_i21	12hr	48hr	9.23	2.04E-02	DHSO_CHICK
TRINITY_DN205990_c1_g1_i4	12hr	48hr	-7.04	2.07E-02	MSH2_CHLAE
TRINITY_DN206108_c0_g1_i9	12hr	48hr	9.82	4.68E-03	KLH24_HUMAN
TRINITY_DN206236_c0_g2_i10	12hr	48hr	9.09	5.99E-03	HMR1_HUMAN
TRINITY_DN206375_c10_g1_i4	12hr	48hr	-8.63	1.20E-02	RL27_RAT
TRINITY_DN206439_c4_g2_i3	12hr	48hr	7.28	7.02E-03	NA
TRINITY_DN206561_c0_g1_i4	12hr	48hr	-9.03	1.08E-02	PRP8_HUMAN
TRINITY_DN206575_c6_g2_i1	12hr	48hr	8.02	2.12E-02	NA
TRINITY_DN206641_c8_g1_i1	12hr	48hr	-7.68	3.20E-02	RVT_1
TRINITY_DN206727_c7_g1_i2	12hr	48hr	-9.68	3.72E-07	CLD10_BOVIN
TRINITY_DN206727_c7_g1_i4	12hr	48hr	4.23	2.70E-02	CLD10_BOVIN
TRINITY_DN206814_c2_g4_i1	12hr	48hr	-6.99	1.62E-02	NA
TRINITY_DN206921_c5_g1_i1	12hr	48hr	-7.12	1.48E-02	NA
TRINITY_DN206921_c7_g1_i6	12hr	48hr	-5.58	4.62E-02	RADIL_DANRE
TRINITY_DN206954_c2_g1_i4	12hr	48hr	8.14	3.46E-02	NUF2A_XENLA
TRINITY_DN207030_c1_g2_i6	12hr	48hr	10.57	8.28E-05	EXOC3_BOVIN
TRINITY_DN207091_c10_g2_i3	12hr	48hr	-7.54	1.48E-03	NA
TRINITY_DN207120_c11_g2_i2	12hr	48hr	4.14	2.64E-02	TM10A_HUMAN
TRINITY_DN207129_c0_g1_i12	12hr	48hr	9.59	1.37E-02	NA
TRINITY_DN207129_c0_g1_i9	12hr	48hr	11.69	5.54E-03	NA
TRINITY_DN207167_c5_g1_i9	12hr	48hr	4.91	3.41E-02	NA
TRINITY_DN207363_c9_g1_i15	12hr	48hr	-9.57	3.61E-02	FBXW9_BOVIN
TRINITY_DN207463_c8_g1_i2	12hr	48hr	-4.87	3.28E-02	NA
TRINITY_DN207541_c9_g1_i1	12hr	48hr	6.65	4.54E-02	NDUA6_PANTR

TRINITY_DN207551_c18_g1_i2	12hr	48hr	-9.02	6.97E-03	NA
TRINITY_DN207557_c8_g1_i22	12hr	48hr	-7.20	3.44E-02	TTC25_DANRE
TRINITY_DN207597_c3_g1_i5	12hr	48hr	7.79	1.01E-02	UHRF1_DANRE
TRINITY_DN207619_c2_g1_i4	12hr	48hr	-10.54	2.62E-03	IF2A_CHICK
TRINITY_DN208145_c6_g2_i6	12hr	48hr	-9.19	1.00E-02	RPB1_HUMAN
TRINITY_DN208205_c1_g7_i1	12hr	48hr	5.05	3.06E-02	NA
TRINITY_DN208322_c2_g1_i12	12hr	48hr	-8.77	6.56E-03	SGSM3_XENLA
TRINITY_DN208346_c12_g2_i1	12hr	48hr	-9.17	8.12E-03	S20A1_XENTR
TRINITY_DN208415_c4_g1_i5	12hr	48hr	8.77	4.74E-03	CALX_RAT
TRINITY_DN208421_c0_g1_i1	12hr	48hr	-5.76	4.55E-02	NA
TRINITY_DN208465_c1_g2_i15	12hr	48hr	-9.13	1.20E-02	TENS3_HUMAN
TRINITY_DN208537_c1_g1_i7	12hr	48hr	-6.17	4.34E-02	NA
TRINITY_DN208572_c5_g1_i2	12hr	48hr	-9.57	3.59E-02	CATIN_HUMAN
TRINITY_DN208594_c3_g1_i1	12hr	48hr	-8.14	1.55E-02	BL1S3_HUMAN
TRINITY_DN208630_c2_g1_i1	12hr	48hr	8.41	3.59E-02	NA
TRINITY_DN208756_c8_g3_i6	12hr	48hr	10.24	1.32E-02	NA
TRINITY_DN208801_c4_g1_i1	12hr	48hr	-8.34	1.57E-02	NA
TRINITY_DN209081_c3_g3_i10	12hr	48hr	-6.95	4.07E-02	NA
TRINITY_DN209102_c3_g2_i6	12hr	48hr	7.76	9.75E-03	NA
TRINITY_DN209189_c2_g1_i14	12hr	48hr	8.64	2.98E-02	RGL1_HUMAN
TRINITY_DN209201_c4_g1_i6	12hr	48hr	-9.17	8.83E-04	ADDA_HUMAN
TRINITY_DN209249_c7_g1_i9	12hr	48hr	9.01	2.05E-03	NA
TRINITY_DN209290_c0_g1_i1	12hr	48hr	-9.54	3.63E-02	NA
TRINITY_DN209296_c6_g3_i4	12hr	48hr	7.40	3.06E-02	NA
TRINITY_DN209464_c9_g1_i1	12hr	48hr	-5.58	4.67E-02	K132L_MOUSE
TRINITY_DN209563_c5_g2_i4	12hr	48hr	8.83	1.00E-02	NA
TRINITY_DN209642_c7_g1_i8	12hr	48hr	11.40	9.30E-03	COX5A_PONPY
TRINITY_DN209870_c1_g3_i7	12hr	48hr	-7.11	4.00E-02	STOM_HUMAN
TRINITY_DN209954_c6_g1_i1	12hr	48hr	6.65	2.06E-02	NA
TRINITY_DN210043_c6_g1_i7	12hr	48hr	-9.65	3.51E-02	AP4E1_HUMAN
TRINITY_DN210148_c2_g1_i8	12hr	48hr	-8.71	1.41E-02	MYBPH_CHICK
TRINITY_DN210217_c0_g2_i5	12hr	48hr	-8.12	1.57E-02	CEBPZ_HUMAN
TRINITY_DN210285_c3_g1_i24	12hr	48hr	6.03	3.41E-02	VGP_MABVA
TRINITY_DN210495_c3_g1_i8	12hr	48hr	5.46	4.70E-02	NA
TRINITY_DN210526_c6_g1_i20	12hr	48hr	-8.33	1.26E-02	S2538_XENTR
TRINITY_DN210526_c6_g1_i5	12hr	48hr	-6.83	4.56E-02	S2538_XENTR
TRINITY_DN210601_c0_g1_i18	12hr	48hr	-6.68	2.01E-02	RBM5_XENTR
TRINITY_DN210741_c4_g1_i2	12hr	48hr	-7.98	1.57E-02	NA
TRINITY_DN210763_c3_g2_i6	12hr	48hr	7.24	1.56E-02	GTR11_HUMAN

TRINITY_DN210946_c4_g4_i2	12hr	48hr	8.82	4.46E-02	NA
TRINITY_DN211052_c1_g3_i1	12hr	48hr	6.00	2.13E-02	Tm1
TRINITY_DN211062_c4_g1_i8	12hr	48hr	-11.48	2.87E-05	CADH1_CHICK
TRINITY_DN211114_c3_g1_i6	12hr	48hr	-9.50	1.20E-02	NA
TRINITY_DN211119_c7_g2_i1	12hr	48hr	10.31	3.93E-03	NA
TRINITY_DN211128_c9_g1_i4	12hr	48hr	-5.65	1.48E-02	NUCB1_MOUSE
TRINITY_DN211272_c5_g1_i2	12hr	48hr	-9.04	1.50E-03	NDUA7_PONPY
TRINITY_DN211335_c9_g3_i3	12hr	48hr	6.48	2.45E-02	NA
TRINITY_DN211442_c0_g2_i2	12hr	48hr	-9.88	6.90E-03	NA
TRINITY_DN211466_c3_g1_i10	12hr	48hr	-9.10	3.60E-02	COX1_SQUAC
TRINITY_DN211557_c0_g1_i32	12hr	48hr	-10.22	9.36E-05	AOXA_HUMAN
TRINITY_DN211557_c0_g1_i37	12hr	48hr	9.93	1.39E-02	AOXA_HUMAN
TRINITY_DN211583_c1_g1_i1	12hr	48hr	10.37	2.87E-05	SGK1_MOUSE
TRINITY_DN211656_c3_g1_i2	12hr	48hr	-10.09	4.89E-03	I2B2B_DANRE
TRINITY_DN211671_c2_g1_i13	12hr	48hr	-9.47	4.01E-02	PLXB2_MOUSE
TRINITY_DN211671_c2_g1_i3	12hr	48hr	-9.72	7.23E-03	PLXB2_HUMAN
TRINITY_DN211922_c10_g1_i11	12hr	48hr	-8.86	1.21E-03	VMA5A_MOUSE
TRINITY_DN211927_c2_g1_i9	12hr	48hr	12.54	9.72E-20	ITB2_HUMAN
TRINITY_DN212085_c0_g1_i16	12hr	48hr	7.34	1.58E-03	CIB1_RAT
TRINITY_DN212085_c0_g1_i7	12hr	48hr	11.58	3.98E-04	CIB1_RAT
TRINITY_DN212136_c5_g2_i6	12hr	48hr	-5.02	2.38E-02	NA
TRINITY_DN212233_c1_g1_i3	12hr	48hr	11.03	6.90E-03	BACD3_HUMAN
TRINITY_DN212327_c2_g1_i5	12hr	48hr	-6.93	4.62E-02	SPTB2_HUMAN
TRINITY_DN212397_c1_g1_i6	12hr	48hr	4.96	4.26E-02	KV2A2_MOUSE
TRINITY_DN212598_c54_g2_i2	12hr	48hr	-9.46	5.99E-03	NA
TRINITY_DN212659_c3_g3_i2	12hr	48hr	10.79	1.00E-02	PSA7_BOVIN
TRINITY_DN212812_c12_g2_i2	12hr	48hr	4.39	3.27E-02	NA
TRINITY_DN212850_c8_g1_i1	12hr	48hr	-10.52	2.11E-02	CO6_PONPY
TRINITY_DN212864_c3_g2_i1	12hr	48hr	-7.47	2.22E-02	NLRC3_HUMAN
TRINITY_DN212884_c17_g1_i6	12hr	48hr	-9.54	1.39E-02	RPTOR_MOUSE

**Table S2.** Complete list of the differentially expressed genes following 65% SW exposure. Differential expression analysis at the gene level was performed using the edgeR software within the Trinity pipeline and annotation was performed using Trinotate. Log<sub>2</sub>FC represent fold change of time point B relative to time point A. P-values were adjusted using the Benjamin-Hochberg correction for multiple comparisons. The annotation provided states the UniProt protein identifier followed by the species.

Trinity ID	Time point A	Time point B	LogFC	P <sub>adj</sub> value	Annotation
TRINITY_DN115096_c1_g1	0hr	12hr	-3.93	6.33E-04	NA
TRINITY_DN161214_c0_g1	0hr	12hr	3.23	1.09E-02	JUN_SERCA
TRINITY_DN164879_c0_g1	0hr	12hr	-9.53	2.41E-02	NA
TRINITY_DN168075_c0_g1	0hr	12hr	-8.79	3.08E-05	NA
TRINITY_DN172345_c0_g2	0hr	12hr	-8.27	3.36E-02	NA
TRINITY_DN172829_c0_g3	0hr	12hr	4.85	2.12E-02	CCL20_MOUSE
TRINITY_DN174449_c1_g4	0hr	12hr	8.23	2.87E-02	NA
TRINITY_DN175245_c0_g1	0hr	12hr	4.63	1.73E-02	CTF2_MOUSE
TRINITY_DN175494_c15_g1	0hr	12hr	8.51	1.50E-02	NA
TRINITY_DN178092_c7_g1	0hr	12hr	8.29	9.95E-04	NA
TRINITY_DN178599_c10_g1	0hr	12hr	2.83	2.07E-02	NA
TRINITY_DN180265_c9_g1	0hr	12hr	5.01	1.63E-02	TES_MOUSE
TRINITY_DN180795_c11_g1	0hr	12hr	-7.79	3.56E-02	NA
TRINITY_DN181028_c1_g2	0hr	12hr	8.02	4.44E-02	NA
TRINITY_DN181453_c7_g1	0hr	12hr	3.59	4.18E-06	RN186_BOVIN
TRINITY_DN182510_c3_g3	0hr	12hr	3.49	2.94E-02	NA
TRINITY_DN184855_c4_g2	0hr	12hr	8.49	1.75E-02	NA
TRINITY_DN186675_c18_g1	0hr	12hr	7.66	4.66E-02	NA
TRINITY_DN186829_c11_g3	0hr	12hr	-8.97	3.34E-02	NA
TRINITY_DN187025_c1_g2	0hr	12hr	-2.97	1.84E-02	RRBP1_HUMAN
TRINITY_DN187694_c4_g4	0hr	12hr	8.31	1.34E-02	NA
TRINITY_DN188555_c2_g1	0hr	12hr	8.16	2.68E-02	NALP3_HUMAN
TRINITY_DN189072_c9_g1	0hr	12hr	10.07	1.09E-02	NA
TRINITY_DN189124_c7_g1	0hr	12hr	-7.61	4.17E-02	NA
TRINITY_DN189973_c6_g2	0hr	12hr	8.77	4.64E-02	NA
TRINITY_DN191140_c11_g2	0hr	12hr	-8.42	1.93E-04	NA
TRINITY_DN191150_c6_g2	0hr	12hr	-2.93	4.64E-02	NA
TRINITY_DN192644_c9_g10	0hr	12hr	8.56	1.09E-02	NA

TRINITY_DN193142_c5_g9	0hr	12hr	7.51	3.56E-02	NA
TRINITY_DN193830_c8_g1	0hr	12hr	6.59	1.84E-02	NA
TRINITY_DN194170_c8_g1	0hr	12hr	8.4	1.63E-02	NA
TRINITY_DN194300_c7_g1	0hr	12hr	-9.38	9.98E-05	NA
TRINITY_DN194702_c2_g3	0hr	12hr	5.39	4.44E-02	NA
TRINITY_DN194767_c11_g12	0hr	12hr	-2.66	1.09E-02	NA
TRINITY_DN195104_c3_g1	0hr	12hr	9.06	3.36E-02	LV603_HUMAN
TRINITY_DN195469_c3_g9	0hr	12hr	8.15	5.16E-03	ZN227_HUMAN
TRINITY_DN195940_c1_g1	0hr	12hr	2.84	6.12E-03	NA
TRINITY_DN196555_c4_g3	0hr	12hr	8.4	2.16E-02	NA
TRINITY_DN198010_c3_g2	0hr	12hr	5.41	2.68E-02	NA
TRINITY_DN198085_c6_g7	0hr	12hr	-7.95	1.09E-02	NA
TRINITY_DN200001_c6_g1	0hr	12hr	-8.64	1.09E-02	NA
TRINITY_DN200313_c3_g2	0hr	12hr	8.41	3.26E-02	LV601_HUMAN
TRINITY_DN202160_c4_g3	0hr	12hr	5.22	1.09E-02	HS30C_XENLA
TRINITY_DN202247_c12_g1	0hr	12hr	8.19	2.94E-02	NA
TRINITY_DN202479_c1_g4	0hr	12hr	-9.33	5.86E-04	NA
TRINITY_DN202547_c0_g4	0hr	12hr	9.09	6.92E-06	NA
TRINITY_DN202636_c6_g1	0hr	12hr	-8.02	1.50E-02	NA
TRINITY_DN203262_c6_g3	0hr	12hr	-6.81	5.65E-03	PIEZ2_MOUSE
TRINITY_DN203782_c2_g1	0hr	12hr	6.35	4.32E-02	NA
TRINITY_DN203872_c4_g1	0hr	12hr	8.18	6.49E-03	NA
TRINITY_DN204464_c1_g1	0hr	12hr	5.26	3.34E-02	TAR1_KLULA/YEAST
TRINITY_DN204718_c3_g4	0hr	12hr	-3.12	1.88E-03	HMR1_RAT
TRINITY_DN204772_c9_g1	0hr	12hr	8.41	3.36E-02	IRG1_MOUSE
TRINITY_DN204835_c4_g8	0hr	12hr	6.59	1.63E-02	NA
TRINITY_DN205826_c2_g4	0hr	12hr	-8.11	3.26E-02	NA
TRINITY_DN206123_c0_g2	0hr	12hr	5.69	2.94E-02	NA
TRINITY_DN206641_c8_g1	0hr	12hr	9.3	2.68E-02	NA
TRINITY_DN206919_c2_g1	0hr	12hr	8.76	3.59E-02	SPP11_CAEL
TRINITY_DN207620_c4_g2	0hr	12hr	6.64	1.09E-02	TAR1_KLULA/YEAST
TRINITY_DN207660_c0_g4	0hr	12hr	9	3.34E-02	NA
TRINITY_DN208697_c1_g5	0hr	12hr	9.2	1.02E-02	HS71A_MOUSE
TRINITY_DN209372_c7_g6	0hr	12hr	8.07	5.16E-03	NA
TRINITY_DN210800_c6_g3	0hr	12hr	7.9	1.32E-02	NA
TRINITY_DN211457_c5_g1	0hr	12hr	8.08	3.36E-02	NA
TRINITY_DN212136_c5_g3	0hr	12hr	3.42	3.36E-02	NA
TRINITY_DN212571_c6_g1	0hr	12hr	8.58	4.80E-04	NA
TRINITY_DN212573_c13_g3	0hr	12hr	7.99	4.57E-03	NA

TRINITY_DN212642_c396_g1	0hr	12hr	8.05	3.71E-03	NA
TRINITY_DN212778_c8_g3	0hr	12hr	-9.98	1.84E-02	NA
TRINITY_DN297844_c0_g1	0hr	12hr	8.19	5.16E-03	NA
TRINITY_DN351258_c0_g1	0hr	12hr	8.45	3.53E-04	NA
TRINITY_DN131012_c0_g1	0hr	48hr	8.21	1.51E-03	NA
TRINITY_DN168075_c0_g1	0hr	48hr	-8.56	1.51E-03	NA
TRINITY_DN168500_c0_g1	0hr	48hr	-8.85	1.57E-02	ENT1_SCHPO
TRINITY_DN170138_c0_g1	0hr	48hr	9.61	7.63E-03	NA
TRINITY_DN171431_c0_g1	0hr	48hr	-7.85	3.11E-02	NA
TRINITY_DN173533_c0_g1	0hr	48hr	-3.92	2.81E-02	NR4A2_MOUSE
TRINITY_DN174045_c8_g1	0hr	48hr	3.67	1.51E-03	DKK1_HUMAN
TRINITY_DN176813_c3_g1	0hr	48hr	8.71	5.47E-03	NA
TRINITY_DN178151_c0_g1	0hr	48hr	10.33	2.81E-02	LV107_HUMAN
TRINITY_DN179064_c15_g13	0hr	48hr	-8.62	1.37E-02	NA
TRINITY_DN180219_c1_g3	0hr	48hr	8.86	4.45E-03	NA
TRINITY_DN180827_c7_g2	0hr	48hr	-8.36	1.51E-03	NA
TRINITY_DN181107_c21_g1	0hr	48hr	-8.6	1.51E-02	NA
TRINITY_DN181453_c7_g1	0hr	48hr	3.21	5.58E-04	RN186_BOVIN
TRINITY_DN182145_c1_g2	0hr	48hr	-10.61	4.45E-03	NA
TRINITY_DN182222_c3_g8	0hr	48hr	-8.41	3.01E-02	NA
TRINITY_DN182572_c6_g3	0hr	48hr	-9.45	4.96E-02	NA
TRINITY_DN182616_c3_g4	0hr	48hr	9.89	5.47E-03	NA
TRINITY_DN183269_c9_g3	0hr	48hr	5.77	4.02E-02	SCG1_HUMAN
TRINITY_DN184465_c6_g2	0hr	48hr	-9.18	1.96E-03	NA
TRINITY_DN184850_c6_g10	0hr	48hr	8.33	1.51E-03	NA
TRINITY_DN184968_c4_g1	0hr	48hr	-2.67	3.95E-02	NA
TRINITY_DN187914_c0_g1	0hr	48hr	2.72	1.37E-02	MIOX_DANRE
TRINITY_DN188262_c7_g1	0hr	48hr	-2.66	3.11E-02	NA
TRINITY_DN188555_c2_g1	0hr	48hr	7.98	9.75E-03	NALP3_HUMAN
TRINITY_DN190121_c11_g3	0hr	48hr	8.44	1.32E-02	NA
TRINITY_DN191529_c8_g1	0hr	48hr	-8.5	3.48E-02	NA
TRINITY_DN191624_c11_g1	0hr	48hr	9.61	1.32E-02	SCG1_HUMAN
TRINITY_DN191720_c5_g1	0hr	48hr	-2.87	2.00E-02	GTR11_HUMAN
TRINITY_DN194300_c7_g1	0hr	48hr	-9.17	1.67E-03	NA
TRINITY_DN197963_c11_g7	0hr	48hr	-8.83	2.21E-02	NA
TRINITY_DN202056_c17_g1	0hr	48hr	-7.95	1.97E-02	NA
TRINITY_DN202547_c0_g4	0hr	48hr	9.31	1.97E-02	NA
TRINITY_DN203262_c6_g3	0hr	48hr	-6.3	2.63E-02	PIEZ2_MOUSE
TRINITY_DN203614_c5_g1	0hr	48hr	-2.97	2.81E-02	NA

TRINITY_DN204978_c1_g1	0hr	48hr	8.29	1.26E-02	NA
TRINITY_DN206477_c7_g2	0hr	48hr	2.47	1.32E-02	NA
TRINITY_DN207717_c2_g1	0hr	48hr	8.97	3.01E-03	NA
TRINITY_DN208522_c3_g5	0hr	48hr	-2.9	1.97E-02	NA
TRINITY_DN208740_c7_g5	0hr	48hr	2.67	1.32E-02	NA
TRINITY_DN209571_c0_g1	0hr	48hr	8.57	7.72E-03	NA
TRINITY_DN209667_c6_g4	0hr	48hr	8.23	2.61E-03	NA
TRINITY_DN211982_c2_g4	0hr	48hr	-8.59	1.84E-02	IF44L_HUMAN
TRINITY_DN212290_c2_g2	0hr	48hr	-9.92	1.97E-02	LV603_HUMAN
TRINITY_DN212439_c11_g1	0hr	48hr	-3.08	1.19E-02	NA
TRINITY_DN212506_c15_g1	0hr	48hr	8.53	3.21E-02	NA
TRINITY_DN212678_c46_g2	0hr	48hr	-8.62	1.96E-03	NA
TRINITY_DN160434_c0_g1	12hr	48hr	5.97	1.85E-02	MOG2A_XENLA
TRINITY_DN171761_c1_g1	12hr	48hr	-9.54	1.10E-03	NA
TRINITY_DN172518_c0_g1	12hr	48hr	3.73	8.47E-04	PRG4_MOUSE
TRINITY_DN172829_c0_g3	12hr	48hr	-4.74	2.20E-02	CCL20_MOUSE
TRINITY_DN177364_c0_g1	12hr	48hr	-8.06	1.12E-02	NA
TRINITY_DN177788_c9_g1	12hr	48hr	3.75	2.12E-02	NA
TRINITY_DN177880_c8_g13	12hr	48hr	-8.42	2.21E-04	NA
TRINITY_DN178728_c1_g2	12hr	48hr	-7.89	1.52E-02	NA
TRINITY_DN179064_c15_g13	12hr	48hr	-9.04	8.70E-04	NA
TRINITY_DN179816_c0_g3	12hr	48hr	-11.13	1.90E-03	NA
TRINITY_DN180856_c2_g2	12hr	48hr	-8.21	3.45E-02	NA
TRINITY_DN180964_c15_g2	12hr	48hr	-7.91	4.98E-02	NA
TRINITY_DN181077_c0_g1	12hr	48hr	2.7	2.69E-02	NA
TRINITY_DN181383_c11_g1	12hr	48hr	-8.08	2.58E-03	FLOT2_RAT
TRINITY_DN181589_c2_g1	12hr	48hr	3.8	2.19E-02	NA
TRINITY_DN182145_c1_g2	12hr	48hr	-8.38	4.46E-03	NA
TRINITY_DN182415_c7_g2	12hr	48hr	-8.12	2.75E-03	NA
TRINITY_DN182744_c7_g1	12hr	48hr	-8.16	4.98E-02	NA
TRINITY_DN183269_c9_g3	12hr	48hr	5.65	4.21E-02	SCG1_HUMAN
TRINITY_DN184796_c9_g3	12hr	48hr	8.73	8.50E-04	NA
TRINITY_DN184948_c0_g1	12hr	48hr	8.08	3.00E-02	NA
TRINITY_DN186315_c8_g2	12hr	48hr	-11.6	7.66E-04	K2C8_XENLA
TRINITY_DN186936_c17_g2	12hr	48hr	-8.8	9.96E-07	NA
TRINITY_DN187025_c1_g2	12hr	48hr	2.87	2.05E-02	RRBP1_HUMAN
TRINITY_DN187527_c14_g1	12hr	48hr	-8	3.97E-02	NA
TRINITY_DN188046_c17_g1	12hr	48hr	-8.29	3.15E-04	NA
TRINITY_DN188411_c11_g1	12hr	48hr	2.11	1.46E-02	NA

TRINITY_DN189058_c6_g1	12hr	48hr	-7.79	2.11E-02	NA
TRINITY_DN189166_c1_g4	12hr	48hr	2.07	3.45E-02	H10_MOUSE
TRINITY_DN189986_c6_g7	12hr	48hr	8.33	2.10E-02	NA
TRINITY_DN190171_c2_g3	12hr	48hr	8.08	3.61E-02	NA
TRINITY_DN191480_c6_g2	12hr	48hr	-7.86	4.80E-02	NA
TRINITY_DN191624_c11_g1	12hr	48hr	9.64	1.19E-02	SCG1_HUMAN
TRINITY_DN191963_c6_g1	12hr	48hr	-8.04	4.91E-02	NA
TRINITY_DN193830_c8_g1	12hr	48hr	-6.9	2.88E-02	NA
TRINITY_DN193951_c0_g2	12hr	48hr	-9.6	8.50E-04	TRI66_HUMAN
TRINITY_DN194317_c2_g2	12hr	48hr	-7.86	4.22E-02	NA
TRINITY_DN194697_c6_g3	12hr	48hr	8.76	1.91E-02	NA
TRINITY_DN194702_c2_g3	12hr	48hr	-5.41	4.98E-02	NA
TRINITY_DN196186_c1_g1	12hr	48hr	-8.79	4.21E-02	NA
TRINITY_DN196480_c0_g1	12hr	48hr	-6.93	2.23E-02	NA
TRINITY_DN197357_c5_g1	12hr	48hr	-8.94	8.83E-07	NA
TRINITY_DN197874_c2_g1	12hr	48hr	4.72	3.70E-03	NA
TRINITY_DN198213_c4_g1	12hr	48hr	7.84	3.45E-02	NA
TRINITY_DN198229_c7_g3	12hr	48hr	-8.24	3.91E-02	NA
TRINITY_DN200419_c6_g2	12hr	48hr	-8.35	3.05E-02	NA
TRINITY_DN200626_c2_g4	12hr	48hr	-7.8	2.56E-02	ITFG2_HUMAN/MOUSE
TRINITY_DN200715_c8_g1	12hr	48hr	8.56	3.70E-03	NA
TRINITY_DN202022_c2_g2	12hr	48hr	-9.24	1.20E-06	MT_SCYTO
TRINITY_DN202056_c17_g1	12hr	48hr	-7.77	3.97E-02	NA
TRINITY_DN202108_c5_g2	12hr	48hr	-9.59	2.90E-10	NA
TRINITY_DN202479_c1_g4	12hr	48hr	8.65	1.45E-03	NA
TRINITY_DN203822_c0_g4	12hr	48hr	-8.66	1.01E-04	CC135_HUMAN
TRINITY_DN203872_c4_g1	12hr	48hr	-7.87	3.91E-02	NA
TRINITY_DN204061_c2_g4	12hr	48hr	-8.39	1.89E-02	NA
TRINITY_DN204835_c4_g8	12hr	48hr	-6.3	1.85E-02	NA
TRINITY_DN205245_c0_g1	12hr	48hr	-10.51	3.61E-02	NA
TRINITY_DN205447_c8_g4	12hr	48hr	8.49	6.05E-05	NA
TRINITY_DN205927_c3_g9	12hr	48hr	8.06	3.97E-02	NA
TRINITY_DN205960_c0_g4	12hr	48hr	-8.13	8.91E-03	NA
TRINITY_DN206056_c1_g1	12hr	48hr	-9.42	5.44E-03	NA
TRINITY_DN206123_c0_g2	12hr	48hr	-5.9	2.07E-02	NA
TRINITY_DN206641_c8_g1	12hr	48hr	-9	3.97E-02	NA
TRINITY_DN206839_c6_g2	12hr	48hr	8.42	2.20E-02	NA
TRINITY_DN207081_c14_g7	12hr	48hr	-8.38	1.16E-03	PTRF_HUMAN

TRINITY_DN207143_c1_g5	12hr	48hr	4.35	4.80E-02	HV01_HETFR
TRINITY_DN207835_c1_g1	12hr	48hr	-4.16	4.74E-02	YCX91_PHA AO
TRINITY_DN208039_c1_g6	12hr	48hr	-8.62	4.98E-02	SESD1_XENTR
TRINITY_DN209347_c8_g1	12hr	48hr	8.13	1.12E-02	NA
TRINITY_DN209437_c3_g5	12hr	48hr	-8.57	5.28E-04	NA
TRINITY_DN209485_c0_g2	12hr	48hr	-8.44	1.85E-02	NA
TRINITY_DN210658_c7_g1	12hr	48hr	-7.7	3.06E-02	NA
TRINITY_DN210969_c7_g2	12hr	48hr	-8.46	2.73E-02	RTJK_DROME
TRINITY_DN211052_c1_g3	12hr	48hr	7.78	1.46E-02	NA
TRINITY_DN211131_c5_g3	12hr	48hr	-7.79	3.61E-02	NA
TRINITY_DN211805_c0_g1	12hr	48hr	-8.97	2.56E-02	HVCS_HETFR
TRINITY_DN212020_c11_g1	12hr	48hr	7.91	4.83E-02	NA
TRINITY_DN212533_c4_g1	12hr	48hr	-7.74	2.56E-02	NA
TRINITY_DN212573_c13_g3	12hr	48hr	-7.67	2.56E-02	NA
TRINITY_DN212678_c46_g2	12hr	48hr	-8.53	9.18E-05	NA
TRINITY_DN242605_c0_g1	12hr	48hr	-9.8	1.46E-02	NA
TRINITY_DN374867_c0_g1	12hr	48hr	-7.97	4.21E-02	RBBP9_MOUSE
TRINITY_DN416841_c0_g1	12hr	48hr	-8.04	1.05E-02	NA

**Table S3.** RNA purity and integrity of extracted total RNA from kidney tissue

The RNA purity (via Nanodrop) and integrity (via Bioanalyzer) were both measured to ensure high quality samples were used in the cDNA library synthesis. Ideal ratios for 260/280 and 260/230 for RNA are ~2.0 and ~2.2. Mean RIN values for all samples was 9.33.

Sample	Time point	RIN	260/280 ratio	260/230 ratio
K11	0hrs	9.5	1.9	1.95
K12	0hrs	9.4	1.91	1.99
K15	0hrs	8.5	1.96	2.27
K18	0hrs	8.8	2.92	2.34
K24	0hrs	8.5	2.06	2.14
K07	12hrs	9.5	1.99	2.07
K08	12hrs	9.1	2	2.17
K16	12hrs	9.5	1.95	2.1
K19	12hrs	9.9	1.92	2.29
K21	12hrs	9.6	1.96	2.06
K03	48hrs	9.5	1.94	2.37
K04	48hrs	9.3	2.01	2.17
K17	48hrs	9.6	2	2.13
K20	48hrs	9.6	2	2.08
K23	48hrs	9.7	2.01	2.14

**Table S4.** Concordant and discordant alignment rates

Bowtie2 software was used to examine alignment of individual samples back to the *de novo* assembled transcriptome.

Mapping type	% Mapped
Paired reads with 0 concordant alignment	26.99
Paired reads with exactly 1 concordant alignment	16.84
Paired reads with more than 1 concordant alignment	56.17
Of paired reads with 0 concordant alignments, those with 1 discordant alignment	2.94
Of paired reads with 0 concordant alignments, mates that aligned 0 times	30.15
Of paired reads with 0 concordant alignment, mates that aligned 1 time	8.56
Of paired reads with 0 concordant alignment, mates that aligned >1 times	61.29
Overall alignment rate	92.75

**Figure S1.** Sum of transcript expression in each replicate.

The Trinity PtR pipeline was used to obtain transcript counts that were CPM transformed and then  $\log_2$  transformed. The expression for each transcript was then summed to give the total mRNA expression from animals in (A) 0hrs, (B) 12hrs in 65% SW, and (C) 48hrs in 65% SW.

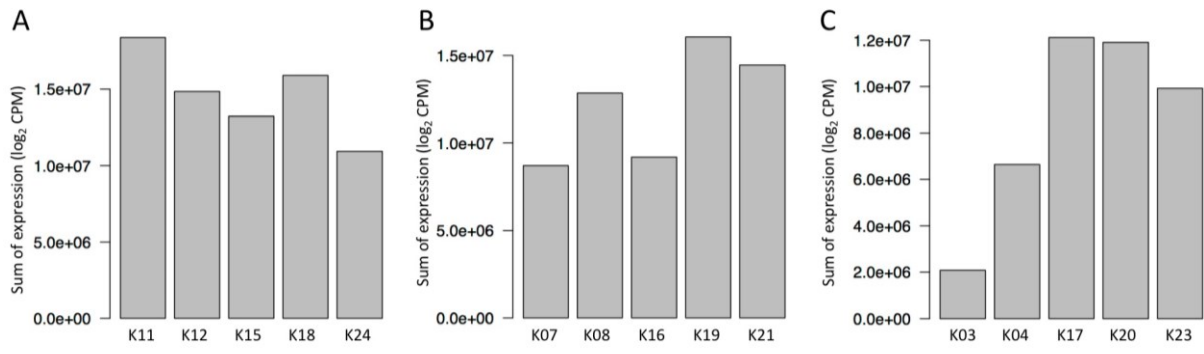


**Figure S2.** Estimation of true number of different transcripts in the kidney transcriptome

A method of approximating a more realistic level of gene (or transcript) expression is supported by the Trinity script *count\_matrix\_features\_given\_MIN\_TPM\_threshold.pl* which plots the number of transcripts as a function of minimum TPM threshold. The green line indicates the linear regression of transcripts below the cut a negative minimum TPM of 10. Where  $x=0$  is the estimation of the approximate number of contigs in the kidney transcriptome while ignoring the numerous lowly expressed contigs. The value approximated using this technique is 15082 transcripts.

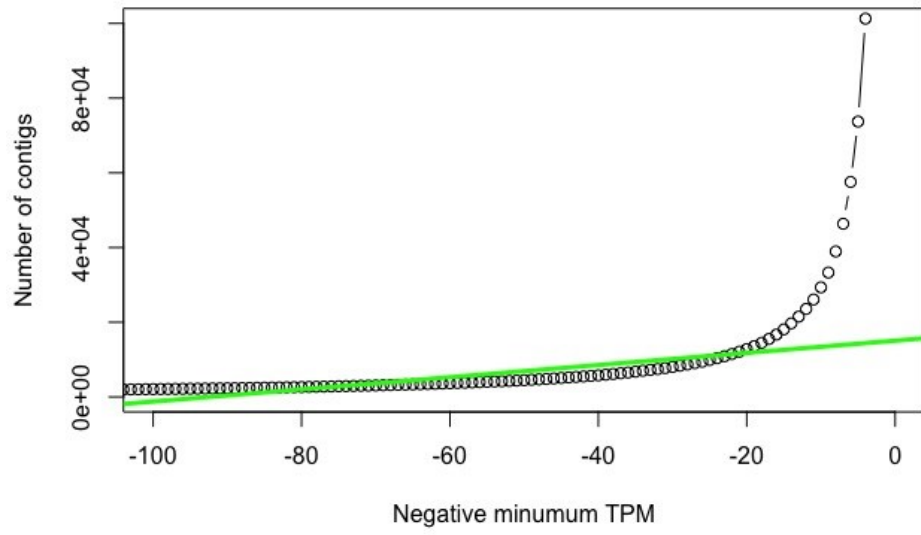


**Figure S3.** Analysis of ExN50 values of the *de novo* assembled kidney transcriptome  
The Ex90N50 value is a better measurement of the quality of the transcriptome than the N50 value. Trinity script *contig\_ExN50\_statistic.pl* was used to generate N50 values for each percentile of the total normalized expression data. The red line indicates the Ex90 value where the contigs below this value comprise 90% of the highest expression data. The Ex90N50 value was calculated as 1,855 bp.

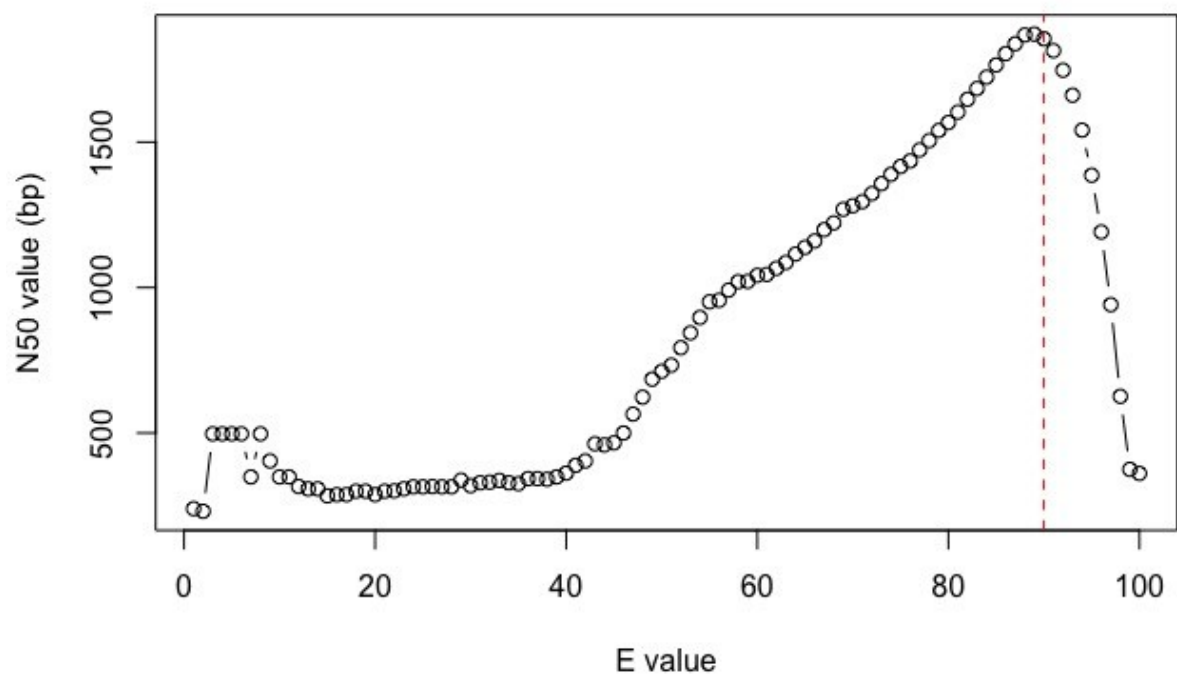


**Figure S4.** MA and Volcano plots for each statistical comparison

MA (left) and volcano (right) plots were generated using the Trinity PtR pipeline to visualize the trends (based on FC, counts, and  $P_{adj}$  value) of the differentially expressed transcripts (red dots) and their unresponsive counterparts (black dots) in each statistical comparison; (A) 0 vs 12, (B) 0 vs 48, and (C) 12 vs 48.

